Listeriolysin O and Pneumolysin: Effects on intracellular calcium homeostasis and epithelial barrier integrity

Martin Leustik

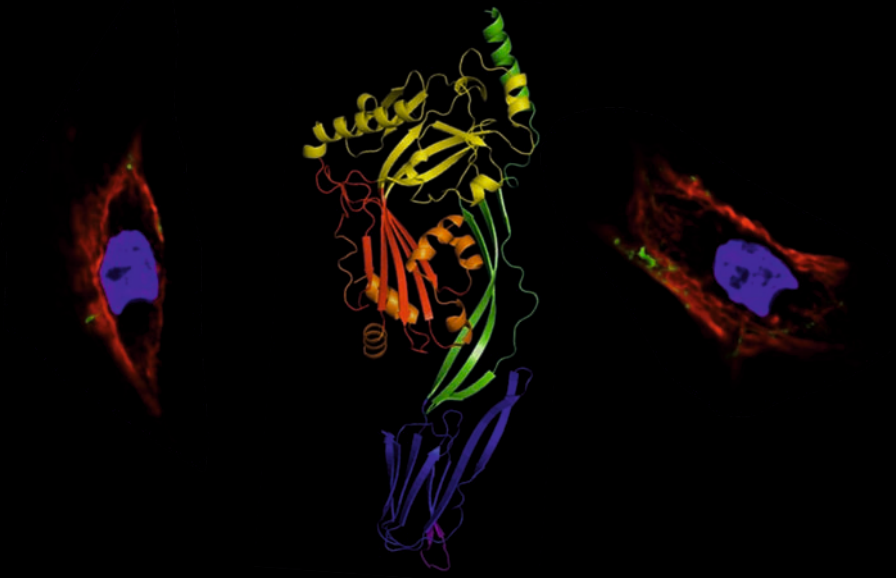

INAUGURAL DISSERTATION
submitted to the Faculty of Medicine
in partial fulfilment of the requirements
for the PhD-degree
of the Faculties of Veterinary Medicine and Medicine
of the Justus Liebig University Giessen, Germany

édition scientifique
VVB LAUFERSWEILER VERLAG

1. Auflage 2013

1st Edition 2013

Printed in Germany

édition scientifique
VVB LAUFERSWEILER VERLAG

STAUFENBERGRING 15, D-35396 GIESSEN
Tel: 0641-5599888 Fax: 0641-5599890
email: redaktion@doktorverlag.de

www.doktorverlag.de

Listeriolysin O and Pneumolysin:
Effects on intracellular calcium homeostasis and epithelial barrier integrity

Inaugural Dissertation

submitted to the Faculty of Medicine

in partial fulfillment of the requirements

for the PhD-Degree

of the Faculties of Veterinary Medicine and Medicine

of the Justus-Liebig-University Giessen

by

Martin Leustik

of

Klagenfurt, Austria

Giessen 2012

From the Institute of Medical Microbiology
Director: Prof. Dr. Trinad Chakraborty
Faculty of Medicine of the Justus-Liebig-University Giessen

First Supervisor and Committee Member:	Prof. Dr. T. Chakraborty
Second Supervisor and Committee Member:	Prof. Dr. W. Kühlbrandt
Committee Members:	Prof. Dr. M. Diener
	Prof. Dr. J. Lohmeyer

Date of Doctoral Defence: 4th February 2013

Declaration

“I declare that I have completed this dissertation single-handedly without the unauthorized help of a second party and only with the assistance acknowledged therein. I have appropriately acknowledged and referenced all text passages that are derived literally from or are based on the content of published or unpublished work of others, and all information that relates to verbal communications. I have abided by the principles of good scientific conduct laid down in the charter of the Justus Liebig University of Giessen in carrying out the investigations described in the dissertation.”

Martin Leustik

Table of Contents

List of abbreviations

α	Alpha
A	Alanine
aa	Amino acid(s)
Ach	Acetylcholine
ADP	Adenosine diphosphate
AJ	Adherens junction
ALO	Anthrolysin O
AM	Acetoxymethyl ester
APC	Antigen presenting cell
ATP	Adenosine-5'-triphosphate
ATCC	American Type Culture Collection
ALV	Alveolyin
β	Beta
BFL	Bifermentolysin
BHI	Brain heart infusion
BLY	Botulinolysin
BoNT	Botulinum neurotoxin
BSA	Bovine serum albumin
C	Cysteine
℃	Degree Celsius
Ca^{2+}	Calcium ion
$[Ca^{2+}]_i$	Intracellular Ca^{2+} concentration
CDC	Cholesterol dependent cytolysin
CFU	Colony forming units
CLO	Cereolysin O
cPKC	Conventional PKC
CTx	Cholera toxin.
CVL	Chauveolysin
DAPI	4',6-diamidino-2-phenylindole
DTT	Dithiothreitol
E	Glutamic acid
ECad	E-Cadherin
EDTA	Ethylenediaminetetraacetic acid
e.g.	*exempli gratia* (for example)
ER	Endoplasmic reticulum
et al.	*et alii* (and others)
FBS	Foetal Bovine (calf) Serum
Fig.	Figure
γ	Gamma
g	Relative centrifugal force or gram
G	Glycine
GILT	γ-interferon-inducible lysosomal thiol reductase
GTP	Guanosine-5'-triphosphate
h	Hour(s)
HEPES	4-(2-hydroxyethyl)-1-piperazineethanesulfonic acid
HTL	Histolyticolysin O
HUS	Haemolytic Uremic Syndrome
$IC_{(50)}$	Half maximal inhibitory concentration
IL1	Interleukin-1

ILO	Ivanolysin O
ILY	Intermedilysin
Inl	Internalin
Iono	Ionomycin
IP_3	Inositol trisphosphate
IP_3R	Inositol trisphosphate receptors
kDa	Kilodalton
k	Kilo [10^3]
l	Litre
L	Leucine
La	Lanthanum
La^{3+}	Lanthanum ion
LLO	Listeriolysin O
LPS	Lipopolysaccharide
LSL	Laterosporolysin
LSO	Seeligerolysin O
LytA	Autolysin A
µ	Micro [10^{-6}]
m	Milli [10^{-3}] or metre
M	Molar (mol/l)
MAPK	Mitogen-activated protein kinase
MDT	Membrane damaging toxin
MEM:	Minimal essential medium (Eagle)
MHC II	Major histocompatibility complex II
min	Minute(s)
MLC	Myosine light-chain
MLY	Mitilysin
MM	Minimal medium
MΩ	MegaOhm
MOI	Multiplicity of infection
mQH_2O	Water cleaned by water purification system
n	Nano [10^{-9}] or number of independent experiments
NADPH	Nicotinamide adenine dinucleotide phosphate
NEA	Non-essential amino acids
nr.	Number
NVL	Novyilysin
OD	Optical density
Osm	Osmole(s)
PBS	Phosphate buffered saline
PFO	Perfringolysin O
PFT	Pore forming toxin
PI3K	Phosphoinositide 3-kinase
PKC	Protein kinase C
Plc	Phospholipase
PLO	Pyolysin
PLY	Pneumolysin
PRR	Pathogen recognition receptor
PVL	Panton-Valentine-leukocidin
R	Arginine
RNA	Ribonucleic acid
ROCK	Rho-associated kinase

rpm	Revolutions per minute
RPMI	Roswell Park Memorial Institute medium
RT	Room temperature
RTX	Repeats in toxin
Rya	Ryanodine
RyR	Ryanodine receptor
SAg	Superantigen
SDL	Sordellilysin
sec	Second(s)
SEM	Standard error of the mean
SERCA	Sarco / endoplasmic reticulum Ca^{2+}ATPase
ShlA	*Serratia marcescens* haemolysin
siRNA	Small interfering RNA
SLO	Streptolysin O
SLY	Suilysin
SPH	Sphaericolysin
SPL	Septicolysin O
STEC	Shiga-like toxin-producing *Escherichia coli*
sTIP	Scrambled TIP
STSS	Streptococcal toxic shock syndrome
STx	Shiga toxin
SUMO	Small ubiquitin-like modifier
T	Threonine
Tab.	Table
TCR	T-cell receptor
Thaps	Thapsigargin
TMH	Transmembrane helix
TJ	Tight junction
TeNT	Tetanus neurotoxin
TIP	Lectin-like domain of TNF or a peptide mimicking it
TLR4	Toll-like receptor 4
TLO	Thuringiolysin O
TLY	Tetanolysin
TNF	Tumor necrosis factor
TSS	Toxic shock syndrome
VLY	Vaginolysin
(v/v)	Volume fraction
W	Tryptophan
WT	Wild type
(w/v)	Mass concentration
XeC	Xestospongin C

1 Introduction

1.1 Bacterial toxins

Bacteria produce a large number of different molecules that are toxic to eukaryotic hosts. Some of these molecules are structural components that form part of the bacterial cell and are released during the growth and death of microorganisms. These structural molecules are referred to as endotoxins because they are not actively released but just appear whenever bacteria are multiplying or being lysed. Endotoxins usually have no toxic effect by themselves, but trigger deleterious reactions because host cells recognize them as warning signals for the presence of invading pathogens. The most well-known example is lipopolysaccharide (LPS), the main building block of the outer membrane of Gram-negative bacteria. LPS consists, as the name suggests, of a lipid part (lipid A) that is linked to a so-called core polysaccharide and faces towards the inside of the cell. Bound to the core polysaccharide is the O side chain or O antigen, a polysaccharide chain extending outwards. As LPS forms the outermost barrier around Gram-negative bacteria it has fundamental function in protecting the microorganisms from environmental influences, such as bile salts, antibiotics or antibodies produced by the host immune system. The toxicity of LPS is conferred by lipid A. As it is the most conserved portion in Gram-negative bacteria it is recognized by the innate immune system's pathogen recognition receptors (PRR). The specific receptor for LPS is toll-like receptor 4 (TLR4) (Poltorak, 1998), which, upon activation, triggers the release of proinflammatory cytokines like IL1, IL6 and tumor necrosis factor alpha (TNFα). Whenever excessive amounts of LPS enter the host a possibly lethal hyperinflammatory reaction is induced due to uncontrolled cytokine release (endotoxin shock). During persistent or systemic infections patients often succumb to septic shock, caused by circulating endotoxin that, via the hyperactivated immune system, damages the endothelium. This leads to a loss of perfusion and subsequent multiple organ failure. Endotoxin-free equipment and materials are of great importance in modern medicine, as even very small doses (500pg/kg body weight; FDA, 2009) of parenterally administered endotoxin are dangerous to patients. Removal of endotoxins is difficult and expensive; their inactivation requires temperatures of at least 250℃. When heating is not possible, endotoxins can also be removed by treatment with hydrogen peroxide or sodium hydroxide. In sensitive

samples like protein extracts, techniques like ion exchange chromatography or ultrafiltration are used.

While endotoxin-like molecules are found in all bacteria, exotoxins are generally produced in pathogenic strains. Exotoxins are, in most cases, actively secreted and have toxic effects on the host, either by directly killing cells or otherwise disturbing the functions of the organism. Bacterial exotoxins are a large and heterogeneous group of proteins with diverse modes of action that include the most potent biological toxins known. The deleterious actions of different toxins range from apparently non-specific lysis of eukaryotic cells by pore forming toxins from the group of cholesterol-dependent cytolysins to highly specific blocking of the release of acetylcholine (Ach) by botulinum toxin in stimulatory motor neurons at neuromuscular junctions. The classification of a bacterial toxin is possible with regard to the microorganism producing it, its specific action or the affected tissue. Here, they will be listed according to their structure and general function.

1.1.1 AB Toxins

This group of exotoxins is the largest and includes toxins with several different activities and potencies. The name AB toxins originates from their shared organisation into one binding (B) and one enzymatically active (A) portion. The B portion is responsible for the specificity of the toxin as it binds to the cellular receptor on the plasma membrane of host cells. The A portion is responsible for the toxic effect after translocation to its destination inside the cell. The ratio of A to B is variable between the different toxins in this group. Depending on the specific toxin the two portions are either released as one protein that is cleaved by host proteases, as a disulfide-linked protein complex, or as single proteins that combine only after the specific cell surface ligand is bound by the B subunit (Figure 1.1.1). The ligand of the B subunit on the plasma membrane together with the intracellular target of the A subunit account for the tissue specificity of the toxins. Some exotoxins, like tetanus toxin, target only neuronal cells while others, like cholera toxin, can enter all kinds of cells because their ligand is ubiquitously expressed. The two most potent members of this group are botulinum neurotoxin (BoNT) and tetanus neurotoxin (TeNT). With lethal quantities in humans of 1.0 and 2.5 ng/kg body weight, respectively, these two are the deadliest biological toxins known today (Gill, 1982; Meyer and Eddie, 1951;

Bolton and Fish, 1902). The extremely low lethal dose is due to the specific action of the toxins at neuromuscular junctions in motor nerve termini.

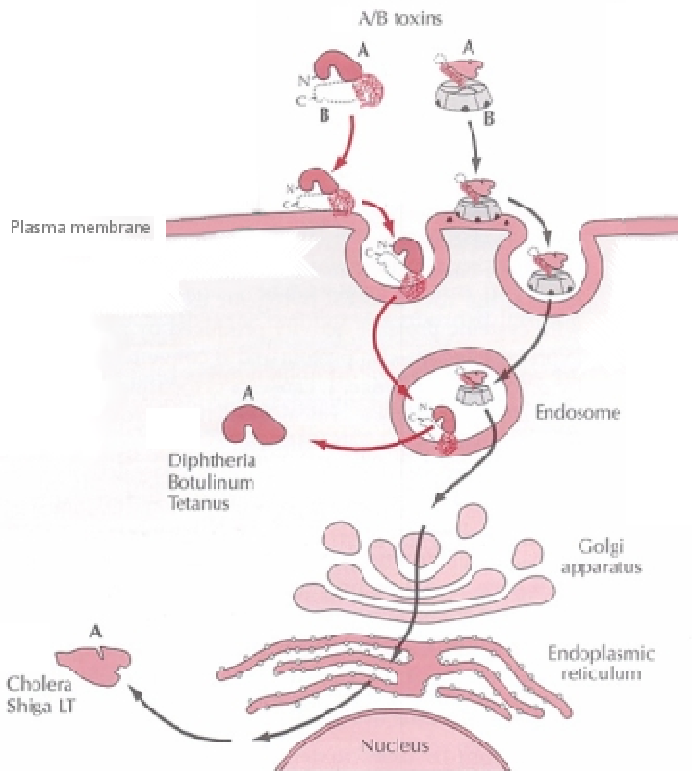

Fig 1.1.1 Entry and retrograde transport of different AB toxins. Adapted from Sandvig *et al.*, 2010.

Here, both BoNT and TeNT find the ligands of their respective B subunit, bind it and are subsequently endocytosed. Thereafter, the A subunit is released into the cytoplasm. In the case of BoNT it inhibits the membrane fusion of synaptic vesicles by degradation of SNARE proteins and the release of acetylcholine, which leads to a long-lasting relaxation of affected muscles (Schiavo, Shone, *et al.*, 1993; Schiavo, Rossetto, *et al.*, 1993; Binz *et al.*, 1994; Foran *et al.*, 1996). A systemic muscle paralysis, called botulism, can develop if *Clostridium botulinum*, the bacterium producing BoNT, is able to colonize the digestive tract or a wound. The first signs of botulism are loss of facial expressions and the inability to speak or open the eyelids and usually progress to paralysis of the limbs. In severe cases the diaphragm and accessory breathing muscles are affected, which results in asphyxiation if the patient is not mechanically ventilated. Botulism can also occur by ingestion of *C. botulinum* - contaminated food. Tetanus, the medical condition caused by TeNT, develops upon infection with *Clostridium tetani*. The bacterium, like *C. botulinum*, is an obligate anaerobe and usually infects deep cuts or punctures that were not disinfected properly. Once an infection is established the neurotoxin is released and causes

muscle rigidity and spasms. In general tetanus, like botulism, starts to affect the facial and neck area first and spreads downward. Respiratory failure and death occur when the spasms affect the diaphragm and accessory breathing muscles. TeNT disturbs the signal transduction to the muscles at a different point than BoNT. It disrupts the function of inhibitory interneurons and Renshaw cells, leading to unmodulated stimulation of skeletal muscles (Howard and Riley, 1965; Takano, 1985; Curtis *et al.*, 1976). The fatalities due to tetanus have decreased drastically (Hoheisel and Hoheisel, 1968; Blencowe *et al.*, 2010) since the introduction of a successful vaccination campaign.

Enterotoxins form another subgroup of AB toxins. They are produced by bacteria that enter the host via contaminated food or water, have a direct effect on the intestinal mucosa and elicit profuse fluid secretion. The best studied example is cholera toxin (CTx). *Vibrio cholerae* releases it upon reaching the small intestine and attaching itself to the intestinal epithelium. The resulting disease (cholera) manifests itself through profuse painless diarrhoea and vomiting of clear fluid. Untreated cholera patients may loose up to 20 litres of liquid daily, often with fatal results. CTx consists of a pentameric B subunit that is connected to a single A subunit by a disulfide bond. The B subunit binds GM1 gangliosides on the plasma membrane of intestinal epithelial cells and triggers the internalization of the toxin. Once inside the cell the toxin is transported from the Golgi apparatus to the endoplasmic reticulum (ER) via retrograde trafficking. In the ER the A subunit is cleaved off and released in the cytoplasm, where it ADP ribosylates the GTP binding protein Gsα (Hepler and Gilman, 1992; McRoberts *et al.*, 1985). This leads to a massive elevation of intracellular cAMP levels, resulting in active chloride secretion (Field *et al.*, 1972, 1989). As a consequence, large quantities of water osmotically move into the intestinal lumen, exceeding the resorption capacity of the large intestine, resulting in severe secretory diarrhoea and life-threatening dehydration.

Shiga toxin (STx), like CTx, consists of a pentameric B subunit that specifically binds the glycosphingolipid Gb3 in the plasma membrane of host cells (Sandvig *et al.*, 1992). Upon toxin endocytosis the A subunit is cleaved and thereby activated by a cellular enzyme called furin. The presence of this enzyme is a prerequisite for STx activity (Garred *et al.*, 1995). STx follows a retrograde trafficking route like CTx, ending with the transport of the activated A subunit from the ER into the cytosol. Here it inhibits protein synthesis by removing one adenine from the 28S RNA (Endo *et al.*,

1988), thereby killing the affected cells. STx is produced by *Shigella dysenteriae*, which causes hemorrhagic colitis, a disease that, unlike cholera, is characterized by small volumes of bloody stool and a painful inflammatory reaction. There are also strains of *Escherichia coli* (STEC) which are able to produce Shiga-like toxins that are very closely related to STx from *S. dysenteriae*. The main difference in the conditions caused by the two bacterial species is the high incidence of haemolytic uremic syndrome (HUS) in STEC-infected patients, as could be observed in the outbreak of *E. coli* O104:H4 in summer 2011 in Germany.

1.1.2 Superantigens

Superantigens (SAgs) are bacterial proteins disturbing the communication at the interface of the innate and the adaptive immune system. Under normal conditions a reaction of the adaptive immune system is triggered when a specific antigen is taken up by an antigen presenting cell (APC). Within the APC the antigen is processed, fitted into the major histocompatibility complex II (MHC II) and then presented to cells of the adaptive immune system. This way it can be recognized by one of the randomly-generated T-cell receptors (TCR). When a T-cell with a fitting receptor binds the antigen-MHC II-complex it is activated and starts to produce inflammatory cytokines like IL1 and TNFα (Figure 1.1.2, left side). Due to the specificity of the TCR any single antigen usually only activates a very small number of T-cells, which allows the host to react to infections with precision and a minimum of self-destruction due to the controlled inflammatory response. SAgs subvert the specificity of the T-cell activation by binding conserved parts of MHCII-molecules and TCRs, thereby mimicking the presence of a specific antigen (Alouf and Müller-Alouf, 2003; Figure 1.1.2, right side). This can lead to an activation of up to 25% of all T-cells in the body. The resulting massive cytokine release, known as toxic shock syndrome (TSS), is deleterious for the host (Todd *et al.*, 1978). In general the symptoms include high fever, hypotension, shock, respiratory distress and renal failure, mostly due to systemic endothelial damage and hyperinflammation. Many SAgs are produced by the two Gram-positive bacteria *Staphylococcus aureus* and *Streptococcus pyogenes*. While staphylococcal SAgs like Toxic shock syndrome toxin-1 are mostly responsible for TSS, the streptococcal pyrogenic exotoxins can trigger a more acute condition (streptococcal TSS or STSS). While the symptoms of TSS and STSS are very

similar, the fatality rate of STSS is much higher (up to 30%) (Stevens *et al.*, 1989; McCormick *et al.*, 2001).

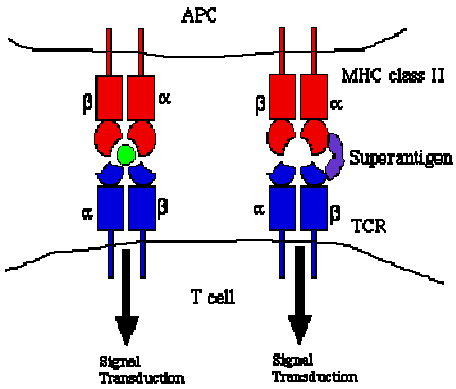

Fig 1.1.2 Schematic representation of antigen and superantigen binding to MHCII and TCR. Normal antigen presentation is shown on the left side while superantigen stimulation in the absence of antigen recognition is featured on the right side: Adapted from Janeway *et al.*, 2001.

1.1.3 Membrane Damaging Toxins

Membrane damaging toxins (MDTs) exert their function by disruption, perforation or destabilization of the plasma membrane of target cells, which leads to an osmotic imbalance. The effects are always dependent on toxin concentrations and range from perturbations in regular cellular functions to massive release of inflammatory messengers and finally to the lytic destruction of cells. It has been proposed that toxin concentrations produced *in vivo* are mostly not sufficient to cause lysis in host cells, but more likely mediate the release of many different effectors in toxin-damaged cells, especially in cells of the immune system (Billington *et al.*, 2000). This includes cytokines, chemokines, nitric oxide and other molecules that are critical for cell signalling. Hence, a much more subtle mechanism of MDTs in bacterial virulence than just randomly killing host cells has been proposed (Kayal *et al.*, 1999; Bryant *et al.*, 2003; Bhakdi and Tranum-Jensen, 1988). Three distinct families of MDTs can be distinguished based upon the mechanism employed to damage eukaryotic cell membranes:

1) Toxins that feature a detergent-like activity that leads to a solubilisation effect in membranes or partial insertions into their hydrophobic regions. Examples are the delta- and delta-like toxins of *Staphylococcus aureus*, *Staphylococcus haemolyticus*, and *Staphylococcus lugdunensis*, the heat-stable haemolysin from *Pseudomonas aeruginosa*, and *Bacillus subtilis* cyclolipopeptides (Freer and Arbuthnott, 1982; Rowe and Welch, 1994; Bernheimer and Rudy, 1986; Sheppard *et al.*, 1991).

2) Enzymatically active toxins that function as phospholipases or sphingomyelinases and hydrolyse the phospholipids in the plasma membrane of target cells. They include *C. perfringens* α-toxin (phospholipase C) (Macfarlane and Knight, 1941) and *S. aureus* β-toxin (sphingomyelinase C) (Russell *et al.*, 1976).

3) Pore forming toxins (PFTs) that are able to create channel-like pores in the plasma membrane. This is the largest family of the bacterial protein toxins, including over 120 members (Alouf and Popoff, 2005). The concept of proteins that perforate membranes is not limited to bacterial virulence factors but is also used by the immune system in the form of the complement system (Mayer, 1972) or perforin from cytotoxic T-cells to eliminate intruding organisms and silence dysfunctional or infected somatic cells (Podack and Konigsberg, 1984). To account for the differences in structure and mechanism a further sub-classification of the PFTs is necessary.

- The subfamily of RTX (repeats in toxin) toxins are produced by a broad range of Gram-negative bacteria like members of the family Pasteurellaceae, *E. coli*, *B. pertussis*, *V. cholerae*, and other pathogens (Welch, 2001). They share several distinct structural and functional elements such as a series of glycine-rich nonameric repeats in the C-terminal half of the protein, a size over 100 kDa, a calcium (Ca^{2+})-dependent activity and the generation of short-lived, cation-selective pores (Felmlee *et al.*, 1985; Welch, 1987; Lo *et al.*, 1987). The exact mechanism of pore formation remains elusive, as the pores or pore-forming structures have not been detected by electron microscopy yet.
- The *Serratia marcescens* haemolysin (ShlA) is the prototype for a group of toxins that, unlike the rest of the exotoxins, depends on two separate genes for its function. The first gene (*shlA*) encodes the toxin itself while the second (*shlB*) encodes the outer membrane protein required for ShlA secretion and activation (Braun *et al.*, 1987; Poole *et al.*, 1988). *S. marcescens* is a pathogen that opportunistically causes respiratory and urinary tract infections, bacteraemia, endocarditis, keratitis, arthritis, and meningitis (Lyerly and Kreger, 1983; Maki *et al.*, 1973). The haemolysin has been found in over 90% of tested clinical isolates of *S. marcescens*, toxins with similar sequences have been described in *Proteus mirabilis*, *Haemophilus ducreyi*, *Edwardsiella tarda*, and *Photorhabdus luminescens* (Brillard *et al.*, 2002). Until today the exact

mechanism of pore formation is unknown but the experimentally determined pore size is below 1-3 nm in diameter (Hertle *et al.*, 1999).

- The PFTs produced by *S. aureus* are by themselves a heterogeneous family consisting of those with α-helical structures and those rich in β-strands. The staphylococcal δ-haemolysin for example forms a single amphiphilic α-helix that associates in a typical octameric, barrel-like pore (Tappin *et al.*, 1988). This small molecule (26 amino acid residues) can attack a wide range of cell types. Other staphylococcal species like *S. epidermidis, S. simulans* and *S. warneri* were found to carry related toxins. In the group of staphylococcal PFTs rich in β-strand sequences, toxins that form homo-oligomeric pores like α-toxin can be further distinguished from the hetero-oligomeric bicomponent leukotoxins. Staphylococcal α-toxin is a protein of 293 amino acids produced by almost all *S. aureus* strains that assembles to hepta- or hexameric pores with a diameter of about 1.4 nm (Song *et al.*, 1996). Staphylococcal α-toxin was found to preferentially bind membranes containing choline-type phospholipids and cholesterol (Freer *et al.*, 1968). Recently caveolin-1 has been discovered to be essential for toxin binding and membrane penetration (Vijayvargia *et al.*, 2004; Pany and Krishnasastry, 2007). Staphylococcal bicomponent leukotoxins function as a combination of two distinct proteins, a class S (31 kDa) and a class F protein (34 kDa). Together they create bipartite oligomeric pores in the membranes of their target cells, which are monocytes, macrophages, and polymorphonuclear cells (Woodin, 1960; Prevost *et al.*, 1995). Panton-Valentine-leukocidin (PVL) is a prominent example of this toxin class (Woodin, 1961). PVL was found to trigger apoptosis in leukocytes even at low concentrations and therefore plays an important role in the virulence of *S. aureus* (Genestier *et al.*, 2005; Boyle-Vavra and Daum, 2007). Additionally, it is implicated in the increased incidence of community acquired infections with methicillin-resistant *S. aureus* (Tang *et al.*, 2007; Brown *et al.*, 2011). The last group of PFTs are the cholesterol dependent cytolysins (CDCs). This group will be discussed in detail in the following section.

1.2. Cholesterol dependent Cytolysins

CDCs have a long history. The first member of this group was already described in 1898 when Paul Ehrlich (Ehrlich, 1898) reported the presence of a haemolytic agent,

tetanolysin, in culture supernatants from *Clostridium tetani*. Following this first report similar toxins were discovered in other Clostridium species and bacteria from the genera Arcanobacterium, Bacillus, Brevibacillus, Gardnerella, Listeria, Paenibacillus and Streptococcus.

Until this day 25 toxins of this class that are produced by 27 bacterial species are known (Table 1). CDCs are exclusively produced by Gram-positive bacteria and, with the exception of PLY, are secreted into the extracellular medium. The toxin molecules are both water soluble in the secreted form and able to bind and interact with the lipid bilayer of plasma membranes. CDCs non-specifically lyse eukaryotic cells at high concentrations. Their activity can be suppressed by sulfhydryl-group blocking agents and reversibly restored by thiols or other reducing agents (Bernheimer and Avigad, 1970; Morgan *et al.*, 1996). The common features of all CDCs include their dependence on cholesterol in membranes, as they are otherwise unable to bind and perforate them. Additionally, the toxins can be inactivated by preincubation with low cholesterol concentrations. Another common feature of CDCs is their ability to form very large pores, with maximum diameters of up to 45 nm, constituted of up to 50 toxin monomers. CDCs have significant levels of amino-acid similarity and share the same mode of action.

Tab 1.2.1. List of all known CDCs and their bacterial sources. Adapted from Alouf and Popoff, 2005 and completed with Rottini *et al.*, 1990; Jefferies *et al.*, 2007; Nishiwaki *et al.*, 2007.

Genus	**Species**	**Toxin**
Arcanobacterium	*A. pyogenes*	Pyolysin (PLO)
Bacillus	*B. anthracis*	Anthrolysin O (ALO)
	B.cereus	Cereolysin O (CLO)
	B. sphaericus	Sphaericolysin (SPH)
	B. thuringiensis	Thuringiolysin O (TLO)
Brevibacillus	*B. laterosporus*	Laterosporolysin (LSL)
Clostridium	*C. bifermentans*	Bifermentolysin (BFL)
	C. botulinum	Botulinolysin (BLY)
	C. chauvoei	Chauveolysin (CVL)
	C. histolyticum	Histolyticolysin O (HTL)
	C. novyi A (oedimatiens)	Novyilysin (NVL)
	C. perfringens	Perfringolysin O (PFO)
	C. septicum	Septicolysin O (SPL)
	C. sordelli	Sordellilysin (SDL)
	C. tetani	Tetanolysin (TLY)

Genus	Species	Toxin
Gardnerella	*G. vaginalis*	Vaginolysin (VLY)
Listeria	*L. ivanovii*	Ivanolysin O (ILO)
	L. monocytogenes	Listeriolysin O (LLO)
	L. seeligerii	Seeligerolysin O (LSO)
Paenibacillus	*P. alvei*	Alveolyin (ALV)
Streptococcus	*S. intermedius*	Intermedilysin (ILY)
	S. mitis	Mitilysin (MLY)
	S. pneumoniae	Pneumolysin (PLY)
	S. pyogenes *S. dysgalactiae subsp. Equisimilis* *S. canis*	Streptolysin O (SLO)
	S. suis	Suilysin (SLY)

Most of the information available about the structural features and the mechanisms by which the CDCs perforate membranes is from studies on PFO, the first toxin to be crystallized from this family (Rossjohn *et al.*, 1997).

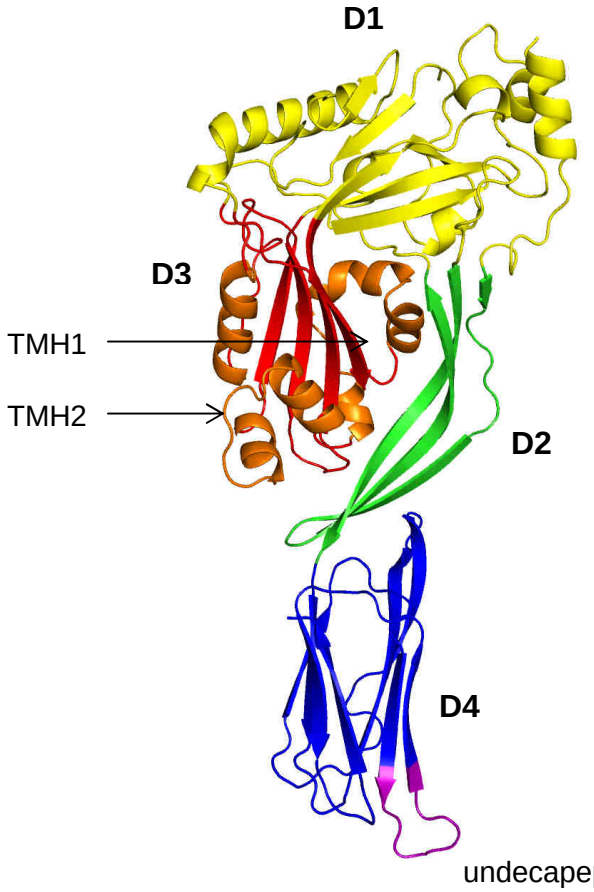

Fig 1.2.1 Crystal structure of pneumolysin. PDB: 2BK2, obtained by fitting the alpha carbon trace of perfringolysin O into a cryo-EM map; created with PyMOL software. D1: amino acids (aa) 25–76, 113–203, 254–299 and 376–398; D2: aa 77–112 and 399–415; D3: aa 204–253 abd 300–375; D4: aa 416–529.

The common structure of CDCs is an elongated, β-sheet-rich shape that can be separated into four domains (Figure 1.2.1). Domain 4 has been recognized to be responsible for membrane binding. Within this domain, all CDCs share a highly conserved motive (ECTGLAWEWWR), the so called undecapeptide (coloured purple in figure 1.2.1), which is necessary for recognition and binding of cholesterol in membranes (Soltani *et al.*, 2007; Smyth and Duncan, 1978; Sekino-Suzuki *et al.*, 1996). Together with the other three downward-facing loops of domain 4 it is anchored in cholesterol-containing membranes. This allows for its movement along the membrane and subsequent association with other toxin monomers to form a prepore complex (Ramachandran *et al.*, 2002; Heuck *et al.*, 2003). After prepore formation an unknown signal triggers conformational changes in domains 2 and 3. Structural changes in transmembrane helices THM1 and 2 in domain 3 – from three α-helices (coloured orange in figure 1.2.1) to one long amphipathic β-hairpin – initiate the formation of a membrane-spanning β-barrel, which is required for perforation of the cell membrane. In detail, these two amphipathic β-hairpins are injected into the plasma membrane and form the walls of the toxin pore (Shepard *et al.*, 1998; Shatursky *et al.*, 1999; Hotze *et al.*, 2001).

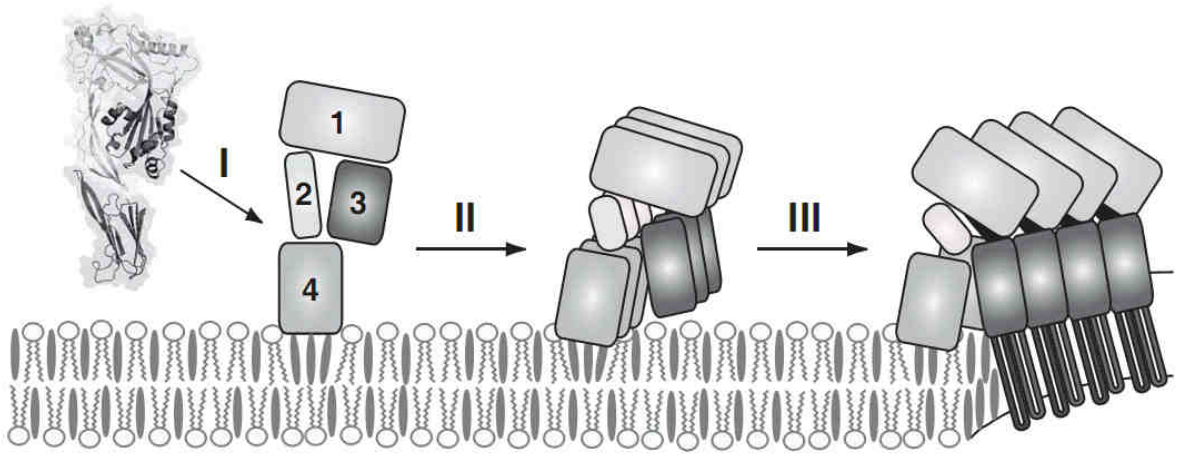

Fig 1.2.2 Proposed pore formation mechanism of CDCs. The toxin domains are indicated by numbers 1-4. CDCs are secreted as water-soluble monomeric proteins that bind cholesterol-containing membranes (I). Single molecules oligomerize into a ring-like structure called the prepore complex (II). An unknown trigger starts conformational changes that lead to the insertion of the TMHs into the membrane bilayer to form the aqueous pore. Adapted from Heuck *et al.*, 2010.

A prerequisite for the insertion of the hairpins into the membrane is the collapse of domain 2, which brings domain 3 much closer to the surface of the membrane. This step is necessary because the hairpin structures formed by THM1 and 2 are

otherwise too short to span the distance through a lipid bilayer (Czajkowsky *et al.*, 2004). Monoclonal antibodies that are able to neutralize the cytolytic activity of CDCs were found to inhibit only pore formation but not membrane binding and oligomerization into a ring-shaped prepore (Darji *et al.*, 1996; Nato *et al.*, 1991). This indicates a stepwise process in pore formation that can be stopped after membrane binding and oligomerization of toxin monomers (Figure 1.2.2).

1.2.1 Listeriolysin O

LLO is the most important virulence factor of *Listeria monocytogenes*, a foodborne facultative intracellular pathogen. The production of a soluble haemolysin by the pathogen was discovered in 1941 (Harvey and Faber, 1941) and since then the toxin has been expressed, purified and extensively studied (Geoffroy *et al.*, 1989).

L. monocytogenes establishes infections via an intracellular life cycle after it comes into contact with human hosts (Figure 1.2.2) (Tilney and Portnoy, 1989). The bacteria express virulence factors called internalins (InlA and InlB) that enable them to invade epithelial, endothelial and liver cells. Once they are taken up into the cytoplasm by internalin-triggered endocytosis they are able to escape the vacuole, proliferate and spread from cell to cell without being detected by the immune system. The control of *Listeria* infections is dependent on macrophages, which phagocytose the bacteria and kill them by fusion of phagosomes with lysosomes. Virulent strains are able to block the fusion event and escape into the cytoplasm, where they multiply and move like in other cell types. The escape from macrophage phagolysosomes and hence destruction is dependent on LLO (Gedde *et al.*, 2000). Deletion mutants or strains lacking the toxin gene are avirulent, as they are digested in phagolysosomes and hence rapidly cleared from the host. There is solid evidence that the phagosomal escape is the main function of LLO in the life cycle of *L. monocytogenes*. It was discovered early that the toxin functions best under acidic conditions with the highest activity at pH 5.5 (Kingdon and Sword, 1970), a property that is unique among the family of CDCs. Only recently it was found that LLO is not activated by low pH values like it was hypothesized for a long time but is quickly disabled by unstructured aggregation under alkaline conditions (Bavdek *et al.*, 2012). When exposed to an acidic milieu, as within phagolysosomes, the toxin molecules are protected from forming inactive aggregates by a controlled dimerization process. Furthermore, CDCs *in vitro* must be activated by reducing agents, a task that is fulfilled inside a

macrophage phagosome by a thiol reductase called γ-interferon-inducible lysosomal thiol reductase (GILT).

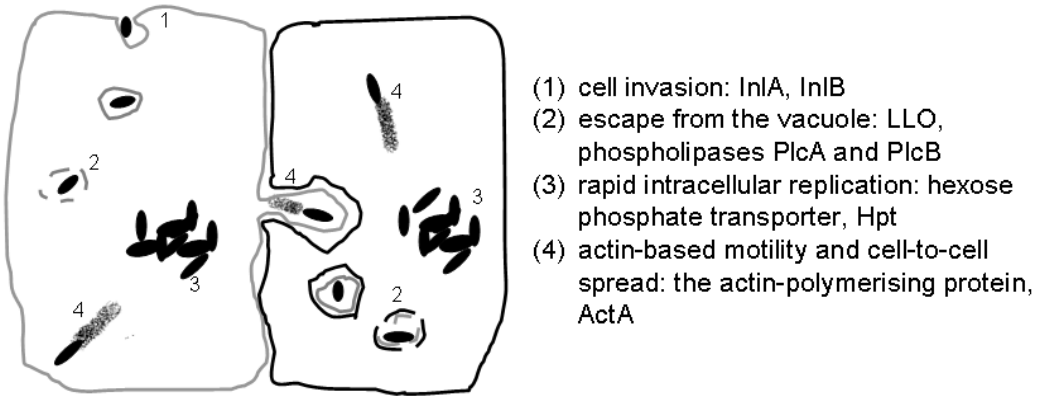

Fig 1.2.2 The intracellular life cycle of *Listeria monocytogenes* and the required virulence factors. Adapted from Alouf and Popoff, 2005. (InlA, B: Internalin A, B)

The effects of purified LLO on cells have been extensively tested. It was found to trigger a number of effects at low concentrations which did not lyse the target cells. LLO triggers apoptosis in some lymphocytes (Carrero *et al.*, 2004; Guzmán *et al.*, 1996). It also leads to an influx of extracellular Ca^{2+} in HEK293 cells (Repp *et al.*, 2002), this disturbance of the cellular homeostasis seems to promote bacterial invasion in Hep-2 epithelial cells (Dramsi and Cossart, 2003) and activate Ca^{2+}-dependent kinases like PKC (Wadsworth and Goldfine, 2002; Shaughnessy *et al.*, 2007; Richter *et al.*, 2009). Similar Ca^{2+}-signalling induces bacterial uptake into J774 macrophages and the escape from phagosomes (Goldfine and Wadsworth, 2002). It was also reported that the toxin is able to release Ca^{2+} from intracellular stores of mouse bone marrow-derived mast cells (Gekara *et al.*, 2008). Recently, LLO was found to increase the permeability of HT-29/B6 colon epithelial cell monolayers in a Ca^{2+}-dependent manner (Richter *et al.*, 2009). Furthermore, the toxin can disturb mitochondrial function and thereby the internal energy supply of cells, presumably to reduce the cellular resistance to infection (Stavru and Cossart, 2011). Other effects of LLO which promote bacterial survival inside cells were also discovered recently. Lam *et al.* (Lam *et al.*, 2011) could show that NOX2 NADPH-oxidase localization to phagosomes is inhibited by the toxin, allowing the bacteria to survive in the phagosomes and ultimately escape into the cytoplasm. Ribet *et al.* (Ribet *et al.*, 2010) reported that LLO pore formation interferes with the posttranslational modification system of SUMOylation by triggering the fast degradation of an enzyme

essential for this protein modification. The overall reduction of SUMOylated proteins promoted bacterial invasion. The authors suggested the involvement of TGF-ß signalling, the exact mechanism behind this finding is still obscure.

Based on the information available, it is clear that LLO disturbs the cellular homeostasis in multiple ways to promote bacterial invasion and intracellular survival. The possibilities of inhibiting the deleterious effects of the toxin on single cells and whole tissue are scarce; the only recent description of a way to ameliorate the complex LLO-induced damages is about the so called TIP peptide. This is a circular 17 amino acid peptide that mimics the lectin-like (TIP) domain of tumor necrosis factor (Lucas *et al.*, 1994). In an acute lung injury model the peptide was able to restore the fluid balance and reduce the vascular permeability (Elia *et al.*, 2003; Vadász *et al.*, 2008; Hamacher *et al.*, 2010; Bloc *et al.*, 2002). It could also be shown to limit LLO-induced hyperpermeability in endothelial cells by inhibiting MLC phosphorylation (Xiong *et al.*, 2010; Lucas *et al.*, 2009; Yang *et al.*, 2010).

1.2.2 Pneumolysin

PLY is found in all clinically relevant isolates of *S. pneumoniae* and is classified as one of its most important virulence factors (Paton *et al.*, 1983; Kanclerski and Möllby, 1987). Since its discovery as a haemolytic factor (Libman, 1905), several characteristics typical for the CDC family, like cholesterol dependence, oxygen lability and increased activity under reducing conditions (Cole, 1914; Cohen *et al.*, 1937, 1942; Avery and Neill, 1924), have been identified. After being cloned, sequenced and purified (Mitchell *et al.*, 1989; Walker *et al.*, 1987; Paton *et al.*, 1986) it was further tested in order to understand its function in pneumococcal pathogenesis. *S. pneumoniae* carries an array of virulence factors enabling it to cause severe and persistent diseases. A major complication of pneumococcal pneumonia is the loss of epithelial and endothelial barrier function. When the pathogen succeeds in undermining the integrity of the lung epithelium it can enter the blood stream, causing sepsis. Another result of *S. pneumoniae* overcoming host barriers is meningitis, which requires the pathogen to cross the blood-brain barrier that is constituted by endothelial cells (Hippenstiel and Suttorp, 2003; Nassif *et al.*, 2002). While there are reports of *S. pneumoniae* entering cells, this phenomenon seems to be restricted to a very low percentage of infecting bacterial cells in the host (Ring *et al.*, 1998).

Therefore, the pathogen seems to be able to damage epi- and endothelial barriers in a way that allows the bacteria to transmigrate between cells.

In the light of PLY being indispensable for pneumococcal pathogenicity, it seems curious that PLY, unlike all the other members of the CDC family, is stored in the cytoplasm of streptococci instead of being actively released. This is due to the lack of an N-terminal secretion signal sequence (Jedrzejas, 2001; Johnson and Aultman, 1977). Host cells are exposed to PLY after lysis of the bacteria by a virulence factor called autolysin. The activation of autolysin can be triggered by the immune system, antibiotics or other bacterial virulence factors (Jedrzejas, 2001; Balachandran *et al.*, 2001; Anderson *et al.*, 2007; Charpentier *et al.*, 2000). Moreover, it is active when the bacteria reach a plateau in their growth phase *in vitro* (Sanchez-Puelles *et al.*, 1986). This seemingly suicidal behaviour favours bacterial survival in the host because PLY has many immunomodulatory effects. It was found to inhibit migration, respiratory burst, degranulation and other bactericidal activities in polymorphonuclear leukocytes and monocytes (Ferrante *et al.*, 1984; Nandoskar *et al.*, 1986; Paton and Ferrante, 1983). In addition, it is able to modify epigenetic regulation (Hamon *et al.*, 2007) of host cells and influences the expression of several genes of cytokines, chemokines, caspases and adhesion molecules (Rogers *et al.*, 2003; Thornton and McDaniel, 2005).

The structural basis for the pore formation by PLY was resolved by Tilley *et al.* (2005) with electron microscopy. The group was able to picture prepore and pore complexes, thereby confirming that oligomerization precedes the conformational changes in domain 2 and the refolding of the two α-helices in domain 3 into the membrane-perforating ß-hairpins. It is also shown that the collapse of domain 2 is necessary for pore formation, as domain 3 is previously too high above the membrane for the hairpins to insert.

Like all CDCs, pneumolysin acts in a concentration-dependent manner on host cells. While higher amounts instantly lyse and kill cells in an unspecific manner, sublytic concentrations can interfere with cell signalling events by inducing an influx of extracellular Ca^{2+} and disturbances of osmotic homeostasis through the toxin pores. This activates host kinases like rho and rac GTPases rac-1 and rho-associated kinase (ROCK) (Iliev *et al.*, 2007), mitogen-activated protein kinases (MAPK) like p38 (Ratner *et al.*, 2006) and phosphoinositide 3-kinase (PI3K) γ (Maus *et al.*, 2007). When purified PLY is introduced into rat lungs it causes reactions very similar to the

symptoms of pneumonia, featuring neutrophilic alveolitis and lung injury (Feldman *et al.*, 1991). It also alters alveolar permeability and affects epithelial tight junction integrity (Rubins *et al.*, 1993; Rayner *et al.*, 1995). The toxin is highly cytotoxic on alveolar epithelial cells and causes cytoplasmic blebbing, mitochondrial swelling and cell death (Steinfort *et al.*, 1989). Its haemolytic activity also impairs ciliary function (Feldman *et al.*, 2002) and damages endothelial cells, which contributes to pulmonary haemorrhage and oedema (Rubins *et al.*, 1992; Lucas *et al.*, 2012). In mouse experiments PLY-deficient *S. pneumoniae* mutants are cleared faster from the respiratory tract and have a reduced lethality upon intranasal application compared to toxin-producing strains (Kadioglu *et al.*, 2002; Berry *et al.*, 1989). Lung injury induced by PLY was suggested to result from direct pneumotoxic effects on the alveolar-capillary barrier, rather than from resident or recruited phagocytic cells (Maus *et al.*, 2004). All these findings indicate a major role of PLY in the modulation of inflammatory reactions during infection with *S. pneumoniae*. However, the exact mechanism by which the toxin promotes pneumococcal virulence is not fully understood.

1.2.3 Comparison of listeriolysin O and pneumolysin

The comparison of the DNA and amino acid sequences of LLO and PLY with the EMBOSS Matcher tool (http://www.ebi.ac.uk/Tools/psa/emboss_matcher/) results in 56% shared identity on the genetic level and 43% shared identity and 67% similarity between the two proteins. For this purpose the signal peptide and PEST sequence of LLO were disregarded, as PLY is missing both (see figure 1.2.3).

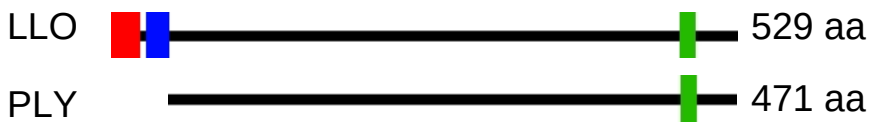

Fig. 1.2.3 Motifs found in the amino acid sequences of LLO and PLY. LLO has two N-terminal motifs, the signal peptide (aa 1-24, red) and the PEST sequence (aa 32-50, blue). The undecapeptide (aa 482-493, green) is found on the C-terminal end of the protein. PLY contains only the C-terminally located undecapeptide (aa 426-437, green).

While the sequences are quite similar there are differences in the way the toxins are deployed during infection. The signal peptide of LLO mediates its active secretion into the extracellular space while PLY, for its lack of a signal peptide, is mainly released by lysed bacteria. As described before, LLO is highly adapted to the

phagolysosomal environment; the increased stability under acidic conditions and the PEST sequence are unique traits among the members of the CDC family. Besides these differences the activation through reducing agents, cholesterol dependence and mechanism of pore formation are shared by the both toxins.

1.3 Objective

The pore forming protein toxins LLO and PLY of *Listeria monocytogenes* and *Streptococcus pneumoniae* are indispensable for establishing infections in the human host. This study focused on the toxins known ability to disturb the cellular Ca^{2+} homeostasis at sublytic concentrations (Stringaris *et al.*, 2002; Repp *et al.*, 2002) and the subsequent effects on epithelial cells.

In the case of *L. monocytogenes* a successful invasion of the host starts with crossing of the epithelial barrier in the small intestine. The pathway by which Listeria reaches its cellular receptor, E-Cadherin, to induce its uptake into epithelial cells is not entirely understood. In healthy tissue E-Cadherin is protected by tight junctions. Current models support the idea that the bacteria overcome this obstacle by attacking at sites of cell extrusions (Pentecost *et al.*, 2006). The first part of this work dealt with the ability of purified LLO to induce disturbances in cellular Ca^{2+} homeostasis and hence its ability to interfere with size and volume of cells in closed epithelial monolayers to make E-Cadherin available. Furthermore, LLO mutants with selected amino acid substitutions were tested on their haemolytic activity and their ability to induce an influx of extracellular Ca^{2+} and thereby trigger a loss in cell volume.

S. pneumoniae induced lung damage and bacterial invasion of the blood stream and the central nervous system are detrimental to patients. The second part of this work was aimed to elucidate the effects of PLY on alveolar epithelial cells. It was examined whether purified PLY alone is able to impair alveolar epithelial integrity by increasing intracellular Ca^{2+} concentrations and the connected loss of cell volume. Furthermore, it was tested whether PLY could trigger the release of Ca^{2+} ions from intracellular stores and whether this is dependent on cellular ion channels. The way cells reacted to the toxin was compared to cells suffering hypertonic stress and it was tried to block the associated loss in cell volume and barrier integrity with inhibitors of Ca^{2+} channels and kinases.

2 Materials and Methods

Glass pipettes and flasks, microcentrifuge tubes (1.5 ml) und pipette tips were autoclaved (121℃, 20 min) or heat sterilized at 180℃ for 4h. Media and solutions were prepared using H_2O from water purification systems (U>18 mΩ; mQH_2O). Sterile media and solutions for cell culture applications were either autoclaved or sterile filtered (filter cut-off 0.22 µm). All concentrations for media and solutions are given as final concentrations.

2.1 Equipment and consumables

Table 2.1 List of the equipment and consumables used.

Item	Manufacturer
General use	
Analytical balance	Mettler, Kern
Autoclave	Getinge
Centrifuges	Eppendorf Centrifuge 5415D
	Heraeus Biofuge 15
	Heraeus Megafuge 1.0 R
	Merck Gelaxy Mini
Combitips 5 ml	Eppendorf
Cryovials	Sarstedt
Disposable scalpels	Feather
Disposable syringes	Braun
Electric pipette aid	Integra
Examination gloves	Ansell
Freezer (-20℃)	Bosch, Liebherr
Freezer (-80℃)	Heraeus
Fridge (4℃)	Bosch, Elektrolux, Liebherr
Glassware	Schott
Incubator	Heraeus
Light microscope	Wilovert
Magnetic stirrer	IKA
Microcentrifuge tubes 1.5 ml	Roth
Microliter pipettes	Gilson, Biohit, Eppendorf
Microwave	AEG
Multipipette	Biohit, Eppendorf
Paper towels (lintless)	Kimberly-Clark
Parafilm	Pechiney Plastic Packaging
pH-Meter	Knick (Electrode Nordantec)
Pipette tips	MBT Brand
Pipette tips (with filter)	Nerbe
Plastic tubes 50 ml, 15 ml	Greiner Bio-One
Sterile filter (0.22 µm)	Millex
Sterile work bench	Heraeus, Nuaire
Thermomixer	Eppendorf
Vortex mixer	VWR, IKA, Scientific Industries
Water purification system	TKA, Milipore

Item	Manufacturer
Bacterial culture	
CO_2-incubator	Labotect
96-well heated shaking photometer	Tecan
8-channel pipette	Biozym
Shaking incubator	Infors
96-well plates flat bottom	Greiner
Inoculating loops	Nunc
Photometer	Thermo Fisher Scientific, GeneQuant
Cuvettes	Ratiolab
Petri dishes (13.5 cm)	Greiner
Calcium measurements	
CCD camera	TILL Photonics
Software	TILL Photonics
Dichroic filter	Olympus
Emission filters	Olympus
Inverse light microscope	Olympus
Monochromator	TILL Photonics
Xenon arc lamp	TILL Photonics
Cover slips	Menzel
Cover slip incubation chamber	self-made by the Institute of Physiology, JLU Gießen
Cell culture	
Water bath	Grant
CO_2-incubator	Thermo Forma
Freezing chamber for eukaryotic cells	Nalgene
Inverted light microscope	Hund
Tissue culture dishes	Becton Dickinson
Multiwell tissue culture plates	Becton Dickinson
Disposable pipettes	Greiner Bio-One
Immunofluorescence	
Confocal microscope	Leica
Cover slips	R. Langenbrinck
Glass slides	R. Langenbrinck

2.2 Chemicals, inhibitors and media

Table 2.2 List of the chemicals, inhibitors and media used.

Item	Manufacturer
General use	
4-(2-hydroxyethyl)-1-piperazineethanesulfonic acid (HEPES)	Serva
Dimethyl sulfoxide (DMSO)	Merck
Dithiothreitol (DTT)	Serva
Ethanol	Sigma-Aldrich
Glucose	Merck
Hanks´ Salt Solution	Biochrom AG

Item	Manufacturer
Hydrochloric acid	Merck
LLO	Product of the Institute
Magnesium chloride	Merck
Magnesium sulfate	Merck
Methanol	Fluka
Monopotassium phosphate	Merck
Phosphate buffered saline (PBS)	Biochrom AG
PLY	Product of the Institute
Potassium chloride	Merck
RNase-free water	Thermo Scientific
Sodium chloride	Roth
Sodium hydroxide	Roth
Sorbitol	Merck
Bacterial culture	
Brain heart infusion (BHI)	Difco
Gentamicin	Invitrogen
Glycerol	Merck
Calcium measurements	
Ethylene glycol tetraacetic acid (EGTA)	Sigma-Aldrich
(1-(2-(5-Carboxyoxazol-2-yl)-6-aminobenzofuran-5-oxy)-2-(-2´-amino-5´methylphenoxy)-ethan-N,N,N´,N´-tetraacetate (Fura-2-AM)	Invitrogen
Ionomycin	Sigma-Aldrich
Ryanodine	Enzo Life Sciences
Thapsigargin	Sigma-Aldrich
Xestospongin C	Enzo Life Sciences
Cell culture	
Fetal bovine serum (FBS)	PAA Laboratories
MEM medium	Invitrogen
Non essential amino acids (NEA)	Biochrom AG
RPMI 1640 medium	Invitrogen
Isopropanol	Fluka
Trypsin	PAA Laboratories
Immunofluorescence	
Bovine serum albumin (BSA)	Sigma-Aldrich
Formaldehyde	Merck
ProLong Gold Antifade with 4',6-diamidino-2-phenylindole (DAPI)	Invitrogen
Triton X-100	Serva

2.3 Handling of bacteria

The bacterial strain used for this work was *Listeria monocytogenes* EGDe serotype 1/2a (Glaser *et al.*, 2001). Bacteria were handled exclusively under a sterile work bench. Sterile buffers, media, solutions, glass ware and reaction vessels were used while working with bacteria.

2.3.1 Media and solutions for bacteria

BHI medium:	3.7% (w/v) BHI in sterile mQH_2O
BHI solution for agar plates:	BHI medium 1.5% (w/v) Agar
10x PBS:	27 mM KCl 1.4 M NaCl 81 mM Na_2HPO_4 15 mM KH_2PO_4 pH 7.4 (adjusted with HCl)

2.3.2 Growing of bacterial cultures

Initial cultures were generated by inoculating 10 ml BHI medium with one bacterial colony. The cultures were then incubated overnight at 37℃ with a shaking speed of 180 rpm. Bacteria were prepared for long-term storage by mixing 750 µl of an overnight culture with 750 µl of 60% (v/v) glycerol in BHI in a cryovial. They could be stored for several years at -80℃ un this way. For short term storage, bacteria from an overnight culture or a cryovial were plated out on BHI agar plates that were then incubated overnight at 37℃. The bacteria grown on agar plates could be stored for up to eight weeks at 4℃.

2.3.3 Preparation of bacterial cultures for infection experiments

The overnight grown bacterial culture was diluted 1:50 in fresh BHI medium. This new culture was incubated for approximately 2 h at 37℃ and shaking at 180 rpm until it reached the middle of its exponential growth phase (=OD value between 0.4 and 0.8). For infection experiments, it was necessary to reproducibly achieve a multiplicity of infection (MOI = ratio of bacteria to eukaryotic cells) of 10, meaning that for each cell there should be ten bacteria to infect it. It was possible to determine the amount of bacteria (or colony forming units, CFU) in each ml of liquid culture with a previously established growth curve for *L. monocytogenes* (growth curve by Juri Schlarenko). Thus, the OD value of a culture in mid-exponential growth could be converted into the number of CFU/ml. When the amount of cells to be infected was known the calculated volume of liquid culture was pipetted into a microcentrifuge tube (1.5 ml) and spun down [13000 rpm, 1 min, room temperature (RT), Eppendorf 5415D centrifuge]. The bacterial pellet was then taken up in 1x PBS, resuspended and spun down again (13000 rpm, 1 min, RT). The bacteria were finally resuspended in FBS-free MEM medium, vortexed and added to the cells.

2.3.4 Establishing bacterial growth curves

Growth curves of *L. monocytogenes* in different media and with different concentrations of $LaCl_3$ were established by using a plate reader capable of incubating and shaking 96-well flat bottom plates for several hours. 180 µl of medium and 10 µl of sterile filtered $LaCl_3$ dilutions were pipetted onto the plate before 10 µl of an overnight bacterial culture were added to yield a total volume of 200 µl in each well. Sterile BHI medium was added to control wells instead of overnight culture for background correction. All $LaCl_3$ concentrations used were measured on the same plate without bacteria to correct for the precipitate formation in medium containing higher amounts of the inhibitor. The plates were then transferred into the plate reader (Tecan) and the OD at 600 nm was measured every 20 min for 10h under constant shaking (200 rpm) and temperature control (37℃). A ll samples were measured as triplicates on each plate and each experiment was repeated at least three times independently. The results of all replicates were used to calculate the mean values and standard errors.

2.4 Handling of eukaryotic cells

The cell lines used in this work were H441, a human lung adenocarcinoma epithelial cell line (ATCC, order nr. HTB-174) and Caco-2, a human colorectal adenocarcinoma epithelial cell line (ATCC, order nr. HTB-37). Eukaryotic cells were handled routinely in a clean room under a sterile work bench. Sterile buffers, media, solutions, glass ware, reaction vessels and consumables were used while working with eukaryotic cells.

2.4.1 Media and solutions for eukaryotic cells

MEM:	Minimal essential medium (Eagle) with Earle's Salts, 6.0 g/l D-glucose, L-glutamine
RPMI 1640:	RPMI 1640 with 4.5 g/l D-glucoseand L-glutamine
FBS:	100% foetal calf serum; inactivated at 56℃ for 30 min
NEA:	100x non essential amino acids
Hanks´ Salt Solution:	1x Hanks´ Salt Solution; w/o Ca^{2+}, Mg^{2+}; w/o Phenol red

PBS:	1x PBS; w/o Ca^{2+}, Mg^{2+}
Trypsin/EDTA:	1x trypsin/EDTA; 0.05% / 0.02% in D-PBS
Freezing medium:	90% FBS, 10% DMSO
HEPES medium:	1.2 mM KH_2PO_4 2.6 mM KCl 2.25 mM $MgSO_4$ 1.2 mM NaCl 25 mM HEPES pH 7.4 at 37°C (adjusted with NaOH) 2.5 mM Glucose (sterile filtered) 1.3 mM $CaCl_2$ (sterile filtered)
Hyperosmotic RPMI 1640 medium:	70% RPMI 1640 30% 1 M Sorbitol in mQH_2O, sterile filtered

2.4.2 Cultivation of eukaryotic cells

Cells were generally kept in 10cm dishes filled with cell culture medium at 37°C in an atmosphere of 5% CO_2. The media used were RPMI 1640 for H441 cells and MEM for Caco-2 cells. If not stated differently, FBS was added to both media at a concentration of 10% (v/v). MEM medium was also supplied with 1% NEA (v/v).

Cells were split every two to three days when reaching confluence. For splitting the medium was removed completely and the cells were washed twice with 4 ml of 1x Hanks´ Salt Solution. To remove the adherent cells from the bottom of the dishes they were incubated with 1.5 ml trypsin at 37°C in a CO_2-incubator until they were detached from the culture dish. The plates were also tapped gently to completely detach all cells. The enzymatic reaction of trypsin was stopped by adding 1.5 ml of medium containing 10% FBS. Detached cells were resuspended and distributed in the required dilutions onto new cell culture dishes containing fresh medium. The total volume of medium in each 10 cm dish was 10 ml.

For storage detached cells were carried over into 15 ml tubes and centrifuged (1200 rpm, 2 min, RT, Heraeus Megafuge 1.0 R centrifuge). The cell pellets were resuspended in freezing medium and transferred into cryovials. The cryovials were then placed in an isopropanol-filled freezing chamber that assured a cooling rate of 1°C/min. This chamber was then placed in a -80°C fr eezer overnight. Afterwards the cryovials were either kept at -80°C or in liquid ni trogen for long-term storage.

To reuse frozen cells from cryovials, they were thawed at 37°C, pipetted on a cell culture dish and mixed gently with 9 ml of fresh medium. To completely remove

DMSO, which is toxic to the cells, the medium was exchanged again after the cells had attached to the bottom of the dish.

2.4.3 Preparing eukaryotic cells for calcium measurements and immunofluorescence.

H441 and Caco-2 cells were seeded three to five days before experiments. Adherent cells in 10 cm dishes were detached using trypsin as described in chapter 2.4.2. Resuspended cells were mixed with fresh medium and distributed in 6-well tissue culture plates for calcium measurements and 24-well tissue culture plates for immunofluorescence experiments. The wells of the plates had been previously equipped with one sterile cover slip in each well. The total volume of medium per well was 2 ml in 6-well plates and 0.5 ml in 24-well plates. The plates were then incubated at 37°C in an atmosphere of 5% CO_2 until the cells had grown to 50-80% confluence. On the day of the experiment, the old medium was completely removed and fresh medium was added to the cells, which were then kept at 37°C and 5% CO_2 for 1 h. After this time the medium was completely removed again and the cells were washed five times with prewarmed (37°C) 1x Hanks' Salt Sol ution. The cells were then kept in fresh medium without FBS (in case of MEM also without NEA) for 2 h at 37°C and 5% CO_2. After this time they were ready to be used for calcium measurements and immunofluorescence.

2.4.4 Preparing eukaryotic cells for infection assays

Caco-2 cells were seeded two to three days before experiments. Adherent cells in 10cm dishes were detached as described in chapter 2.4.2. Resuspended cells were mixed with fresh medium and equally distributed in 24-well tissue culture plates to yield a total volume of 0.5 ml per well. The plates were then incubated at 37°C in an atmosphere of 5% CO_2 until the cells had grown to full confluence. Care was taken to avoid overgrowing, as Caco-2 cells tend to grow in multiple layers when cultured too long or seeded too dense. On the day of the experiment, the old medium was completely removed and fresh medium was added to the cells, which were then kept at 37°C and 5% CO_2 for 1 h. The medium was completely removed again and the cells were washed carefully three times with prewarmed (37°C) 1x Hanks' Salt Solution. The cells were then kept in fresh medium without FBS for 2 h at 37°C and 5% CO_2. After this time they were ready to be used for infection assays.

2.5 Measuring the intracellular calcium concentration and total area covered by cells

A video imaging system for fluorescence microscopy was used to measure the changes in intracellular calcium concentrations. The experimental setup allowed the simultaneous recording of the total surface area covered by cells. All calcium measurements were performed in the Calcium Lab (Institute of Physiology, JLU Gießen), where the required equipment was kindly provided for this work.

All solutions, including toxins, inhibitors and other reagents, added during calcium measurements were diluted in HEPES medium to a final volume of 100 µl per administration and were carefully pipetted into the medium-filled chamber. This was necessary to assure adequate mixing while avoiding any movement of the coverslip during measurements.

2.5.1 Video imaging system for fluorescence microscopy

The basis for measuring the intracellular calcium concentration and total cell surface area was fluorescence microscopy. The light was generated by a xenon arc lamp and the required wavelengths were selected by a monochromator. From there the light was directed through a dichroic mirror and an object lens onto cells that were previously loaded with a fluorescent dye. The fluorescent light emitted by the cells was directed through the same object lens and dichroic mirror and an emission filter to a digital camera that was connected to a computer. The data generated were interpreted using the TILL Photonics-Software. The fluorescence dye used was Fura-2-AM, an acetoxymethyl (AM) ester that is able to permeate the cell membrane and accumulate in the cytoplasm. Here, the AM groups are cleaved off by endogenous esterases and Fura-2, being a charged molecule, can not leave through the membrane again. Fura-2 is excited at wavelengths of 340 and 380 nm, depending on the presence of free Ca^{2+} ions. Calcium-saturated Fura-2 is excited at 340 nm calcium-free Fura-2 at 380 nm. Its emission maximum lies at 510 nm. Changes in intracellular calcium concentrations were recorded by the software as changes in the ratio of 340/380 nm. The data collected from these experiments were either shown as percentage of the maximum possible signal induced by giving 5 µM Ionomycin or as fold change in arbitrary fluorescence of the 340/380 nm ratio.

2.5.2 Measuring intracellular calcium concentrations

Cells were prepared for calcium measurements as described in chapter 2.4.3. For the experiments, they were loaded with 5 µM Fura-2 AM, incubated for 40 min at 37℃ and 5% CO_2 and then placed in microscopy chambers with 1 ml of HEPES medium. When Ca^{2+}-free conditions were required the HEPES medium used was prepared without $CaCl_2$. Before treating cells as described they were monitored for 10 min in order to get a baseline for the 340/380 nm ratio.

The toxins used were prediluted to concentrations between 10 and 100 ng/ml. It is known that proteins in highly diluted solutions bind to the wall of microcentrifuge tubes and are not available at the desired concentrations. Therefore, bovine serum albumin was added at a concentration of 0.1% to the prediluted solutions to avoid this loss of toxin. When the toxins were activated in reducing conditions they were preincubated with 5 mM DTT for 10 min at RT. Activated toxins were stored at -20℃ and could be used for several weeks.

2.5.3 Measuring the total area covered by cells

The fluorescence microscopy equipment used recorded images in grey scale that could be used for the evaluation of the total surface area covered by cells. For doing so, a small space within the recorded images that was not covered by cells was set as a background marker. Once the background was defined the software could mark each pixel of the images as “0” (not covered by cells) or “1” (cells). The amount of pixels standing for cell-covered areas in each acquired image was used to measure the change in the total surface covered by cells. This was expressed as percentage of “1”-pixels in cells at rest before any treatment was started.

2.6 Infection assay

Cells were prepared for infection assays as described in chapter 2.4.4. $LaCl_3$ was added at indicated concentrations 10 min before the bacteria and was in the medium throughout the infection. The bacteria used were prepared as described in chapter 2.3.3 and were added to the cells. After careful swivelling the cell culture plates were incubated for 1 h at 37℃ and 5% CO_2. The supernatant was removed and pipetted into microcentrifuge tubes. The cells were then carefully washed three times with 1x Hanks´ Salt Solution and incubated for 30 min with FBS-free medium containing 50 µg/ml Gentamicin to inactivate the remaining extracellular bacteria. Gentamicin is not

cell permeable at the concentration used and therefore did not act on intracellular bacteria. The cells were then washed carefully three times with 1x Hanks´ Salt Solution to completely remove Gentamicin and lysed in 0.5 ml of cold (4℃) 0.2% (v/v) Triton X-100-containing H_2O for 20 min at RT. The bacteria in the cell lysates were diluted in 1x PBS and plated out on BHI agar plates. The plates were incubated overnight at 37℃ and the colonies were counted on the next day.

2.7 Bacterial survival assay

The bacteria were prepared as described in chapter 2.3.3. The bacterial numbers used were calculated from the mean amount of CFUs used for the infection assays. Bacteria were pipetted into microcentrifuge tubes containing 0.5 ml HEPES medium with the indicated concentrations of $LaCl_3$. After being shortly vortexed the microcentrifuge tubes were incubated for 1 h at 37°C and 5% CO_2. The bacteria were then diluted in 1x PBS and plated out on BHI agar plates. The plates were incubated overnight at 37℃ and the colonies were counted on the next day.

2.8 Immunofluorescence

This method employs antibodies coupled with fluorescent markers to visualize proteins within cells. E-Cadherin was visualized directly using an Alexa®488-coupled anti-E-Cadherin antibody (Cell Signalling), while NFAT5 was detected using an anti-NFAT5 primary antibody (from rabbit, Thermo Scientific) in combination with an anti-rabbit Alexa®555-coupled secondary antibody (Cell Signalling).

Cells were prepared as described in chapter 2.4.3. PLY was activated before being added to the cells as described in chapter 2.5.2. The cells were treated as indicated in the specific experiments. When comparing the effects of PLY to those of hyperosmotic stress, the medium was changed again right before the start of the experiment. Control cells and cells to be treated with the toxin received fresh medium without FBS while the medium for the hyperosmotic group was also FBS-free but additionally contained Sorbitol to increase the osmolality to 500 mOsm/kg H_2O. The toxin was administered immediately after the medium change.

The cells were then incubated for the indicated times. After the incubation period the medium was completely removed and the cells were fixed with 500 µl of 3.7% formaldehyde (v/v) in 1x PBS for 10 min at RT. Fixed cells could be stored in 1x PBS overnight at 4℃. The coverslips were carefully washed three times in 1x PBS and

permeabilized with either 0.2% Triton X-100 (v/v) in 1x PBS at RT or with ice-cold 100% methanol at -20℃, both for 5 min, depending on the recommendation of the antibody manufacturer. The cover slips were washed carefully three times in 1x PBS and incubated in 500 µl of blocking buffer [1% BSA and 0.3% Triton X-100 (v/v) in 1X PBS] for 1 h at RT. In the meantime, an incubation chamber was lined with a wet sheet of 3MM-Whatman paper covered with a layer of Parafilm. Antibodies were diluted in blocking buffer as described by the manufacturer (anti-E-Cadherin 1:1000 and anti-NFAT5 1:2000). Then 5 µl of the diluted antibodies were pipetted on the Parafilm sheet and the blocked cover slips were placed on the droplets with the cells facing down. The incubation chamber was closed with a lid and incubated protected from light at 4℃ overnight. 2 h of incubation with a secondary antibody were necessary for indirect labelling. To remove the primary antibody, the cover slips were washed three times in 1x PBS. The incubation with anti-rabbit secondary antibody (dilution 1:1000) was carried out as described for primary antibodies, only this time at 37℃. During the incubation period glass slides were labelled and prepared with 3 µl of ProLong Gold Antifade with DAPI for each cover slip. DAPI (4',6-diamidino-2-phenylindole) is a fluorescent stain that binds strongly to A-T rich regions in DNA and is therefore used to label nuclei in fluorescence microscopy. Finally the cover slips were washed three times in 1x PBS, carefully dried of excess liquid and placed on the ProLong droplets with the cells facing down. The glass slides were kept in the dark at 4℃ for 24 h to allow the antifade reagent to dry and were then viewed under the confocal microscope.

2.9 Purification of Listeriolysin O and Pneumolysin

Both toxins were purified and measured for their haemolytic activity by Martin Hudel in the Institute of Medical Microbiology, Justus-Liebig-University Gießen. The haemolytic activity was determined with a haemolytic titer assay under reducing conditions, using a serial dilution of the toxin in question. One haemolytic unit (HU) is defined as the amount of toxin needed to lyse 50 % of red blood cells in a 0.1 % solution of sheep erythrocytes.

2.9.1 Listeriolysin O

Listeria innocua strain NCTC 11288 was transformed with a pERL3 plasmid construct containing the structural genes *hly*, encoding LLO, and *prfA*, encoding the regulator

protein (Leimeister-Wächter and Chakraborty, 1989). The transformed bacteria were grown in minimal medium for several hours and the supernatant was subsequently concentrated using a filtration apparatus with a cut-off point of 10 kDa. Further purification was achieved by batch absorption of contaminants with Q-Sepharose and sterile filtration. The final step was the loading of the pre-filtered supernatant on a Mono-S HR5/5 column and the elution of retained material with a linear gradient of NaCl. The eluted fractions were tested for their haemolytic activity and finally dialysed against PBS (Darji *et al.*, 1995).

The used fraction of purified LLO had 1.0 x 10^7 HU/mg. In experiments with Caco-2 cells loaded with Fura-2 it was determined that at a concentration of 250ng/ml of LLO+DTT (= 2.5 x 10^6 HU) had the same effect as the treatment with 5 µM Ionomycin, indicating immediate lysis of the cells.

2.9.2 Pneumolysin

A pIMK2 vector construct containing the gene encoding for pneumolysin, a His-tag and the signal peptide sequence from the *hly* gene was generated by Dr. Silke Silva in an unpublished recombinant strain. This vector was integrated into the chromosome of Listeria innocua strain NCTC 11288. After several hours of growth in minimal medium the supernatant was separated from the bacteria by centrifugation. It was concentrated using a filtration apparatus with a cut-off point of 10 kDa and subsequently batch loaded on a His-Trap column. After washing the retained material was eluted with imidazole, which was dialysed out against PBS. Finally the eluted fractions were tested for their haemolytic activity.

The used fraction of purified PLY had 3.73 x 10^6 HU/mg. The lytic concentration of PLY on H441 cells was not determined as the toxin was only used in sublytic amounts in this work. It can be estimated by assuming that the same amount of HU of PLY should have similarly drastic effects on H441 cells as 2.5 x 10^6 HU of LLO+DTT had on Caco-2 cells. That would amount to a lytic concentration of 670ng of PLY+DTT. This must be considered as a rough approximation as the tolerance to LLO and PLY might differ between cell lines.

2.10 Crystal structure of LLO and target selection for mutations

The highly purified and concentrated LLO produced in the Institute of Medical Microbiology was used by Stefan Köster and Özkan Yildiz from the Department of Structural Biology of the Max Planck Institute for Biophysics to resolve the crystal structure of the toxin (Köster, 2010). The data generated were jointly analyzed in both institutes. The alignment of the single LLO molecules in the crystals was similar to toxin oligomerization on the surface of cholesterol containing membranes. This circumstance allowed a novel insight into the assembly of toxin pores. In the crystal structures, the neighbouring LLO molecules had several contact points in domain 1. Especially the first 50 amino acids were in close proximity to the next toxin monomer. This area contains the PEST sequence that was found to be crucial for *L. monocytogenes* virulence (Decatur and Portnoy, 2000; Lety *et al.*, 2001). These results led to the generation of several novel LLO mutants that were predicted to disrupt interacting interfaces, and hence LLO activity, in the 3D model.

The crystal structure showed interactions between amino acids 39-43 with the residues S176, N179, N180 and N183 of the neighbouring toxin molecules. Therefore, mutants were designed carrying residues with opposite charges or much larger side chains to induce sterical hindrances at these allegedly important sites for oligomerization. In other mutants a permanent phosphorylation was simulated by exchanging serine for aspartic acid and glutamic acid. Furthermore, one polar and one acidic side chain were swapped for a large hydrophobic one to find out whether they have a specific function. As other members of the CDC family lack the N-terminal PEST motive it was tested for its importance in LLO by deleting the first 51 amino acids in one mutant. Mutants having a combination of changes within the N-terminal region and substitutions in amino acids 175 and 176 were established to further investigate interactions between these sites during pore formation.

2.10.1 Generation, expression and purification of LLO mutants

The LLO mutants used in this work were generated, expressed and purified by Stefan Köster in the Department of Structural Biology of the Max Planck Institute for Biophysics in Frankfurt am Main.

For the generation of LLO mutants with amino acid substitutions and deletions the QuikChange kit from Stratagene (Agilent Technologies, Waldbronn) was used. Following the instructions from the kit a set of two mutagenesis primers containing

the changed amino acid sequence was synthesized for each *hly* mutant. For deleting parts of the *hly* gene the primers were designed to bind upstream in sense direction and downstream in antisense direction of the region to be deleted. The mutated *hly* genes were cloned into a pET16b plasmid, which was introduced into competent *E. coli* cells. Transformed bacteria were grown in media containing selective antibiotics and expression was induced with 1 mM isopropyl β-D-1-thiogalactopyranoside at 30℃ for four hours. The cells were then pelletised , lysed and centrifuged to remove all debris. For purification of the His-tagged proteins the supernatant was loaded on a Ni-NTA column. After washing the proteins were eluted by cleaving off the His-tag with thrombin. The eluates were concentrated using a 30 kDa cut-off and then afterwards loaded on a Superdex200 gel filtration column. The toxin-containing fractions were finally concentrated to 5 mg/ml and stored at -80℃.

2.11 Statistical Analysis

The data were calculated and represented as mean value +/- standard error of the mean (SEM) from *n* experiments using independent preparations. For infection and bacterial survival assays the statistical analysis toolkit included in the Microsoft Office Excel 2003 software package was used to test variances between experimental groups and subsequently run the appropriate t-tests. The “F-test two sample for variances” tool was used to test for equality of variances. If $p > 0.1$, the variances were treated as equal and if $p < 0.1$, as unequal. In case of equal variances the student’s t-test (“t-Test: Two-Sample Assuming Equal Variances”) was used to check for significant differences between the groups. The Welch test (“t-Test: Two-Sample Assuming Unequal Variances”) was used when unequal variances were found. For comparing curves of calcium and area measurements the linear mixed model tool from the SPSS software package was used. For all statistical operations p-values < 0.05 were considered significant.

3 Results

3.1 Sublytic concentrations of Listeriolysin O disturb cellular calcium homeostasis, weaken epithelial monolayers and enable the effective invasion of *L. monocytogenes*

Listeriolysin O has long been identified as the major virulence factor of *L. monocytogenes* (Goebel *et al.*, 1988). Its known function in the intracellular life cycle of the pathogen is to mediate the escape from phagosomes, thereby allowing movement within and between host cells without immune recognition (Gedde *et al.*, 2000). In 2002, Repp *et al.* discovered that LLO pore formation in the plasma membrane leads to a direct influx of Ca^{2+} ions from the extracellular space (Repp *et al.*, 2002). This would explain most of the immunomodulatory effects of LLO on host cells that are dependent on Ca^{2+}-signaling (Tang *et al.*, 1996; Nishibori *et al.*, 1996; Kayal *et al.*, 1999). Recent studies revealed a connection between the deregulation of intracellular Ca^{2+} concentration ($[Ca^{2+}]_i$) by LLO and the activation of calcium-dependent kinases like PKC (Wadsworth and Goldfine, 2002; Shaughnessy *et al.*, 2007; Richter *et al.*, 2009). The recruitment and phosphorylation of PKC has direct effects on the actin cytoskeleton and the regulation of tight junctions (Larsson, 2006; Stuart and Nigam, 1995; Tsukamoto and Nigam, 1999). The ability of purified LLO to damage epithelial barriers in the gut was described with regard to fluid loss due to uncontrolled ion efflux in diarrhoea (Richter *et al.*, 2009). Its effect on invasiveness in connection to Ca^{2+}-permeable pores has been briefly addressed by Dramsi and Cossart in 2003 (Dramsi and Cossart, 2003).

The connection between Ca^{2+}-dependent changes in cell morphology, junctional constitution and invasion of epithelial monolayers by *L. monocytogenes* is still unknown. Therefore, the following experiments aimed to elucidate LLO's role in the early stages of Listeria infection.

3.1.1 Purified LLO triggers an increase in $[Ca^{2+}]_i$ in Caco-2 cells

To test the effect of toxins from Gram-positive bacteria on epithelial cells, it was of great importance to ensure that no contaminations of lipopolysaccharides (LPS) were present. Epithelial cells are very sensitive to trace amounts of endotoxin and react in a manner indistinguishable from effects produced by CDCs (Allen, 1965; Shen *et al.*, 1989; Yamada *et al.*, 1981; Raichvarg *et al.*, 1982). The expression and purification

of recombinant LLO was done following an established protocol (Darji *et al.*, 1995) in the non-pathogenic species *Listeria innocua* with some adjustments towards better yield and purity (see section 2.9.1 in Materials and Methods). The purified toxin was tested for protein concentration and lytic activity before employing it in cell culture experiments. LLO expression, purification, the protein concentration and activity assays were performed by Martina Hudel. All experiments were conducted with toxin from the same batch in order to ensure reproducibility.

To measure the impact of LLO on epithelial barriers, Caco-2 cells were grown on glass coverslips to about 80% confluence. Fully closed monolayers could not be used, as small patches of free, non-cell covered surface were required for the determination of changes in the total cell covered area. Cells were loaded with Fura-2 AM, incubated for 40 minutes and then placed in microscopy chambers in HEPES medium. Before treating cells as described, they were monitored for ten minutes in order to obtain a baseline for the 340/380 nm ratio. At the end of the experiments, the ionophore Ionomycin (Iono) was added to a final concentration of 5 µM to perforate the plasma membrane and allow for free exchange of Ca^{2+} ions with the medium. This was necessary to set a maximum signal, representing the equilibrium of $[Ca^{2+}]_i$ with the concentration in the medium. The amount of calcium influx after LLO-treatment was calculated as percentage of the maximum signal. In this way, it was possible to compare experiments and eliminate variations from cell status, optical equipment, light source and different batches of the calcium indicator.

When treated with LLO, each single cell measured reacted differently. Figure 3.1.1 shows the change in 340/380 nm ratio of four selected cells to illustrate recorded variations between single cells. To produce comparable results, at least 30 cells were measured in each experiment. Thereafter, the mean value of all cells for each time point was calculated. When experiments were repeated, the single mean values were again used to calculate a collective mean value and SEM (if n = 3, at least 90 individual cells were measured).

Different concentrations of LLO caused dose dependent reactions of the cells. 1000 ng/ml of toxin triggered an increase in $[Ca^{2+}]_i$ of about 50% maximum, cells treated with 500 ng/ml raised the $[Ca^{2+}]_i$ by 20% and 250 ng/ml to about 5% of the maximum. When LLO was heat inactivated at 65°C for 5 minutes, the cells did not react to it while responding normally to Iono at the end of the experiment.

A)

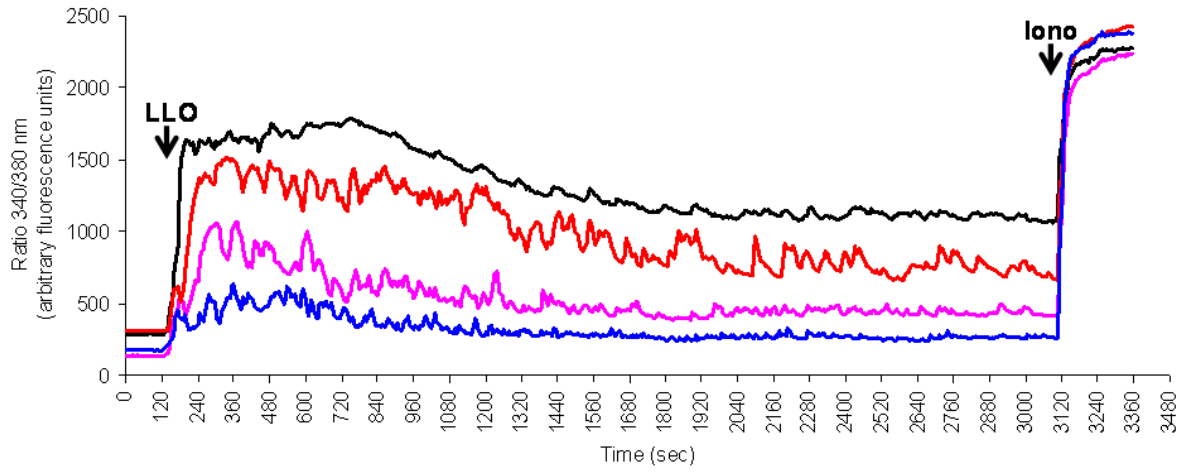

B)

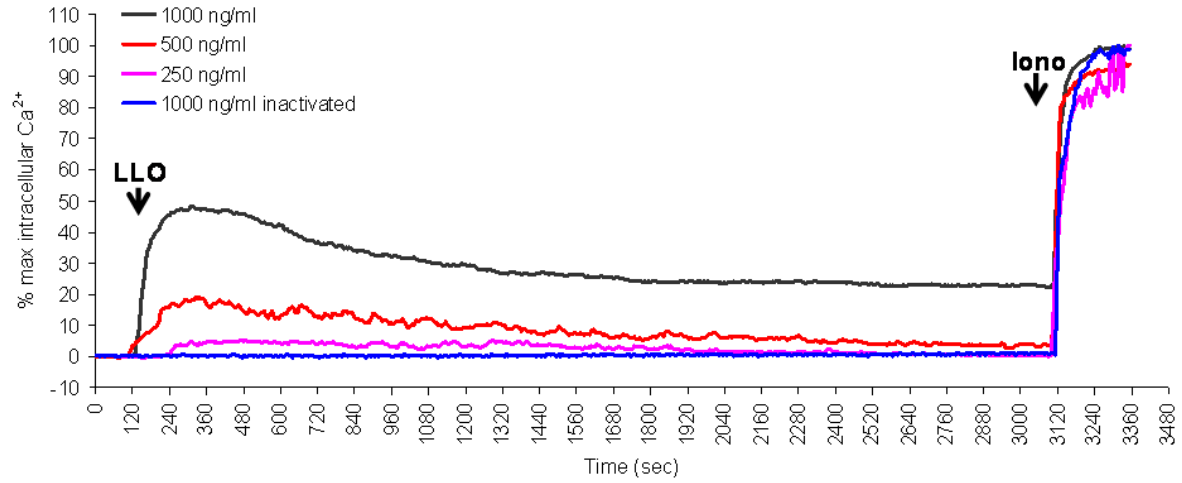

Fig 3.1.1 Individual cells respond differently to incubation with LLO while the average $[Ca^{2+}]_i$ of >30 cells reacts in a dose-dependent manner when treated with increasing toxin concentrations. Caco-2 cells were loaded with Fura-2 AM and monitored for changes in the emission at 340 and 380 nm when excited at 510 nm. The 340/380 nm ratio was calculated from the emission readings. The maximum signal measured after adding Iono (5 µM) at the end of the experiment was used to express the relative change in $[Ca^{2+}]_i$. LLO was added at indicated concentrations and cells were measured for 50 min before Iono was added.
A) Each line shows the changes in $[Ca^{2+}]_i$ in an individual cell during the same experiment. The four depicted cells were chosen to represent the whole spectrum of reactions that could be observed when cells were treated with 1000 ng/ml LLO.
B) To compare the effects of the different toxin concentrations, all values are given in % maximum $[Ca^{2+}]_i$. The experiments consisted of at least 30 cells each. The results are shown as mean values of all measured cells.

3.1.2 The activity of LLO is markedly increased after exposure to reducing conditions

The family of CDCs was at first named thiol activated cytolysins. This term came up due to the observation that oxidizing conditions reversibly inactivated them. When incubated with cysteine or hydrogen sulphate, the activity could be restored (Cohen *et al.*, 1937). The addition of the reducing agent DTT was found to increase not only the activity of purified toxin, but also to enhance the cytotoxicity of *L. monocytogenes* on cell lines (Westbrook and Bhunia, 2000). It is speculated that the reduction of the thiol group of the single cysteine found in LLO is responsible for this effect.

A direct comparison of the percentage of maximum $[Ca^{2+}]_i$ increase triggered by toxin with and without DTT (5 mM) preincubation revealed a considerable gain in activity under reducing conditions (Figure 3.1.2). The amount of LLO used for a 50% maximum change in $[Ca^{2+}]_i$ could be reduced from 1000 ng/ml to 20 ng/ml when preincubated with DTT, allowing for a more economical use of the toxin and a closer resemblance to conditions likely present inside the host GI tract during an infection with *L. monocytogenes*. This concentration is also well below the lytic concentration of 400 ng/ml of LLO+DTT that was found by Pillich *et al.* on another cell line (Pillich *et al.*, 2012).

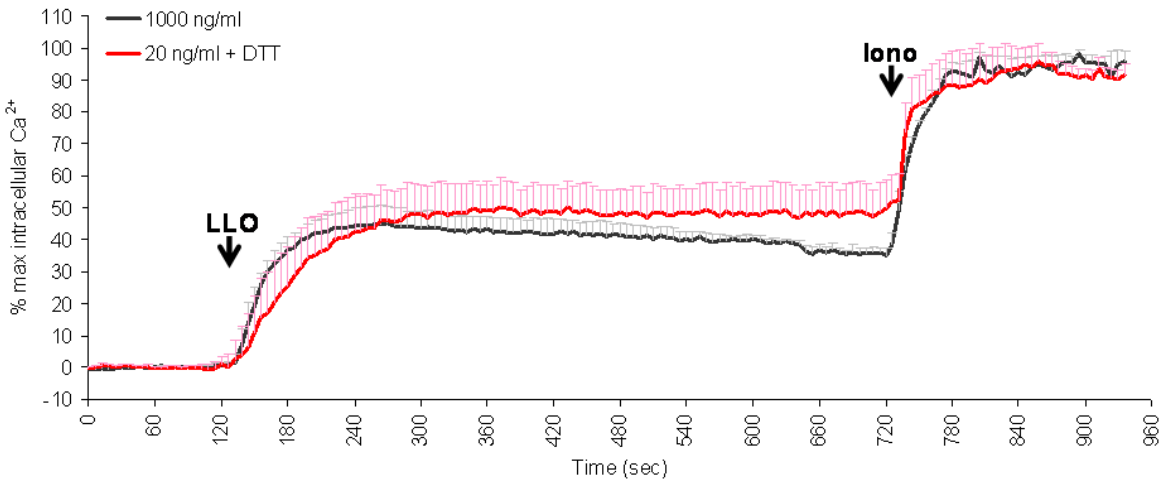

Fig 3.1.2 Preincubation of LLO with DTT increases its ability to form Ca^{2+}-permeable pores and reduces the amount of toxin needed for a strong cellular response. Caco-2 cells were loaded with Fura-2 AM and monitored for changes in the emission at 340 and 380 nm when excited at 510 nm. The 340/380 nm ratio was calculated from the emission readings. The maximum signal measured after adding Iono (5 µM) at the end of the experiment was used to express the relative change in $[Ca^{2+}]_i$. LLO was added at indicated concentrations and cells were measured for 10 min before Iono was added.
The graph shows the mean values + SEM of three independent experiments for each group.

3.1.3 Treatment with LLO leads to a reduction of the overall surface area covered by epithelial cells that depends on the influx of calcium ions into the cytoplasm

The setup of the microscopy equipment used for the measurement of changes in the $[Ca^{2+}]_i$ as well recorded images in grey scale that could be used for the evaluation of the total surface area covered by cells. To do so, the software needed a small space within the recorded images that was not covered by cells throughout the whole experiment as a background marker. Once the background was defined, the area covered by cells could be counted as the amount of pixels in each image that were not background. The amount of pixels standing for cell-covered areas in each acquired image was used to measure the change in total surface covered by cells.

Figure 3.1.3 A shows the microscopic images of Fura-2 AM loaded cells before and after treatment with LLO. The signal of the emission wavelength at 380 nm was markedly decreased shortly after the addition of LLO, illustrating the reduction of the Ca^{2+}-unbound form of the fluorophore once extracellular Ca^{2+} started to flow into the cytoplasm through the toxin pores. After about five minutes post LLO-treatment, the cell monolayer started to shrink. To visualize this effect, the white line in the five and ten minute frames was drawn exactly at the same position in both images. The overall loss of cell surface area after toxin incubation is shown in Figure 3.1.3 B. Important additional information gained from these images is that LLO treatment did not result in cells becoming necrotic or apoptotic. This would have been visible as a sudden drop of fluorescence in the Ca^{2+} measurement and, in the case of apoptosis, as rapid shrinking of single cells or as rupturing and total loss of intracellular fluorescence signal in necrotic cells. In each experiment, the calcium graphs of each single cell measured and the images taken were checked for signs of cell death. Experiments that showed events of cell death were excluded so that the surface area measurements were not faulted by dying cells.

A)

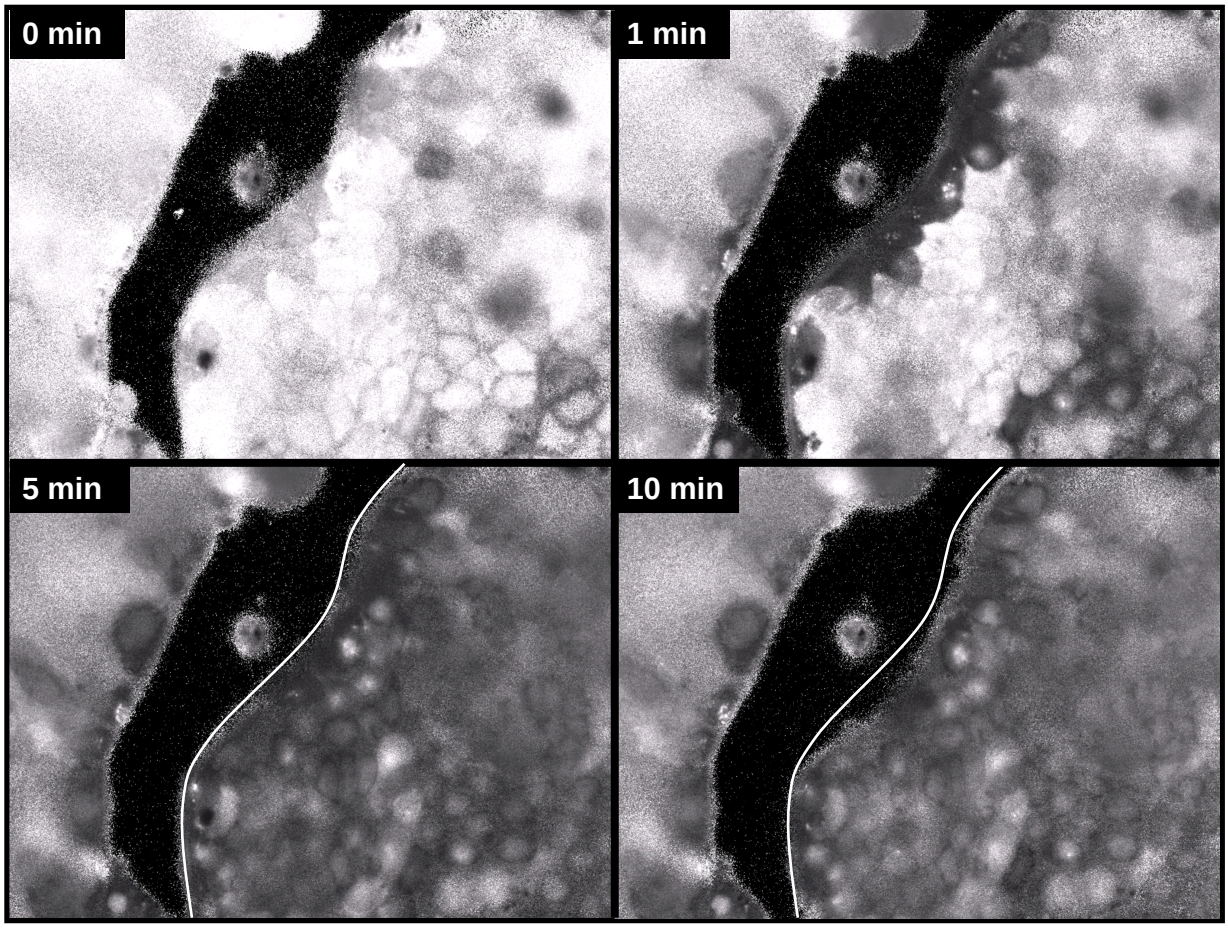

B)

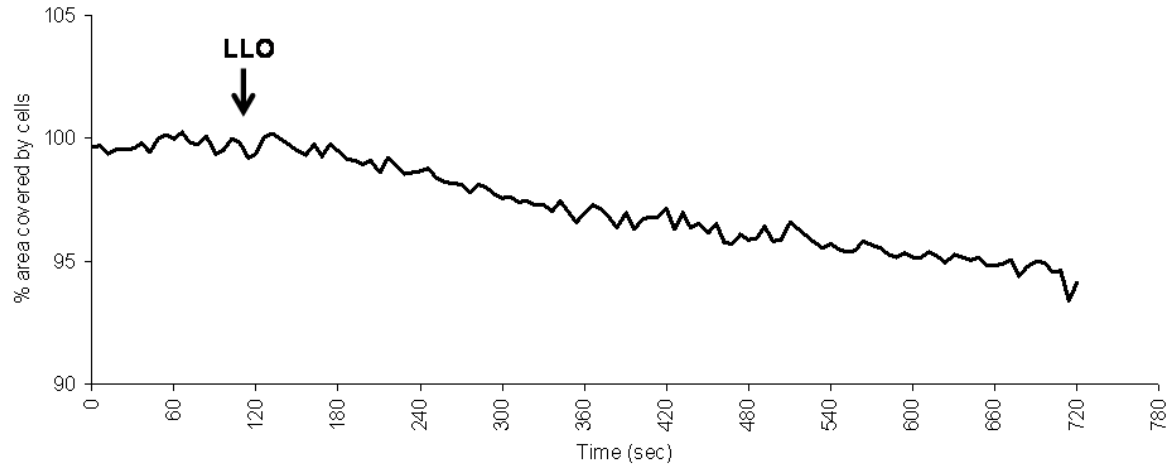

Fig. 3.1.3 The total cell surface area of epithelial monolayers is negatively affected by LLO. Caco-2 cells were loaded with Fura-2 AM and monitored for changes in the emission at 380 nm when excited at 510 nm.
A) Cells at rest had a low $[Ca^{2+}]_i$, therefore the emission of the free Fura-2 AM molecules at 380 nm was high (=cells are white). Shortly after LLO+DTT at 20 ng/ml was administered, the 380 nm signal dropped (=cell are dark grey), indicating that most of the fluorophore was Ca^{2+}-bound and the emission shifted to 340 nm (not shown). The white lines in the five and ten minutes' frame were placed at the same position in both images, allowing a comparison of the area loss between the two time points.
B) The cell surface area was determined by counting the pixels in the acquired images that had a signal above background levels. The pixel count before addition of LLO was set to 100%. The graph represents the area loss in the same experiment from which the images in A were acquired.

To test if the shrinking of cells is linked to the increase in $[Ca^{2+}]_i$ observed after LLO treatment, the long known non-specific Ca^{2+}-channel blocker lanthanum was used in the form of lanthanum(III) chloride ($LaCl_3$). Different studies reported that trivalent metal cations are able to inhibit an array of different ion channels in eukaryotic cells (Rangel-González *et al.*, 2002; Huettner *et al.*, 1998; Bryan-Lluka and Bönisch, 1997). The ability of different trivalent cations to inhibit ion channels correlates with the ionic radius (Mlinar and Enyeart, 1993). La^{3+} has the largest ionic radius in the group of lanthanides and was also determined to have the lowest $IC_{(50)}$ on LLO pores (Bittenbring, 2005). The diameter of LLO pores was determined by electron microscopy to be as large as 50 nm (Vadia *et al*., 2011).The group of Vadia *et al.* used toxin concentrations in the milligram range which produce large pores that are highly lytic. When electrophysiological methods for the examination of membrane pores like patch clamp are applied, it is possible to use very low LLO concentrations and hence operate under sublytic conditions as used here. Researchers following this approach reported the existence of much smaller pores consisting of only few LLO monomers (Repp *et al.*, 2002; Butler, 2004). These small pores occur at nanomolar toxin concentrations and offer an explanation for the blocking effect of trivalent metal ions.

In the experiments described above, Iono could not be used to determine the maximum $[Ca^{2+}]_i$ as La^{3+} at the used concentration completely blocked the ion flux through pores in the plasma membrane. The measurements therefore were expressed as the change in arbitrary fluorescence units from the 340/380 nm ratio. The respective 340/380 nm ratio of cells at rest before the start of the experiments was set to a value of one.

When cells were preincubated with 10 mM $LaCl_3$, the addition 250 ng/ml of LLO had no effect on the $[Ca^{2+}]_i$ (Figure 3.1.4 A, blue line). The addition of $LaCl_3$ to cells one minute after treatment with 20 ng/ml LLO immediately stopped further Ca^{2+} influx and the $[Ca^{2+}]_i$ remained constant (red line) at a slightly raised level but never reached the same elevation as LLO at the same concentration alone (black line). At the end of the experiments, Thapsigargin, a non-competitive inhibitor of the sarco / endoplasmic reticulum Ca^{2+}-ATPase (SERCA), was used to check if the cellular Ca^{2+} stores had remained untouched by the toxin. Thapsigargin was not administered after LLO treatment as the inflow of extracellular calcium ions would have completely masked the little amount released by the ER. When the toxin was interrupted by La^{3+}, the

somewhat elevated $[Ca^{2+}]_i$ could be increased further by Thapsigargin and showed a slow rise that is characteristic for the diffusion of Ca^{2+} out of the ER due to SERCA inhibition. Cells preincubated with $LaCl_3$ also showed a normal reaction after Thapsigargin-treatment, indicating that the ER calcium stores were not affected by the toxin.

A)

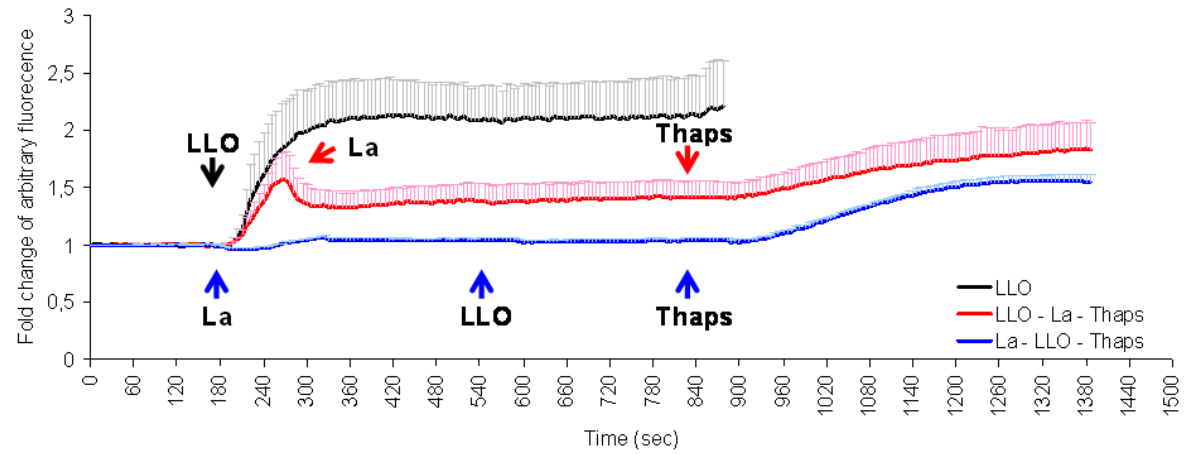

B)

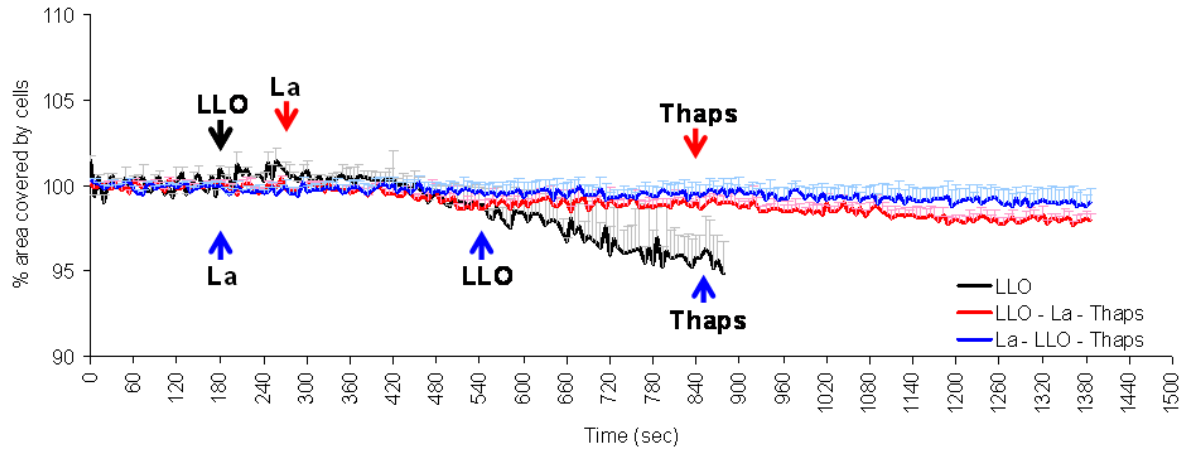

Fig 3.1.4 Lanthanum ions are able to block LLO-induced influx of extracellular calcium and thereby inhibit cell surface loss.
A) Caco-2 cells were loaded with Fura-2 AM and monitored for changes in the emission at 340 and 380 nm when excited at 510 nm. From those emission readings, the 340/380 nm ratio was calculated and the change in arbitrary fluorescence units was set to be one in cells at rest.
B) The cell surface area was determined by counting the pixels in the acquired images that had a signal above background levels. The pixel count in cells at rest was set to 100%. The graphs represent the area loss in the same experiments that are shown in A).
The cells were treated at indicated times with LLO+DTT at 20 ng/ml alone (black line), with LLO+DTT at 20 ng/ml and $LaCl_3$ at 10 mM one minute later (red line) or were preincubated with 10 mM $LaCl_3$ and then treated with 250 ng/ml LLO+DTT (blue line). In the last two experiments, Thapsigargin (Thaps) was added at the end of the experiments at a concentration of 100 nM.
In A) and B) the graphs show the mean values + SEM of at least three independent experiments for each group.

The change in cell surface area was monitored in the same experiments and revealed that there is a direct connection between increase in $[Ca^{2+}]_i$ and cell shrinking (Figure 3.1.4 B). $LaCl_3$-preincubated cells did not show any reduction in cell surface area although they were treated with a very high dose of LLO (250 ng/ml, blue line). When the Ca^{2+}-influx through LLO pores was interrupted shortly after the application of the toxin, the loss in cell surface area was almost completely abolished (red line). In comparison to that, cells incubated with LLO alone lost 5% of their total surface area (black line) within ten minutes of toxin treatment. The treatment with Thapsigargin at the end of the experiments (red and blue line) increased the $[Ca^{2+}]_i$ but had no negative effect on the cell surface area within a ten minutes' time frame.

3.1.4 Lanthanum reduces *L. monocytogenes'* invasiveness in epithelial monolayers and has bactericidal effects at millimolar concentrations

The observation that epithelial monolayers start shrinking upon toxin incubation led to the hypothesis that LLO plays an important role in the pre-intracellular phase of *L. monocytogenes* infection. Upon ingestion, the bacteria enter the GI tract of the host with the epithelium blocking their way into the body. Only when the pathogen is able to invade or otherwise cross the epithelial barrier it can successfully cause infections. *L. monocytogenes* harbours virulence factors that enable it to invade non-phagocytic cells. It expresses a surface protein called Internalin A (InlA), which binds the host-cell receptor E-Cadherin (ECad) and thereby achieves internalization of the bacteria (Hamon *et al.*, 2006; Mengaud *et al.*, 1996). ECad, which is the building block of adherens junctions (AJ), is fenced off towards the apical side of the barrier by tight junctions (TJ) in closed monolayers of polarized epithelial cells. It has been shown by Pentecost *et al* .(Pentecost *et al,.* 2006) that bacteria in need of otherwise inaccessible cellular ligands can attach at sites where apoptotic cells are budded off. The pathogens use the gaps that are produced by extrusion of senescent cells to find their way to the appropriate binding partner, enabling them to enter or cross the epithelial barrier. The authors found that most adhesion and invasion by *L. monocytogenes* on cultured polarized epithelial monolayers occurred at sites where multicellular junctions were formed after exclusion of single cells. The finding of reduction in cellular surface area upon LLO incubation lead to the hypothesis that the release of a pore forming toxin might allow the pathogen to get to its closed-off binding site.

To test whether active LLO secretion is sufficient for the break-up of TJs between cells and the release of ECad, closed monolayers of Caco-2 cells were infected with apically-applied *L. monocytogenes* strain EGDe. EGDe is used as a wild type control and expresses the full set of virulence factors known in Listeria, including LLO and Internalin A. The infection experiments showed that $LaCl_3$ inhibits invasion in a concentration dependent manner (Figure 3.1.5).

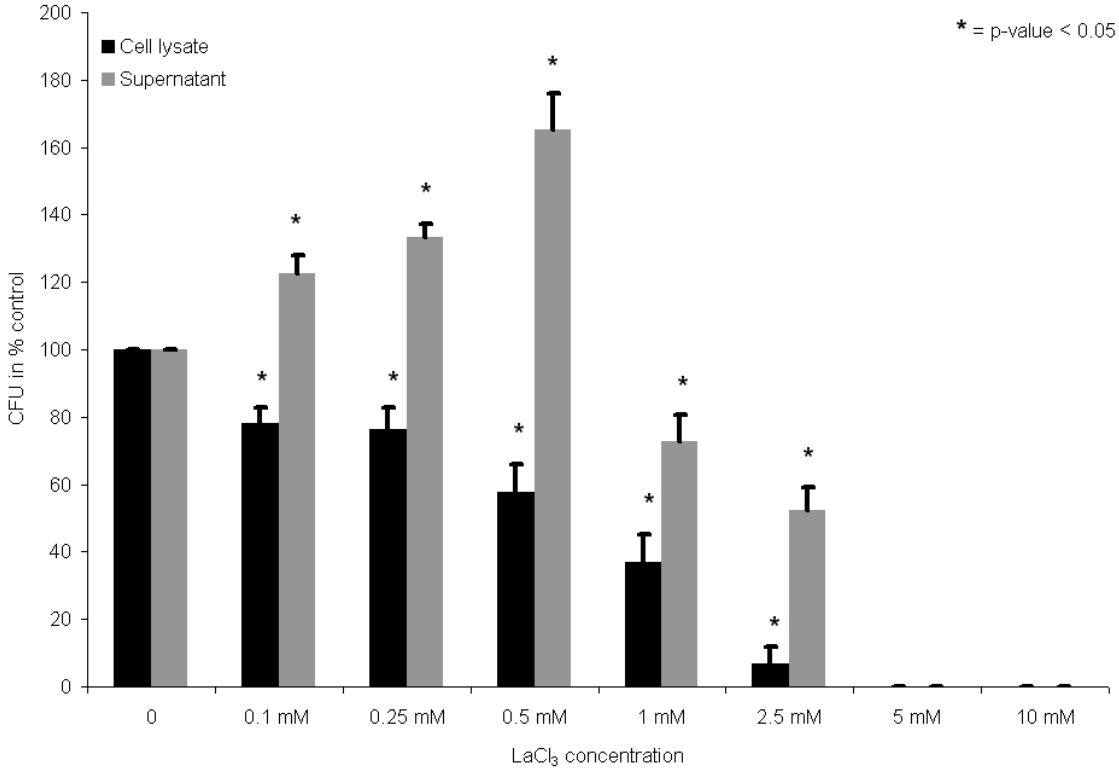

Fig 3.1.5 Preincubation with $LaCl_3$ protects Caco-2 monolayers from *L. monocytogenes* invasion. Caco-2 cells were grown to confluence and, on the day of the infection, were washed four times with PBS to remove all cholesterol from the FCS-containing growth medium. After washing, cells were kept in HEPES medium ($+Ca^{2+}$) for 2 h to recover from the washing and the medium change. $LaCl_3$ was added to the cells at indicated concentrations 10 min before infection. Cells were counted and infected with *L. monocytogenes* EGDe at MOI 10. After 1 h, the supernatant was collected and the cells were incubated with 50 µg/ml Gentamicin for 30 min. Then the antibiotic was washed off and the cells were lysed. Supernatants (gray bars) and cell lysates (black bars) were plated out and CFU were counted the next day. In the case of 5 and 10 mM $LaCl_3$, undiluted samples were plated out.
Results are shown as the percentage of control values. Each bar represents the mean value + SEM of at least three independent experiments. Significant differences from to the controls are indicated as ***** above the bars ($p<0.05$).

Concentrations of 0.1; 0.25 and 0.5 mM $LaCl_3$ reduced the amount of intracellular CFU (black bars) and at the same time increased the number of bacteria found in the supernatant (grey bars). This indicates that, when the action of LLO on the epithelial cells is blocked by La^{3+}, the bacteria are not able to invade the cells efficiently. Higher concentrations of $LaCl_3$ reduced the overall amount of bacteria, both in the cell

lysates and in the supernatants. 2.5 mM $LaCl_3$ almost completely blocked the invasion of cells and the extracellular bacteria were reduced to about 50% of control. When 5 or 10 mM were employed, no more CFU were detected in either fraction. The changes in the amount of extracellular and intracellular bacteria were found to be significant in comparison to control values for all of the tested $LaCl_3$ concentrations.

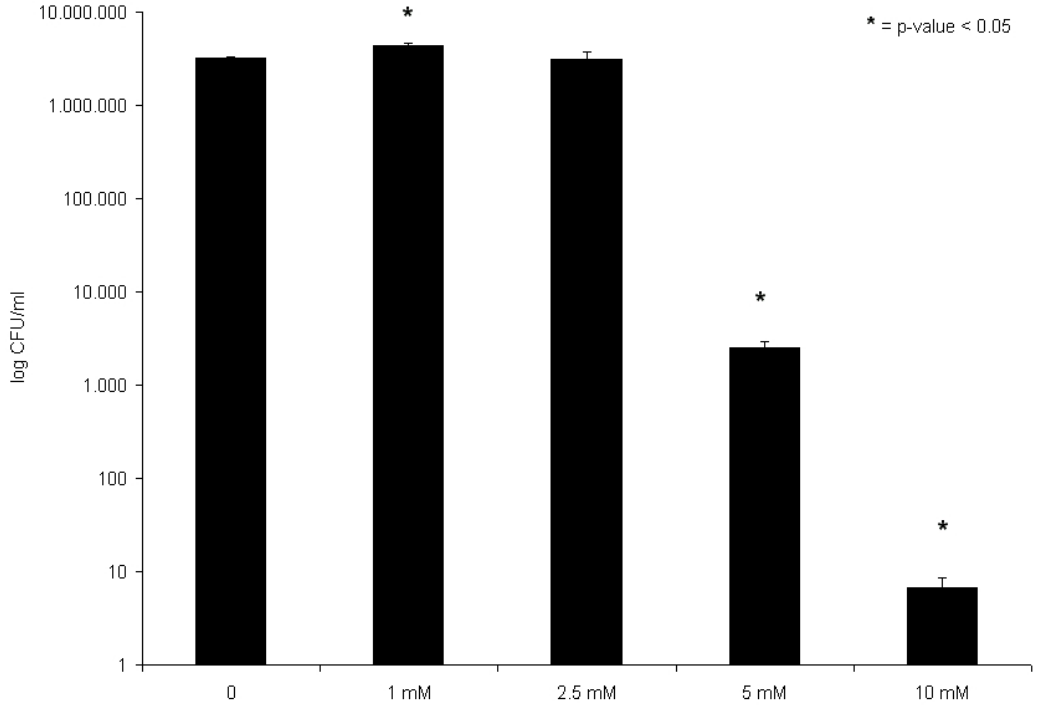

Fig 3.1.6 When incubated without cells, *L. monocytogenes* is more resistant to high $LaCl_3$ concentrations. An amount of bacteria comparable to MOI 10 in the previous experiment was incubated in the same volume of HEPES (+ Ca^{2+}) medium for 1 h with indicated $LaCl_3$ concentrations before the samples were diluted, plated out and counted.
The graph shows the counted CFU on a logarithmic scale. Each bar represents the mean value + SEM of at least three independent experiments. Significant differences from to the control are indicated as ***** above the bars ($p<0.05$).

The next step was to distinguish whether bacterial killing was due to the high $LaCl_3$ concentrations or induced cellular defence mechanisms. The bacteria were incubated in HEPES (+Ca^{2+}) medium containing $LaCl_3$ concentrations that caused a reduction in overall CFU for the same time but without cells. The results (Figure 3.1.6) were unexpected, as 1 mM $LaCl_3$ yielded an even higher CFU count than the untreated control ($4.4x10^6$ CFU ± $3.7x10^5$ vs $3.2x10^6$ CFU ± $1.7x10^5$ for 1 mM and control, respectively). 2.5 mM $LaCl_3$ did not change the CFU number when compared to control. At higher concentrations, a drastic reduction in bacterial numbers was observed. A decrease of more than three log was seen with 5 mM $LaCl_3$, and in samples incubated with 10 mM the few residual bacteria could only be counted when

not diluted at all. In this last group, the reduction in bacterial numbers amounted to a loss of six log in comparison to the control.

To better understand the effect of $LaCl_3$ on *L. monocytogenes*, growth curves of the wild type bacteria in different media were generated with the same range of $LaCl_3$ concentrations as used in the previous experiments. To accelerate the process of data generation, the growth curves were run in a system that could automatically control the incubation time, temperature, shaking and OD measurements in 96-well microplates (see Material and Methods section 2.3.4).

The HEPES medium used for the ratiometric calcium measurements and the infection and survival assays is devoid of amino acids and energy sources, except for glucose. Bacterial proliferation under these conditions was expected to be minimal to naught, even over a period of ten hours. The growth curve of untreated bacteria in this medium increased only marginally for about 5 h and then reached a plateau (Figure 3.1.7 A). Wells containing $LaCl_3$ at 5 and 10 mM could not be evaluated because a cloudy, white precipitate formed and produced negative OD values when negative controls were subtracted. These two curves were therefore only plotted until the 220 min time point, after which both groups had only negative OD values. The curve of $LaCl_3$ at 2.5 mM had an uneven course that was also due to slight precipitate formation. The high SEM (plotted as dashed error bars) of this group illustrates the high variability between experimental repetitions. All of the lower $LaCl_3$ concentrations showed a somewhat higher growth rate and yielded about two times higher OD values after 10h than EGDe did untreated.

A minimal medium (MM) (Figure 3.1.7B) that contained low concentrations of amino acids, iron, glutamate and glucose was also tested (see Material and Methods full list of components). This formulation includes the absolute minimum nutrition that *L. monocytogenes* needs for successful multiplication. In MM, all concentrations of $LaCl_3$, except for 10 mM, increased the growth rate of the bacteria. The highest OD values were achieved with 0.5 and 1 mM $LaCl_3$. In the groups of 5 and 10 mM, the uneven curves were caused again by precipitations that interfered with the measurements. The problem was not as serious as in HEPES; the small error bars indicate a better reproducibility in MM. Due to the precipitate formation, it was not possible to judge whether 10 mM $LaCl_3$ was really inhibiting bacterial growth or if the reduction in OD was due to unevenly distributed particle clouds in the negative control.

A)

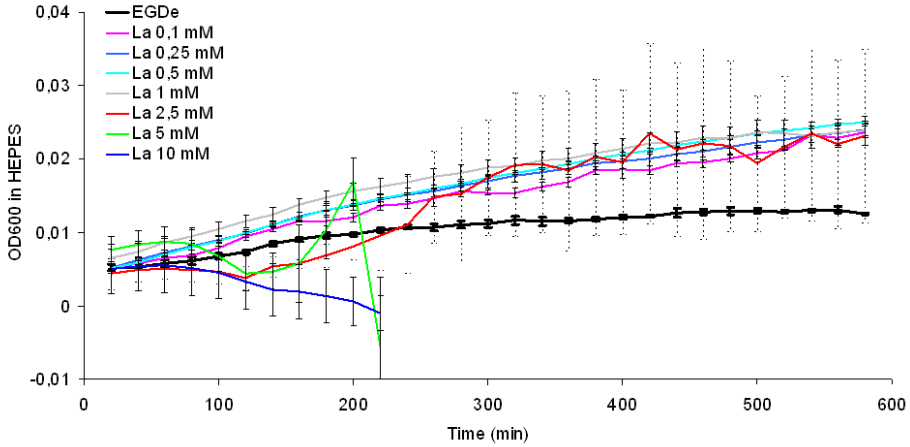

B)

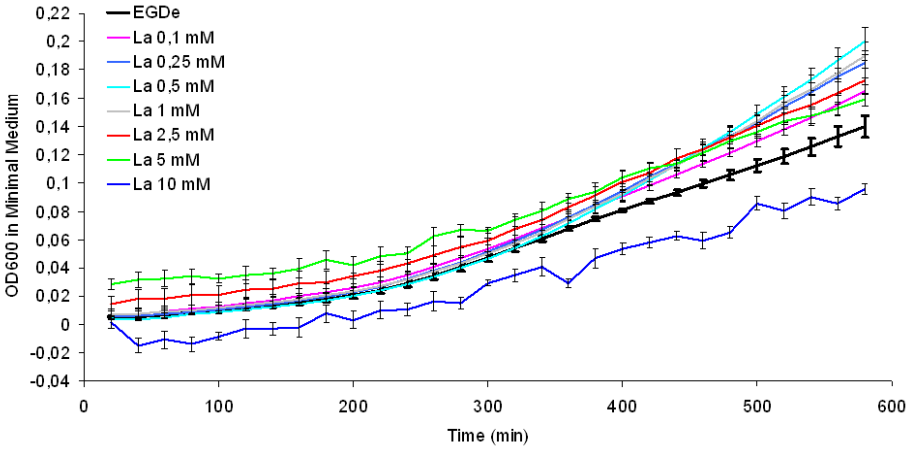

C)

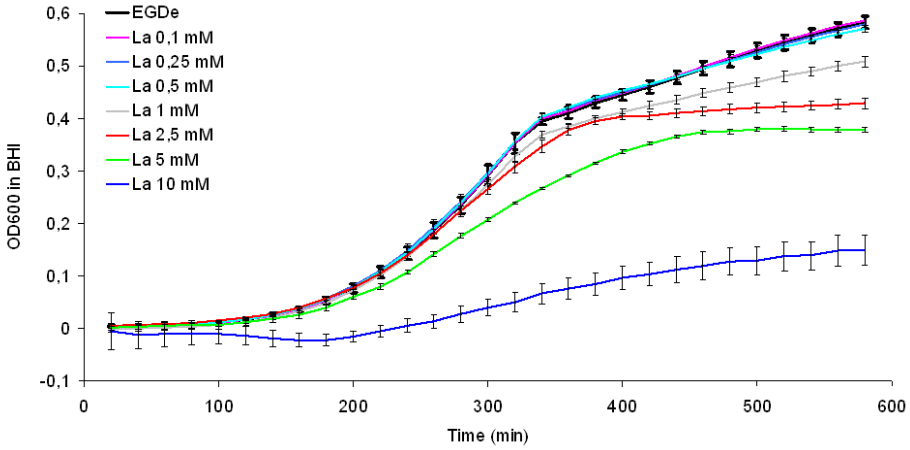

Fig 3.1.7 $LaCl_3$ has different effects on the growth rate of *L. monocytogenes* EGDe in rich and poor media. Growth curves in A) HEPES, B) MM and C) BHI. All experiments were performed in 96-well plates with a total volume of 150 µl in each well for 10h with continuous shaking at 37℃. EGDe cultures for inoculation were grown overnight in BHI and diluted 1:200 before being transferred into the wells containing the indicated $LaCl_3$ concentrations. Bacterial growth was measured every 20 min as the change of optical density at 600 nm. Negative controls of all $LaCl_3$ concentrations were used to account for different background values. Results are shown as mean values ± SEM of at least three independent experiments. SEM for 2.5 mM $LaCl_3$ in A) is shown as dashed lines for better visibility of the other error bars.

Finally, bacteria were grown together with $LaCl_3$ in Brain-Heart-Infusion (BHI) medium (Figure 3.1.7C). This complex and rich medium contains a broad array of nutrients and other essentials for bacterial growth from digested animal tissue and is used to cultivate a range of different microorganisms. In this group, the lower concentrations of $LaCl_3$ from 0.1 to 0.5 mM had no net effect on the growth curves. With higher amounts, there was a dose-dependent inhibition of bacterial multiplication. Growth was almost inhibited with 10 mM $LaCl_3$, 5 mM produced a much shallower rise in OD values and 2.5 and 1 mM showed an exponential growth phase similar to the control group but reached a plateau earlier.

3.2 Assessment of LLO mutants for their ability to form Ca^{2+}-permeable pores

The LLO mutants generated by our cooperation partners at the Max Planck Institute of Biophysics in Frankfurt am Main were assayed for their haemolytic activity on sheep erythrocytes and their ability to form Ca^{2+}-permeable pores in Caco-2 epithelial cells. The ability of the mutants to affect the cell surface area was tested in combination with the ratiometric calcium measurements as explained in chapter 3.1.3. The wild type toxin that was used as reference in the following experiments was produced together with the mutants in the same lab and under the same conditions to ensure comparability. All protein and haemolytic assays with the mutants were performed by Martina Hudel. Following the determination of protein concentrations, Caco-2 cells were treated with the wild type and mutant toxins to assess the resulting increase in $[Ca^{2+}]_i$. Each toxin was preincubated with DTT and tested at a concentration of 50 ng/ml on the same batch of cells as the others to ensure comparability and avoid differences in results due to changes in cell status.

As an example, figure 3.2.1 shows the cellular reactions to wild type toxin (WT) and the mutants A40W and A40W+K175E. The results of all the different mutants are listed in table 3.2.1, the single measurements can be found in the appendix (section 8.1).

A)

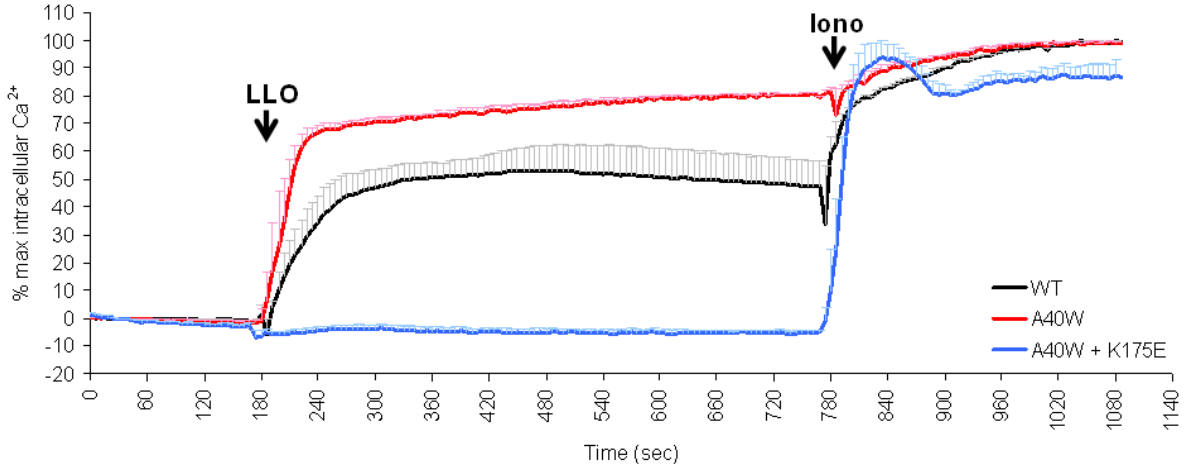

B)

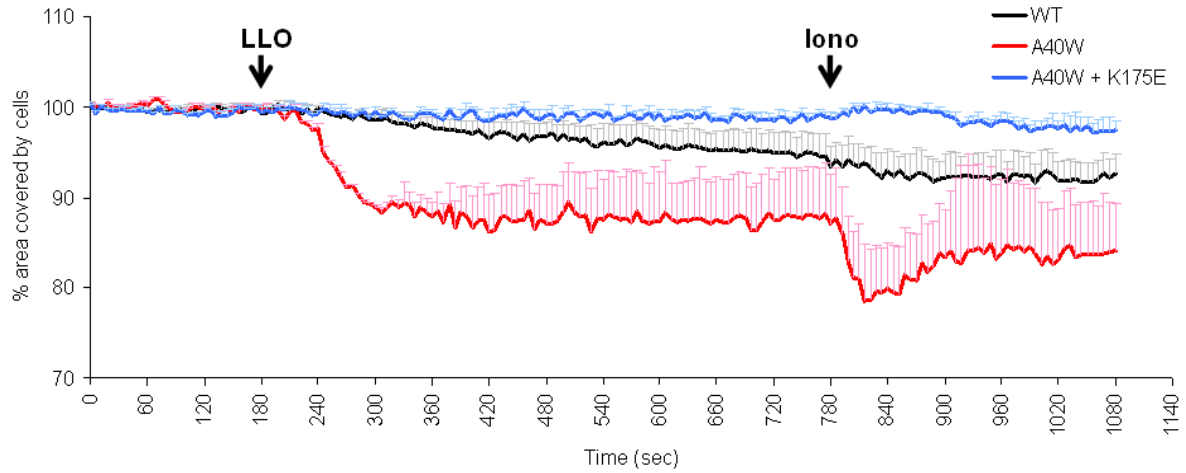

Fig 3.2.1 Comparison between wild type LLO and two mutant toxins
A) Caco-2 cells were loaded with Fura-2 AM and monitored for changes in the emission at 340 and 380 nm when excited at 510 nm. From the emission readings the 340/380 nm ratio was calculated. The maximum signal measured after adding Iono (5 µM) at the end of the experiment was used to express the relative change in $[Ca^{2+}]_i$.
B) The cell surface area was determined by counting the pixels in the acquired images that had a signal above background levels. The pixel count in cells at rest was set to 100%. The graph represents the area loss in the same experiments that are shown in A).
The cells were treated with 50 ng/ml LLO+DTT (WT, black line), with 50 ng/ml mutant LLO A40W+DTT (red line) or with 50 ng/ml mutant LLO A40W+K175E+DTT (blue line).
In A) and B) the graphs show the mean values + SEM of at least three independent experiments for each group.

Mutations that yielded an increased Ca^{2+} influx and cell surface loss were A40W, S44D, delta 51 and N230W (coloured red in table 3.2.1). N230W was the only mutant in this group yielding a lower haemolytic activity than WT, the other three mutants all had a stronger lytic effect on erythrocytes. Mutations that triggered a little less Ca^{2+} influx and cell surface loss were (coloured blue in table 3.2.1) S44E, which had less haemolytic activity but yielded a stronger reduction in cell surface area than WT-LLO,

and N179C and D394W, both of which had a stronger haemolytic activity than WT toxin.

Mutations that had lost almost all haemolytic activity and did not trigger any Ca^{2+} influx or cell surface loss were (coloured grey in table 3.2.1) K175E, S176W, E262W, the combination of A40W+K175E and the deletion of the first 50 aa in combination with K175E and S176W, respectively. It should be pointed out that the mutant E262W retained about 20% of its haemolytic activity on erythrocytes but was unable to form Ca^{2+}-permeable pores in Caco-2 cells.

Tab 3.2.1 Massive differences between the single mutants were found in their ability to lyse erythrocytes, form Ca^{2+}-permeable pores and cause cell surface area loss in cultured epithelial cells. For the haemolytic activity, the wild type was set to be 100%. To determine the toxins ability to form Ca^{2+}-permeable pores, Caco-2 cells were loaded with Fura-2 AM and monitored for changes in the emission at 340 and 380 nm when excited at 510 nm. From the emission readings, the 340/380 nm ratio was calculated, the maximum signal measured after adding Iono at the end of the experiment was used to express the relative change in $[Ca^{2+}]_i$. The change in cell surface area was determined by counting the pixels in the acquired images that had a signal above background levels. The pixel count in cells at rest was set to 100%. The cells were incubated with LLO+DTT at 50 ng/ml and were measured for 10 min before Iono was added.
The table of tested mutated toxins is colour coded: red for toxins with a higher overall activity than WT, blue for toxins that triggered a smaller increase in $[Ca^{2+}]_i$ and less loss in surface area and grey for toxins that lost all ability to perforate epithelial cells.

LLO variety	haemolytic activity in %	% max $[Ca^{2+}]_i$	% max area loss
WT	100	53	5.6
A40W	134	82	13.8
A40W + K175E	1.6	0	0.0
S44D	112	71	6.0
S44E	72	42	7.4
delta 51	125	79	12.4
delta 51 + K175E	1.2	0	0.0
delta 51 + S176W	0.0001	0	0.0
K175E	3	0	0.0
S176W	3	0	0.0
N179C	133	48	2.3
N230W	84	72	6.6
E262W	19	0	0.0
D394W	136	42	3.3

3.3 Pneumolysin has similar effects as Listeriolysin O on calcium homeostasis and epithelial monolayer integrity, releases ER-stored Ca^{2+} and mimics hypertonic stress

S. pneumoniae colonizes the upper respiratory tract in about ten percent of the population and is generally a dangerous pathogen in the very young, old and immunocompromised. When able to establish an infection, it triggers complex immunomodulatory reactions with an array of virulence factors. One present in all clinically relevant isolates is the toxin pneumolysin (PLY) (Paton *et al.*, 1993; Paton *et al.*, 1983), a member of the group of CDC. The toxin was found to be crucial for the establishment of a successful infection in the lung (Berry *et al.*, 1992; Jounblat *et al.*, 2003; Rubins *et al.*, 1996; Alexander *et al.*, 1998) and for the spread of the bacteria into the bloodstream (Kadioglu *et al.*, 2002; Orihuela *et al.*, 2004; Berry, Yother, *et al.*, 1989), where it causes septicaemia. PLY is able to hinder cellular functions like ciliary beating in bronchial epithelial cells, respiratory burst in neutrophils and macrophages, chemotaxis, production of chemokines and antibodies and other antibacterial activities (Rubins and Janoff, 1998). It has also been determined microscopically that human primary epithelial tissue from the upper respiratory tract loses its integrity upon treatment with PLY or toxin-producing *S. pneumoniae* strains (Rayner *et al.*, 1995; Feldman *et al.*, 2002). The effects of PLY on the cellular calcium homeostasis has been studied mostly in immune cells and parts of the nervous system (Stringaris *et al.*, 2002; Hirst *et al.*, 2004; Braun *et al.*, 2002; Fickl *et al.*, 2005). Only recently, Iliev *et al.* (2009) discovered a link between PLY-pores and changes in the actin cytoskeleton but attributed this finding to the activation of endogenous ion channels.

PLY and LLO are closely related and share large parts of their sequence with the exception that pneumolysin has no signal peptide for secretion. To release the toxin and other virulence factors, *S. pneumoniae* produces an amidase called autolysin A (LytA), which lyses the bacteria themselves (Howard and Gooder, 1974; Berry, Lock, *et al.*, 1989). The bacteria produce and store toxin during infection, but only a certain percentage of the pathogens undergo autolysis. When all the bacteria are killed in a narrow timeframe by antibiotics, large amounts of toxin are released, causing a common complication in pneumococcal infections where patients succumb to the disease although the affected tissue is found to be sterile.

To elucidate the connection between the toxins pore forming ability and the changes in calcium homeostasis, cell morphology, junctional constitution as well as epithelial barrier integrity, the following experiments were conducted.

3.3.1 Purified PLY triggers an increase in $[Ca^{2+}]_i$ in H441 cells and is more active under reducing conditions

The expression and purification of recombinant PLY in *Listeria innocua* was established by Martina Hudel and Dr. Silke Silva. The purified toxin was tested by Martina Hudel for protein concentration and lytic activity before it was used in cell culture experiments. All experiments were conducted with toxin from the same batch to ensure reproducibility.

Changes in $[Ca^{2+}]_i$ in H441 cells were measured in the same fashion as described in section 3.1.1. The treatment with 2000 ng/ml PLY led to different reactions of single cells within one experiment. Fig 3.3.1A depicts the changes in the 340/380 nm ratio of four single cells that were chosen to represent the whole spectrum of cellular responses that were observed. Due to the high intercellular variability, at least 30 individual cells were measured in each experiment and the mean value for each time point was calculated. In the case of repetitive experiments, the single mean values were again taken together to calculate a collective mean value and SEM.

To test whether the activity of PLY could be boosted under reducing conditions, like in the case of LLO, it was preincubated with 5 mM DTT before being added to the cells. The activated toxin was also used on cells after being heat inactivated at 65°C for 5 minutes as a control to prove that DTT itself had no effect on the cellular Ca^{2+}-homeostasis. The results of the three differently treated toxins are shown in figure 3.3.1B. When compared to PLY at 2000 ng/ml, the reduced toxin could be used at 100 ng/ml and still triggered the same increase of about 20% maximum $[Ca^{2+}]_i$. This showed that an increase in activity by a factor of 20 is achieved by using DTT-preincubated toxin. Hence, all the following experiments were conducted with PLY+DTT, allowing for a more economic use of the toxin and a better resemblance to *in vivo* infections. The control experiment with reduced and heat inactivated toxin revealed that active PLY is the only source of disturbances of the cellular Ca^{2+}-homeostasis in this experimental setup.

A)

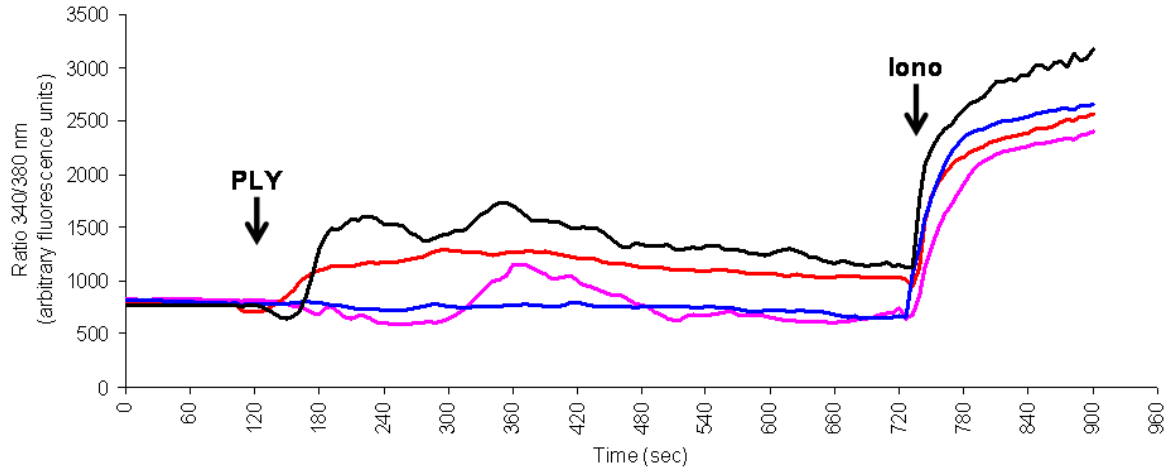

B)

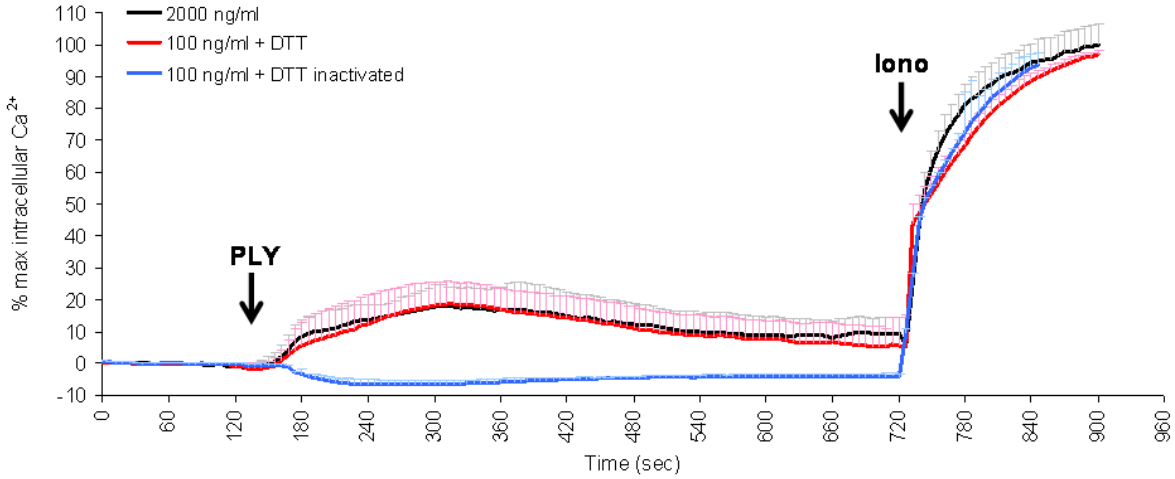

Fig 3.3.1 Single cells respond differently to incubation with PLY, which is more active under reducing conditions and inactive after short heat treatment. H441 cells were loaded with Fura-2 AM and monitored for changes in the emission at 340 and 380 nm when excited at 510 nm. From the emission readings the 340/380 nm ratio was calculated. The maximum signal measured after adding Iono at the end of the experiment was used to express the relative change in $[Ca^{2+}]_i$. PLY was added at indicated concentrations and cells were measured for 10 min before Iono (5 µM) was added.
A) Each line represents the changes in $[Ca^{2+}]_i$ of a single cell during the same experiment. The four depicted cells were chosen to represent the whole spectrum of reactions that could be observed when cells were treated with 2000 ng/ml PLY.
B) To compare the effects of the differently pretreated toxins, all values are given in % maximum $[Ca^{2+}]_i$. Results are shown as mean values ± SEM of at least three independent experiments.

3.3.2 Epithelial monolayers treated with PLY suffer from a reduction of the overall surface area that is caused by the toxin-induced influx of calcium ions into the cytoplasm

The experimental setup used to measure the change in total surface covered by cells was the same as described in section 3.1.3.

The effects of PLY are shown in the microscopy images of Fura-2 AM loaded H441 cells (Figure 3.3.2A). The recorded signal of the emission wavelength at 340 nm was

increased shortly after the addition of PLY when compared to untreated cells (0 min). This illustrates the higher population of the Ca^{2+}-bound form of the fluorophore after extracellular Ca^{2+} entered the cells through the toxin pores. A few minutes after PLY was added, the closed intercellular spaces started to open (blue arrowheads). This was accompanied by the shrinking of cells, increasing the empty space between cells. After ten minutes of PLY incubation, large areas that had been covered by a closed cell monolayer at the beginning of the experiment were turned into cell-free gaps (blue arrowheads). The relative loss of cell surface area after toxin incubation is depicted in Figure 3.3.2B. The red arrowhead in figure 3.3.2A marks a cell that became apoptotic between one and three minutes after the PLY treatment. This event can be seen as a strong increase and following sudden loss of fluorescence in the Ca^{2+} measurement and as rapid shrinking of the affected cell. The rapid drop of the cell surface area shortly after 360 seconds on the x-axis of the graph represents the death of the cell. In all experiments, the calcium graphs of each single cell measured and the images taken were checked for those signs of cell death. Experiments that showed events of cell death, like the one presented in figure 3.3.2, were excluded so that the surface area measurements were not disturbed by dying cells.

To investigate the status of intercellular junction integrity after the incubation of lung epithelial cell with sublytic PLY concentrations, H441 cells treated with PLY were prepared for immunofluorescence and stained for ECad, the protein constituting adherens junctions. Control cells were prepared the same way for comparability. The overall signal strength of ECad was reduced due to PLY treatment and the cells in this group did not present a closed monolayer, which was observed in the control group (Figure 3.3.3). Additionally, large intercellular spaces between cells that are comparable to those in figure 3.3.2 were formed (white arrows).

The non-specific Ca^{2+}-channel blocker $LaCl_3$ was used again to test if the shrinking of cells upon PLY incubation is dependent on the increase in $[Ca^{2+}]_i$. The blocking effect of the trivalent lanthanum ions was described by Schramm (2004). This study used toxin at sublytic (nanomolar) concentrations in electrophysiological experiments and reported the formation of much smaller pores than described before when the toxin was used in lytic amounts (Tilley *et al*., 2005).

A)

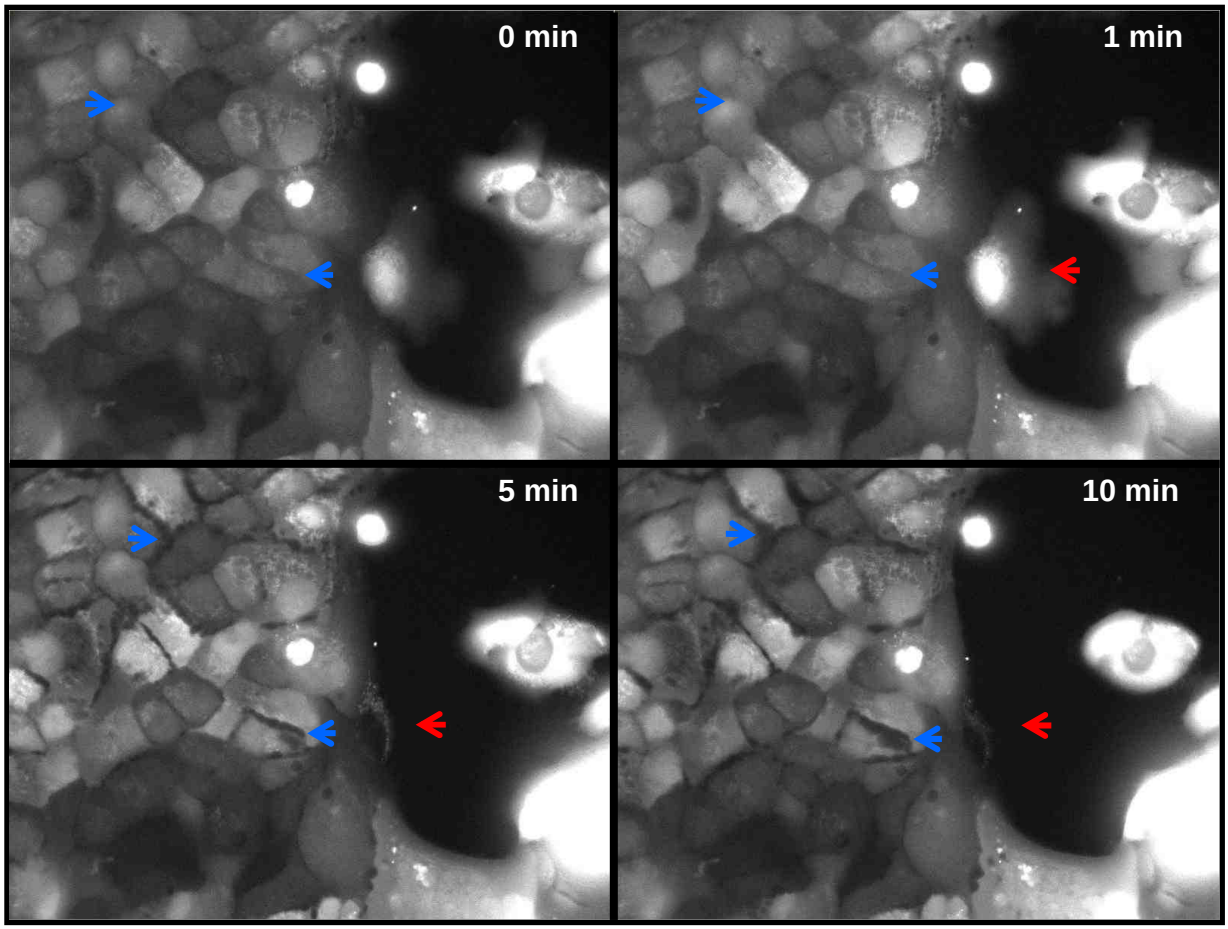

B)

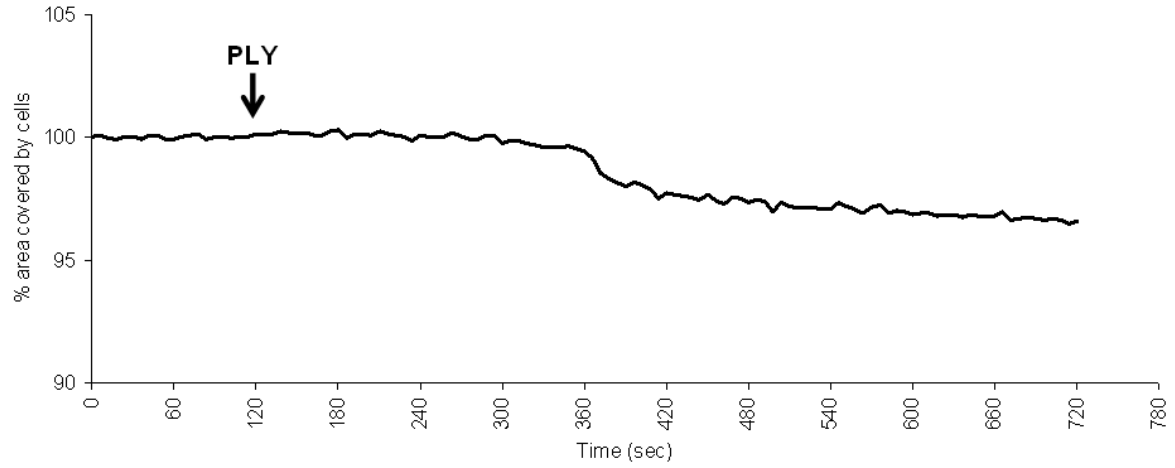

Fig 3.3.2 PLY causes the opening of intercellular gaps in closed cell layers and apoptosis in single cells. H441 cells were loaded with Fura-2 AM and monitored for changes in the emission at 340 nm when excited at 510 nm.
A) Cells at rest had a low $[Ca^{2+}]_i$, therefore the emission of the free Fura-2 AM molecules at 340 nm was also low (= dark grey cells). Shortly after PLY+DTT at 100 ng/ml had been administered, the 340 nm signal increased (= light grey/white cells), indicating that more of the fluorophore was Ca^{2+}-bound. The blue arrowheads point at the largest intercellular gaps formed during the PLY incubation. The red arrowhead marks the cell that became apoptotic shortly after addition of the toxin.
B) The cell surface area was determined by counting the pixels in the acquired images that had a signal above background levels. The pixel count before addition of PLY was set to 100%. The graph represents the area loss in the same experiment that the images in A were acquired from.

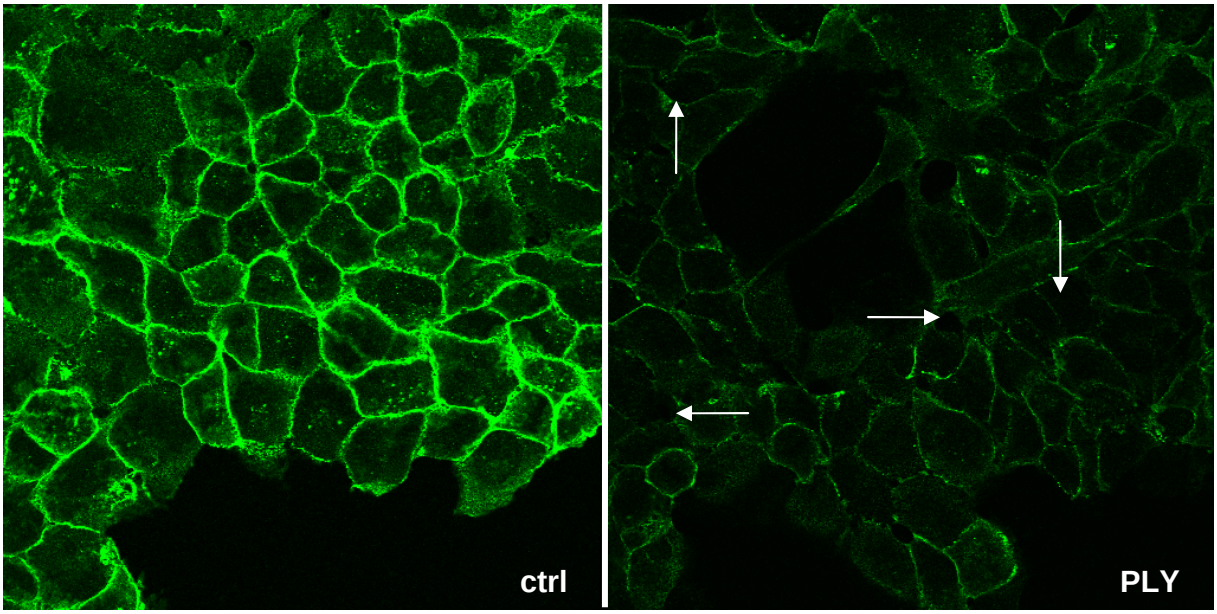

Fig 3.3.3 PLY-treated epithelial cells show a reduced signal from ECad and form large intercellular gaps. H441 cells were grown on glass cover slips and incubated with 100 ng/ml PLY or left untreated for 6 h before being fixed, permeabilized and incubated with an Alexa®488-coupled anti-ECad antibody. Cover slips were mounted on microscope slides and examined by confocal microscopy. White arrows indicate gaps between PLY-treated cells.

The measurements were expressed as the change in arbitrary fluorescence units. The 340/380 nm ratio of cells at rest before starting the experiments was set to a value of one. This was necessary because Iono could not be used to determine the maximum $[Ca^{2+}]_i$ because La^{3+}, at the concentration used, completely blocks the ion flux through its pores in the plasma membrane.

The incubation with 10 mM $LaCl_3$ before the addition 100 ng/ml PLY completely abolished the effect of the toxin on the $[Ca^{2+}]_i$ (Figure 3.3.4A, blue line). The addition of $LaCl_3$ to cells one minute after being treated with 100 ng/ml toxin immediately stopped the influx of Ca^{2+} and the $[Ca^{2+}]_i$ returned to its starting level (red line). PLY alone triggered the highest peak in $[Ca^{2+}]_i$ levels, which slowly declined over the course of the experiment but did not go back to values before toxin treatment (black line). At the end of the experiments, Thapsigargin was administered to check if the ER-stored Ca^{2+} was unaffected by the toxin. In the cells treated with PLY alone Thapsigargin was not used because the inflow of extracellular calcium ions would have completely masked the little amount released by the ER. When the toxin-induced Ca^{2+}-inflow was inhibited by the addition of $LaCl_3$ before or shortly after the toxin, the cells showed a normal reaction to Thapsigargin, indicating that the ER calcium stores were not affected by the toxin.

A)

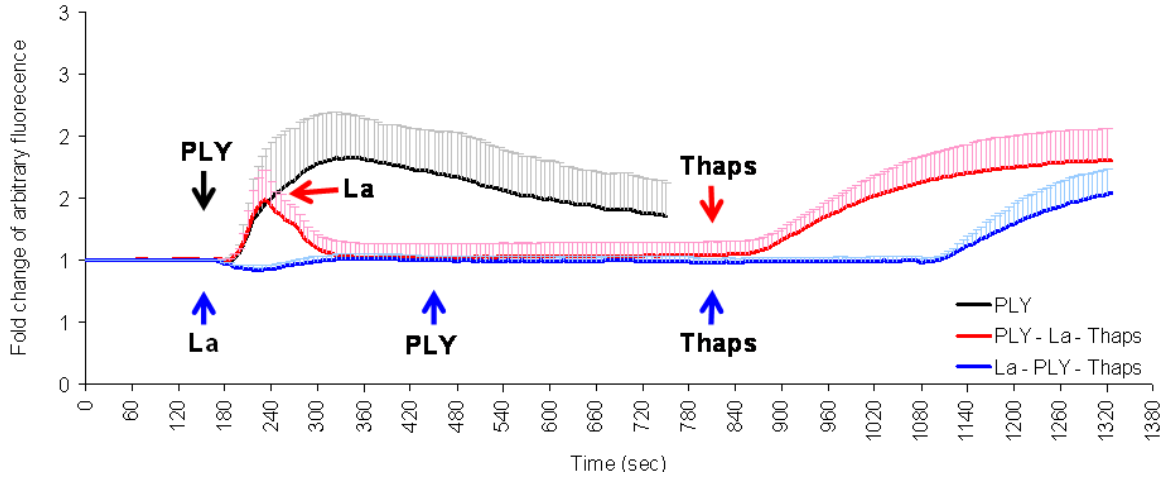

B)

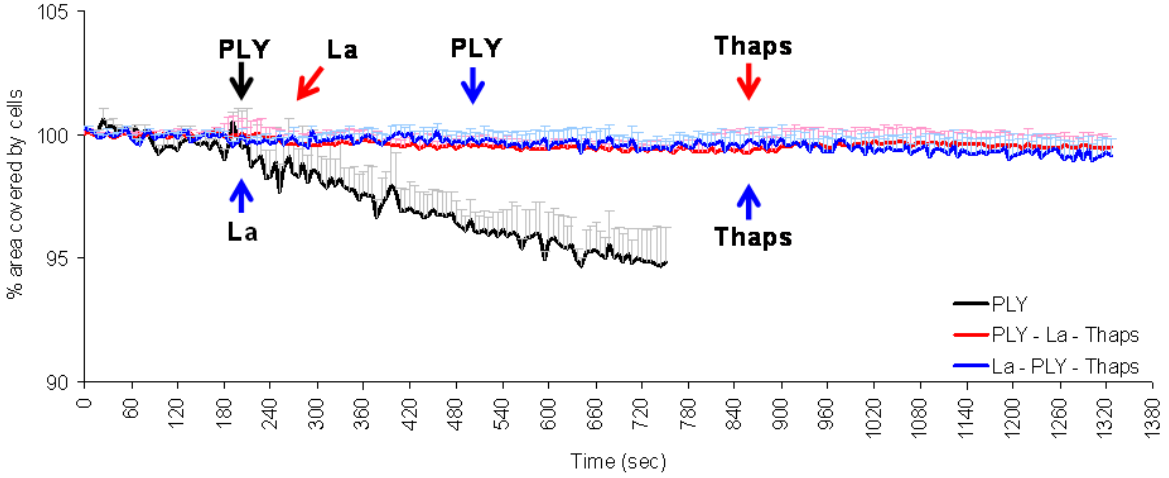

Fig 3.3.4 $LaCl_3$ blocks the PLY-induced influx of extracellular Ca^{2+} and prevents cell surface loss.
A) H441 cells were loaded with Fura-2 AM and monitored for changes in the emission at 340 and 380 nm when excited at 510 nm. From the emission readings the 340/380 nm ratio was calculated and the change in arbitrary fluorescence units was set to be one in cells at rest.
B) The cell surface area was determined by counting the pixels in the acquired images that had a signal above background levels. The pixel count in cells at rest was set to 100%. The graphs represent the area loss in the same experiments that are shown in A.
The cells were treated at indicated times with PLY+DTT at 100 ng/ml alone (black line), with PLY+DTT at 100 ng/ml and $LaCl_3$ at 10 mM one minute later (red line) or were preincubated with 10 mM $LaCl_3$ and then treated with 100 ng/ml PLY+DTT (blue line). In the last two experiments, Thapsigargin (Thaps) was added at the end of the experiments at 100 nM.
In A) and B) the graphs show the mean values + SEM of at least three independent experiments for each group.

The change in cell surface area was monitored in the same experiments (Figure 3.3.4B). Cells that were incubated with $LaCl_3$ before the addition of PLY did not show any reduction in cell surface area (blue line), indicating a direct connection between increase in $[Ca^{2+}]_i$ and cell shrinking. The interruption of the Ca^{2+}-influx through toxin pores by La^{3+} ions shortly after the application of PLY had the same effect, as no loss

in cell surface area was observed (red line). When cells were incubated with PLY alone, they lost more than 5% of their total surface area within ten minutes after toxin treatment (black line). The use of Thapsigargin at the end of the experiments (red and blue line) increased the $[Ca^{2+}]_i$ (see Figure 3.3.4A) but had no negative effect on the cell surface area.

3.3.3 Pneumolysin induces a release of ER-stored calcium into the cytoplasm that is not dependent on cellular ion channels

Calcium ions are important for intracellular signalling events as second messengers. Eukaryotic cells store Ca^{2+} in organelles and release them into the cytoplasm for signal transduction. The $[Ca^{2+}]_i$ in cells at rest is typically four orders of magnitude lower than in the extracellular environment. The low cytoplasmic concentrations can be elevated for messaging by releasing Ca^{2+} from the storage organelles [mostly from the endoplasmic reticulum (ER)]. If an amplification of the signal is required, there are calcium-signalling-activated ion channels in the plasma membrane that mediate the influx of much more calcium ions from the extracellular space. This amplification mechanism also works the other way around. When plasma membrane ion channels increase the $[Ca^{2+}]_i$, there are channels in the ER-membrane activated by calcium signalling events which release additional Ca^{2+} from the intracellular stores to increase the second messenger signal strength.

As mentioned before, the group of CDCs was found to trigger many cellular reactions that are dependent on intracellular calcium signalling. It was long thought that this is due to the influx of extracellular Ca^{2+} through the pores formed by the toxins in the plasma membrane. In a recently published paper the group of Gekara (2007) found that purified LLO and toxin producing *L. monocytogenes* caused physical damage to the ER and possibly directly released ER-stored Ca^{2+} into the cytosol. The experiments were done in mast cells and bone marrow macrophages and the results hinted at two independent ways in which LLO might trigger the release of calcium. The first way was found to be dependent on cellular IP_3R-gated Ca^{2+} channels whereas the second one was probably due to direct injury of intracellular Ca^{2+} stores.

To elucidate whether pneumolysin could have the same effect on epithelial cells the following experiments were performed. H441 cells were monitored for changes in $[Ca^{2+}]_i$ while being incubated in calcium free HEPES medium. To ensure that all traces of Ca^{2+} were gone, the metal ion chelator EGTA was added at a concentration

of 0.5 mM to the cells prior to the start of the experiments. EGTA is not cell permeable, so the intracellular calcium stores were not affected.

The cells were treated with:

i) PLY followed by Thapsigargin, to check whether the intracellular stores were completely emptied by the toxin

ii) Thapsigargin first and then PLY, to deplete the ER-stores before the toxin could do so

iii) Inhibitors of cellular calcium channels previous to PLY and Thapsigargin to determine their involvement in the reaction.

The two classes of calcium-release channels in the ER are ryanodine receptors, which are activated by elevated Ca^{2+}-levels in the cytoplasm and can be blocked with Ryanodine (Rya), and inositol trisphosphate (IP_3) receptors, which are activated by the second messenger IP_3 and can be blocked by Xestospongin C (XeC).

Cells treated with PLY showed a sharp peak in $[Ca^{2+}]_i$ that occurred some seconds later than in experiments with normal extracellular Ca^{2+} concentrations (Figure 3.3.5, black line). Addition of Thapsigargin had no further effect and, together with the transient nature of the reaction to PLY, hinted at the depletion of finite intracellular stores. The decrease in $[Ca^{2+}]_i$ was probably due to disposal of excess calcium outside the cells, where it was immediately chelated by EGTA. When cells were preincubated with the calcium-release channel blockers Rya and XeC their reaction to PLY was slightly weaker in peak height, but showed the same kinetic (red line). Treatment with Thapsigargin showed that the depletion of the ER-Ca^{2+} store was not prevented by the two blocking agents. When Thapsigargin was added prior to the toxin, the increase in $[Ca^{2+}]_i$ was stronger and declined slower (blue line). This difference might be due to the different modes of release, in case of the toxin the ions could flow out through a channel-like structure, whereas the SERCA-inhibition by Thapsigargin resulted in passive diffusion of Ca^{2+} out of the storage organelles following the concentration gradient from the cytoplasm to the extracellular space where it was chelated. The final addition of PLY after Thapsigargin caused minor calcium fluctuations, indicating that the toxin was still able to perforate the plasma membrane but could not interfere with the calcium homeostasis due to the emptied ER-stores.

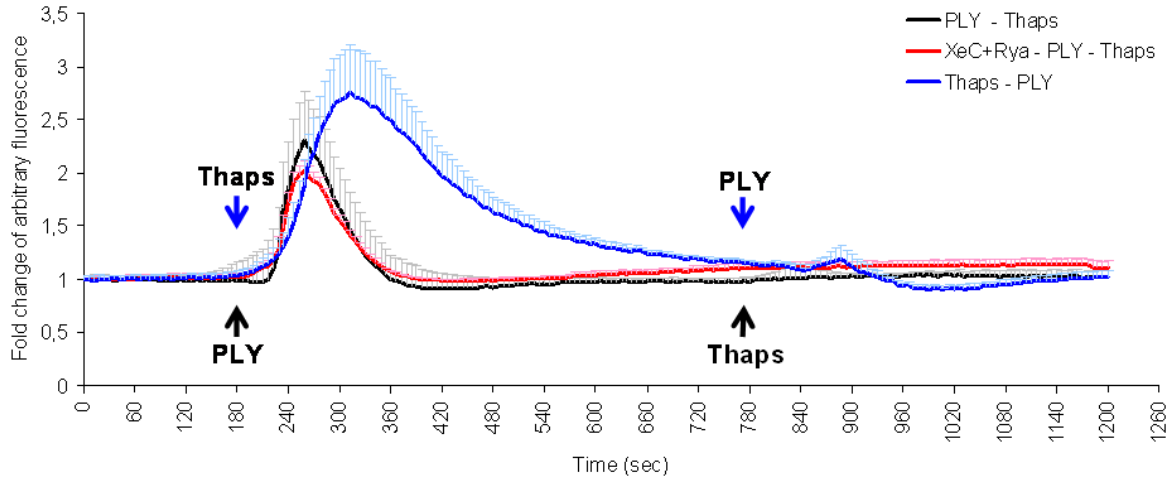

Fig 3.3.5 Peaks in $[Ca^{2+}]_i$ after treatment with PLY in calcium-free medium are caused by the release of ER-stored Ca^{2+} and are not dependent on cellular ion channels.
H441 cells were loaded with Fura-2 AM and monitored for changes in the emission at 340 and 380 nm when excited at 510 nm. From the emission readings the 340/380 nm ratio was calculated and the change in arbitrary fluorescence units was set to be one in cells at rest. Calcium-free HEPES with 0.5 mM EGTA was used in all experiments.
The cells were treated at indicated times with PLY+DTT (100 ng/ml) followed by Thapsigargin (Thaps) (100 nM) (black line), with Rya (5 µM) and XeC (3 µM) ten minutes before PLY+DTT (100 ng/ml) and Thaps (100 nM) (red line) or Thaps (100 nM) before PLY+DTT (100 ng/ml) (blue line).
The graphs show the mean values + SEM of at least three independent experiments for each group.

3.3.4 Pneumolysin triggers changes in epithelial cells that are similar to the cellular reaction to hyperosmotic conditions.

The respiratory epithelium, which functions as a first line of defence against invading pathogens, is regularly exposed to different kinds of bacterial strains that are known to produce pore forming toxins. In this context it is not surprising that lung epithelial cells have been found to be very sensitive detectors of those bacterial toxins (Ratner *et al.*, 2006). The activation of p38 mitogen-activated protein kinases (MAPK) is usually associated with the cellular reaction to hyperosmotic stress (Han *et al.*, 1994). Under this condition, where the cell suffers a loss of water due to a changed osmotic gradient, the cellular volume decreases and the cytoplasm becomes crowded with macromolecules which leads to a series of dangerous changes in the cell like decreased or halted transcription and translation and damaged DNA and proteins. Another effect of increased tonicity on cells that was described early (Homsher *et al.*, 1974) is the fast and transient increase in $[Ca^{2+}]_i$.

To compare the changes in $[Ca^{2+}]_i$ upon hyperosmotic stress to the ones due to PLY, the cells were treated with Sorbitol to increase the osmolarity of the medium from a physiological level of 300 mOsm/kg H_2O to 500 mOsm/kg H_2O. Under these

conditions, the cells experience hyperosmotic stress but are able to adapt to it over time and survive for at least some hours.

A)

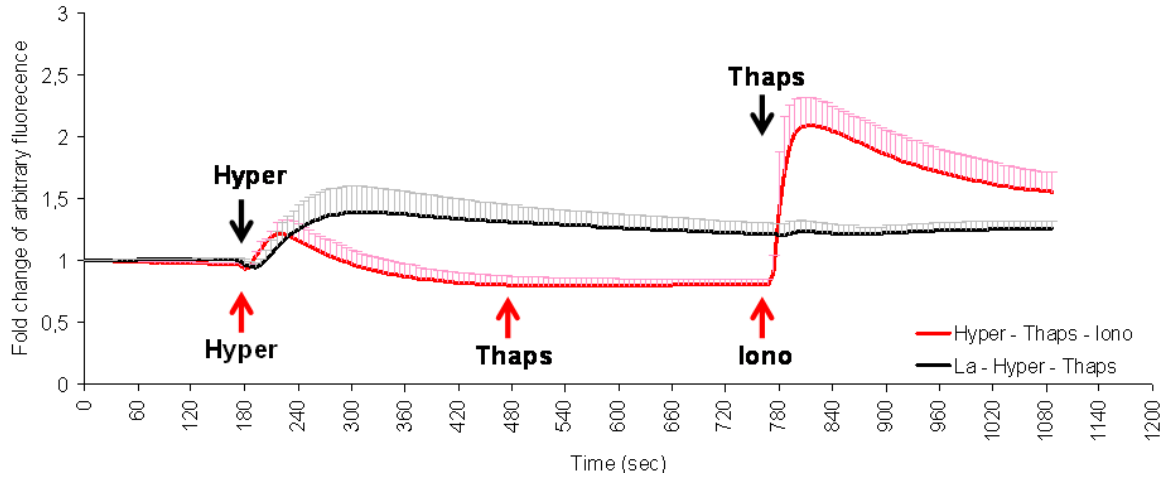

B)

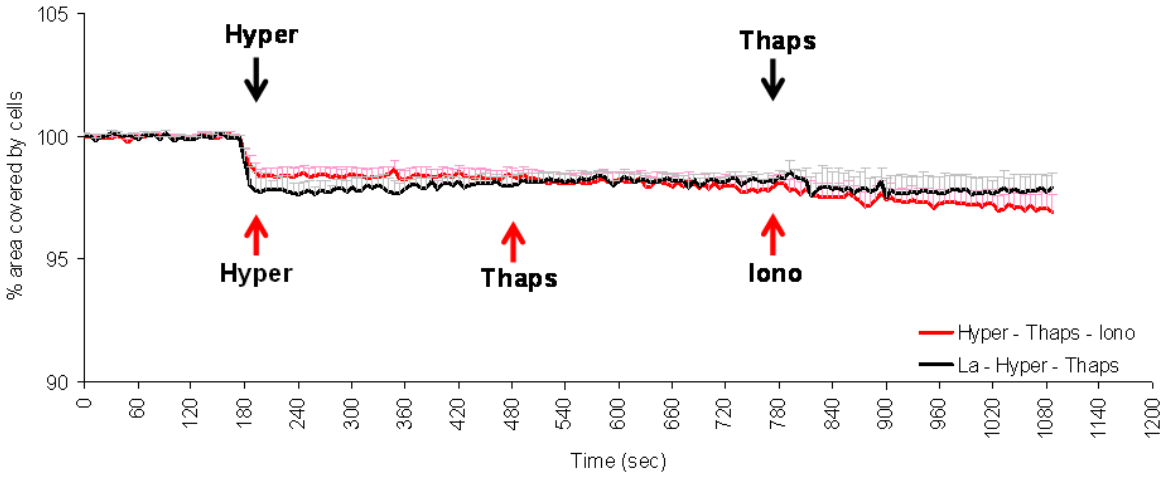

Fig 3.3.6 Hyperosmolarity induced by Sorbitol triggers an increase in $[Ca^{2+}]_i$ that is due to Ca^{2+}-release from the ER.
A) H441 cells were loaded with Fura-2 AM and monitored for changes in the emission at 340 and 380 nm when excited at 510 nm. From the emission readings the 340/380 nm ratio was calculated and the change in arbitrary fluorescence units was set to be one in cells at rest.
B) The cell surface area was determined by counting the pixels in the acquired images that had a signal above background levels. The pixel count in cells at rest was set to 100%. The graphs represent the area loss in the same experiments that are shown in A.
The cells were treated at indicated times with 200 mOsm of Sorbitol (Hyper), Thapsigargin (Thaps) (100 nM) and Iono (5 µM) (black line) or were preincubated with $LaCl_3$ (10 mM) for 5 min before Hyper and Thaps treatment (red line).
The graphs show the mean values + SEM of at least three independent experiments for each group.

Upon changing the osmolarity of the medium by addition of Sorbitol, the cells reacted with a short-lived peak and a subsequent drop in $[Ca^{2+}]_i$ below the level of cells at rest (Figure 3.3.6A, black line). When Thapsigargin was administered there was no

further reaction, indicating that Ca^{2+} was released from the ER into the cytoplasm in response to the hyperosmotic shock. The lower but stable levels of cytoplasmic calcium that occurred after the initial peak might be interpreted as an adaption to the decrease in cell volume. The cells reacted strongly to Iono at the end of the experiment, which shows that the $[Ca^{2+}]_i$ was not saturated. In cells that were preincubated with $LaCl_3$ to exclude the inflow of Ca^{2+} from outside the cells, the treatment with Sorbitol had a different effect on the $[Ca^{2+}]_i$ (red line). The observed peak after initiation of hyperosmotic stress was stronger and did not drop back to or below initial levels. This stable increase was not altered by the addition of Thapsigargin. The different reaction after $LaCl_3$ pretreatment is a hint that the stress-induced Ca^{2+}-release from the ER is cleared by pumping excessive calcium ions out of the cell, a process inhibited by La^{3+} (Herscher and Rega, 1997). These findings are opposing the reaction of an osteoblast cell line to osmotic stimuli described by Dascalu *et al.* (1995). In contrast to the diverging changes in the $[Ca^{2+}]_i$ in both groups, the cell surface area reacted in exactly the same way, which can be seen in figure 3.3.6B as a sharp decrease of about 2% shortly after Sorbitol was added. A striking difference between the toxin- and hyperosmolarity-mediated losses in cell surface area is that the cells do not shrink continuously when treated with Sorbitol but stabilize quickly at a reduced level (compare figures 3.3.6B and 3.3.4B).

Another similarity in the reaction of epithelial cells to hypertonic conditions and PLY at sublytic concentrations is the migration of the transcription factor NFAT5 (TonEBP/OREBP) from the cytoplasm into the nucleus (Figure 3.3.7). In resting cells the transcription factor was located primarily in the cytoplasm, while hypertonic conditions and PLY-treatment led to a colocalization of NFAT5 with the nuclei of H441 cells. NFAT5 is an important player in cellular adaption to hyperosmotic conditions. It induces the transcription of genes that increase the concentration of organic osmolytes inside the cell, facilitate water reuptake and protect from cell death (Woo *et al.*, 2002; Hasler *et al.*, 2005; Burg *et al.*, 2007; Ferraris and Burg, 2004).

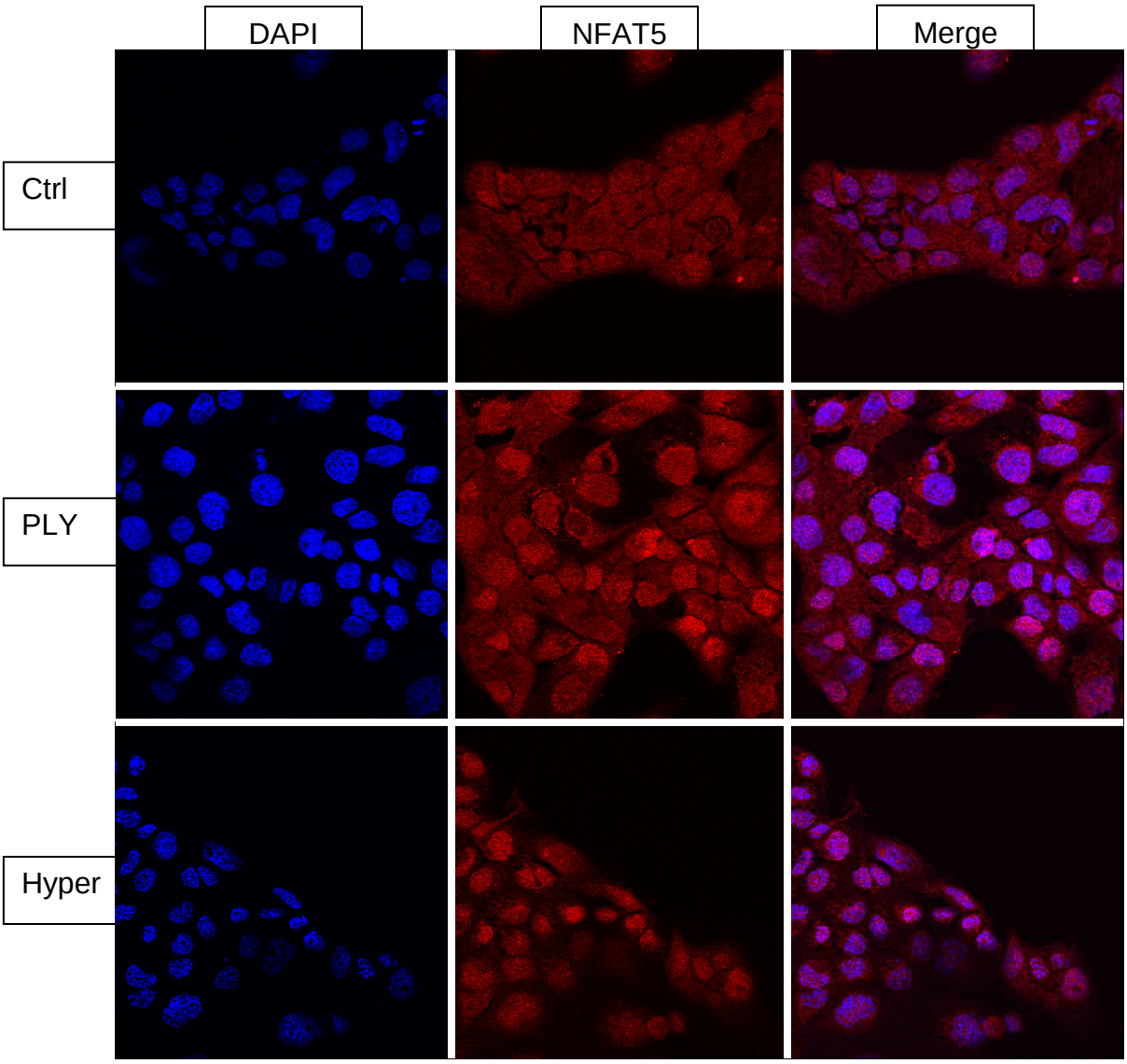

Fig 3.3.7 Hyperosmolar medium and PLY treatment trigger NFAT5 translocation to the nucleus. H441 cells were grown on glass cover slips and incubated with 100 ng/ml PLY+DTT, in medium with 500 mOsm/kg H_2O or left untreated for 6 h before being fixed, permeabilized and incubated with anti-NFAT5 primary antibody and an Alexa®555-coupled secondary antibody. Cover slips were mounted on microscope slides and examined by confocal microscopy.

3.3.5 The pneumolysin-triggered loss in cell surface area is dependent on conventional PKC-activity and is inhibited by the TIP peptide

As mentioned in 3.1, CDC-induced perturbations of the cellular Ca^{2+}-homeastasis were found to activate PKC. There is evidence that conventional PKCs (isoforms α, β I/II and γ, cPKC) are involved in the disassembly of tight junctions in epithelial cells (Tai *et al.*, 1996). To test whether active cPKC was required in PLY-induced intercellular junction breakup and cell shrinking, the specific inhibitor Gö6976 (Martiny-Baron *et al.*, 1993) was used.

A)

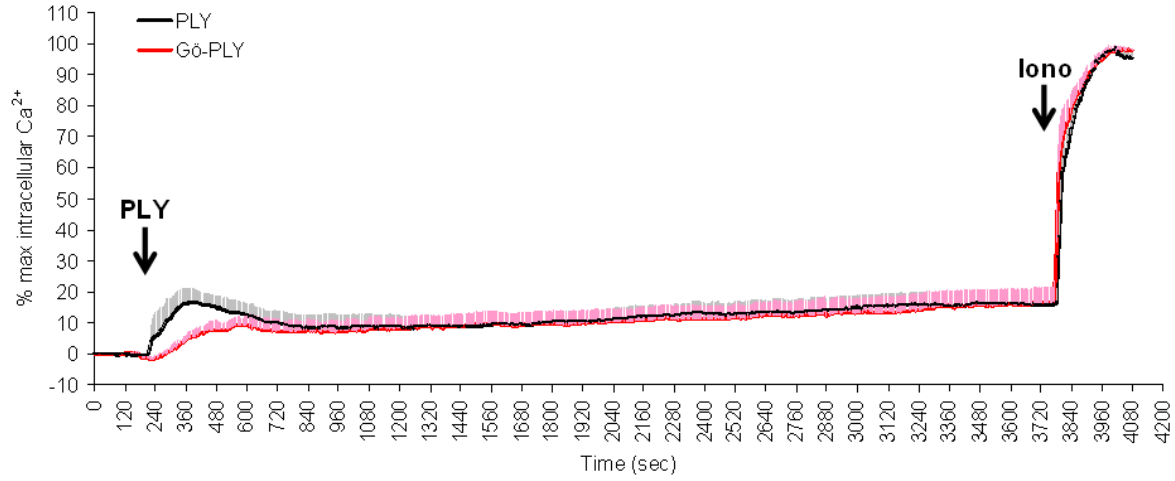

B)

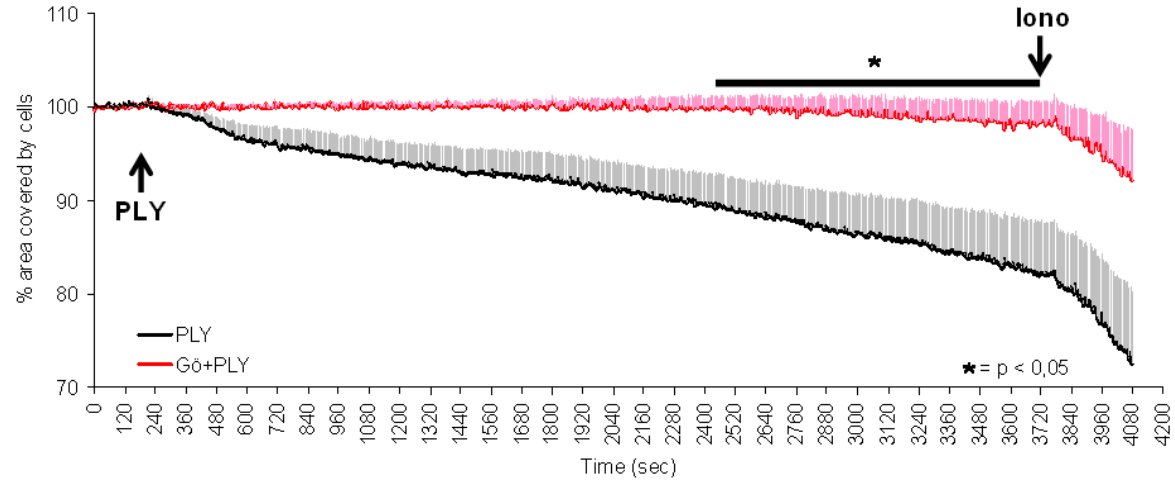

Fig 3.3.8 Cell surface area loss due to PLY is inhibited by Gö6976.
A) H441 cells were loaded with Fura-2 AM and monitored for changes in the emission at 340 and 380 nm when excited at 510 nm. From the emission readings the 340/380 nm ratio was calculated. The maximum signal measured after adding Iono (5 µM) at the end of the experiment was used to express the relative change in $[Ca^{2+}]_i$.
B) The cell surface area was determined by counting the pixels in the acquired images that had a signal above background levels. The pixel count in cells at rest was set to 100%. The graphs represent the area loss in the same experiments that are shown in A.
The cells were treated at indicated times with PLY+DTT at 100 ng/ml (black line) or were pretreated with Gö6976 (1 µM) for 10 min before PLY+DTT at 100 ng/ml was added (grey line).
In A) and B), the graphs show the mean values + SEM of at least three independent experiments for each group.

Cells treated with sublytic PLY concentrations, showed a characteristic peak in $[Ca^{2+}]_i$ that lasted for about ten minutes and then fell to a slightly elevated level that slowly increased over time (Figure 3.3.8A). The reaction in cells pretreated with Gö6976 was initially weaker but not significantly different and adapted the same slowly ascending levels some ten minutes after the PLY addition. In contrast to that, the difference in cell surface loss between the two groups was significant. PLY-treated

cells continued to shrink from shortly after the toxin was administered until the end of the experiment, amounting to a mean loss of over 15% surface area in one hour. The pretreatment with the cPKC inhibitor abolished cell surface area loss almost completely.

The lectin-like domain of tumor necrosis factor (TNF) was found to protect against pulmonary oedema formation in animal models and to alleviate the LLO-induced hyperpermeability of endothelial cells (Xiong *et al.*, 2010; Bloc *et al.*, 2002; Yang *et al.*, 2010; Elia *et al.*, 2003).The effect of the TNF-domain is mimicked by an artificially synthesized peptide called TIP. It was therefore investigated whether TIP was also able to prevent the loss of cell surface area in PLY-treated cells.

Cells treated with PLY alone showed a similar reaction than described before in figure 3.3.8, with an initial Ca^{2+}-peak and a loss of about 10% of the total cell surface area in one hour (Figure 3.3.9A, black line). The same was observed in cells pretreated with a control peptide containing the same amino acids as TIP but arranged in a random order (sTIP, gray dotted line). The only difference to PLY treated cell was a second small, delayed Ca^{2+}-Peak. Cells pretreated with functional TIP (black dotted line) presented an initial peak similar to sTIP pretreated ones but later dropped to a level that was lower than before the toxin was added. There were no significant changes between the three groups regarding $[Ca^{2+}]_i$. No significant difference cell surface area between sTIP pretreatment and PLY alone was detected (Figure 3.3.9B), although the cells that were incubated with the non-functional peptide suffered a somewhat stronger loss in surface area. In cells pretreated with TIP, there was only a small decrease in cell volume that was significantly lower than in the other two groups.

A)

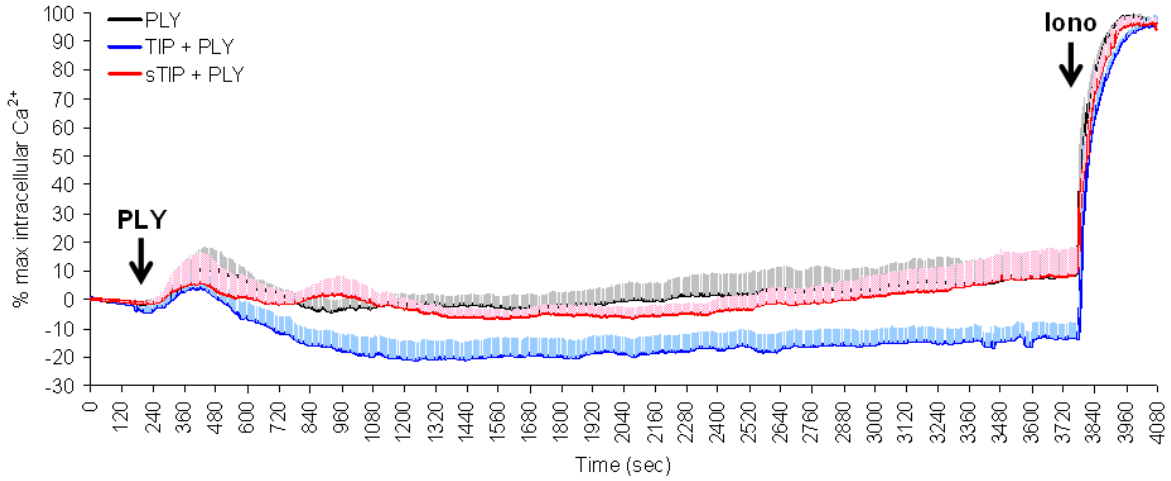

B)

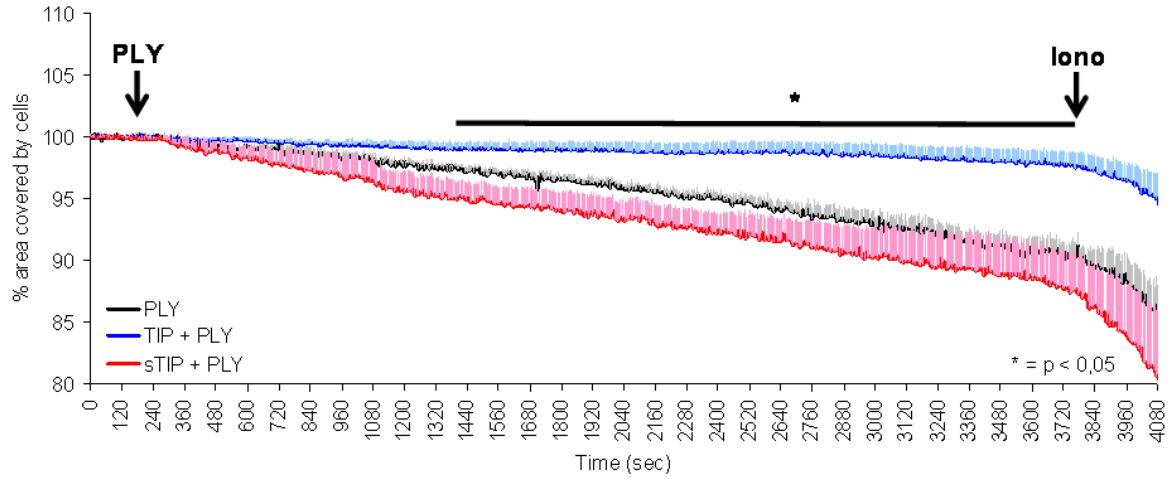

Fig 3.3.9 Cell surface area loss due to PLY is inhibited by TIP.
A) H441 cells were loaded with Fura-2 AM and monitored for changes in the emission at 340 and 380 nm when excited at 510 nm. From the emission readings the 340/380 nm ratio was calculated. The maximum signal measured after adding Iono (5 µM) at the end of the experiment was used to express the relative change in $[Ca^{2+}]_i$.
B) The cell surface area was determined by counting the pixels in the acquired images that had a signal above background levels. The pixel count in cells at rest was set to 100%. The graphs represent the area loss in the same experiments that are shown in A.
The cells were treated at indicated time points with PLY+DTT at 50 ng/ml (black line) or were pretreated with TIP (50 µg/ml) (black dotted line) or sTIP (50 µg/ml) (grey dotted line) for 30 min before PLY+DTT at 50 ng/ml was added.
In A) and B) the graphs show the mean values + SEM of at least three independent experiments for each group.

4 Discussion

4.1 The role of listeriolysin O in *Listeria monocytogenes'* ability to cross the epithelial barrier

The intestinal epithelium forms the first line of defence against food borne pathogens. Exactly how *L. monocytogenes* is able to cross this barrier after being taken up through contaminated food has been an unsolved question for a long time. The requirement of *L. monocytogenes* to establish a successful infection in the human host is its intracellular survival and replication (Tilney and Portnoy, 1989). It is well equipped to invade a range of different cell types, proliferate in their cytosol and spread to neighbouring cells without being detected by the immune system (Vázquez-Boland *et al.*, 2001). The bacterium harbours virulence factors, the internalins, which enables it to trigger its uptake into epithelial cells. Internalin A (InlA) specifically binds the epithelial transmembrane adhesion molecule ECad and induces bacterial uptake into the cytoplasm (Mengaud *et al.*, 1996). The problem that has to be overcome by the pathogen is that ECad, which forms the adherens junctions (AJ) in epithelial monolayers, is protected from access through the apical side of the barrier by tight junctions (TJ). This prevents the bacteria from entering directly into the cytoplasm of epithelial cells and their further spread in the host. Recently, cell extrusions displaying unprotected ECad on the apical side of the intestinal barrier were discovered as sites of *Listeria* attachment and invasion (Pentecost *et al.*, 2006). There is more evidence today from whole tissue samples of animals that some specific areas of the intestine provide windows of opportunity for *L. monocytogenes* to reach behind the epithelial barrier (Nikitas *et al.*, 2011). It was shown that the bacteria can translocate swiftly from the apical to the basolateral side of the epithelium once they find accessible ECad. This process relies solely on InlA and is independent of other virulence factors like ActA and LLO. Yet, the virulence factor LLO is an absolute necessity for the pathogenicity of *L. monocytogenes*. So far, the proposed main function of LLO in *Listeria* infections is its ability to provide a route of escape from macrophage phagosomes (Geoffroy *et al.*, 1987; Gedde *et al.*, 2000). This prevents the destruction of the pathogen by fusion of the phagosome with the lysosome and allows it to proliferate in the cytoplasm and spread to other cells.

This work is based on other theories about possible functions of LLO to explain the invasive abilities of the pathogen. When applied extracellularly, LLO by itself has a

number of effects on eukaryotic cells even at sublytic concentrations (Gekara *et al.*, 2007). It forms permeable pores in the plasma membrane of cells, thereby allowing the influx of extracellular Ca^{2+} (Repp *et al.*, 2002). Ca^{2+} is an important intracellular second messenger and uncontrolled changes in its cytoplasmic concentration can trigger different cellular reactions (Berridge *et al.*, 2000). A connection between LLO-mediated membrane perforation and the invasiveness of *L. monocytogenes* in epithelial cells was only briefly addressed in a single publication (Dramsi and Cossart, 2003). The authors found that bacterial entry is dependent on the influx of extracellular Ca^{2+} through LLO pores but did not identify the responsible mechanism. The main goal of the following experiments was to elucidate whether, and if, how the LLO-induced perturbations of the intracellular calcium homeostasis in epithelial cells facilitate the entry of the pathogen.

Caco-2 cells, a continuous line of heterogeneous human epithelial colorectal adenocarcinoma cells that resemble the enterocytes lining the small intestine in phenotype and polarisation (Hidalgo *et al.*, 1989), were chosen for this approach. The cells form a closed epithelial monolayer if grown to confluence. The use of video-microscopy in combination with a ratiometric method to measure the intracellular Ca^{2+} concentrations ($[Ca^{2+}]_i$) allowed for continuous recordings and the simultaneous evaluation of three parameters: cell viability, the changes in $[Ca^{2+}]_i$ levels and alterations of cellular volume.

4.1.1 Purified LLO forms Ca^{2+}-permeable pores in cultured epithelial cells

At first, it was tested if purified LLO could trigger an increase in $[Ca^{2+}]_i$ when simply added to cholesterol-free growth medium at physiological pH and temperature. In accordance to the findings of Repp *et al.* (Repp *et al.*, 2002) LLO causes a dose dependent increase in $[Ca^{2+}]_i$ (Figure 3.1.1B). The heat inactivation of LLO did not yield cellular responses, thereby proving that the active toxin is indeed responsible for the $[Ca^{2+}]_i$ changes observed. The reactions to LLO varied between single cells. This might be due to an unequal distribution of toxin molecules over the cell layer or the heterogeneity of the used cell line (Figure 3.1.1A). Despite the observed differences, the cellular reaction to LLO followed a common pattern. First, a few seconds after the toxin was added, an initial peak in $[Ca^{2+}]_i$ occurred. Thereafter, the $[Ca^{2+}]_i$ showed a fluctuating curve that slowly decreased and levelled off towards the

end of the experiment. The mean values of the measured curves of at least 30 cells in each experiment were calculated to account for the observed variations.

4.1.2 Preincubation with a reducing agent strongly increases LLO activity

CDCs were formerly known as thiol-activated cytolysins because almost all family members are inactivated under oxidising conditions (Cohen *et al.*, 1937). This can be reversed by incubating the toxins with reducing agents like DTT (Westbrook and Bhunia, 2000). Indeed purified LLO was about 50 times more active when preincubated with 5 mM DTT (Figure 3.1.2). This allowed for a reduction of toxin concentrations in the following experiments. It is still unclear what mechanism is responsible for the activation and stabilisation of the toxin molecules under reducing conditions. A single cysteine residue within the tryptophan-rich C-terminal region (the undecapeptide) that is conserved in most of the CDCs was thought to be responsible for that effect (Smyth and Duncan, 1978). This cysteine residue is, however, not required for pore formation, but responsible for the sensitivity to reducing and oxidising environments (Saunders *et al.*, 1989; Bernheimer and Avigad, 1970; Morgan *et al.*, 1996; Billington *et al.*, 1997). Upon introduction in toxins that naturally do not contain this cysteine residue, the sensitivity to reducing and oxidising agents can be reinstated (Billington *et al.*, 2002). How a single residue with the ability to form disulfide bridges can increase the stability of large toxin complexes (pores) is unclear. An explanation for the importance of this one cysteine would be to invoke the idea of the presence of a so called “cysteine switch”, a mechanism known from matrix metalloproteinases. This switch provides a way of turning on an enzymatic function or a protein activity by intramolecular conformational changes.

LLO within the phagosome of macrophages was shown to be reduced and activated by the thiol reductase GILT (Singh *et al.*, 2008). When secreted by bacteria in the intestinal tract it would also be in its active state due to the lack of oxygen and the ensuing reducing environment.

4.1.3 Treatment with LLO leads to an $[Ca^{2+}]_i$ –dependent reduction of the overall surface area covered by epithelial cells

When the single frames of the recorded measurements were evaluated it became obvious that the cells reacted to the incubation with LLO not only with an increase in $[Ca^{2+}]_i$ but also with a reduction in the total area covered by the cells (Figure 3.1.3A).

About five to ten minutes after the toxin addition the cell monolayer began to shrink back from its original size. This behaviour could be quantified by using the TillVision software package. After defining the intensity background levels the software converted all non-background signals (=cells) to a uniform pixel colour that was subsequently counted frame by frame. The change in amount of pixels representing cells was plotted on a graph as a percentage of the signal before the addition of LLO. Thereby, the loss of cell surface area could be quantified simultaneously to the changes in $[Ca^{2+}]_i$. Employing this method, a continuous shrinking of cells could detected, starting approximately two minutes after toxin-induced Ca^{2+} effects were detectable (Figure 3.1.3B).

An emerging question was whether the loss in cell surface area was directly connected to the disturbance of the intracellular calcium homeostasis. Hence, an unspecific calcium channel inhibitor, $LaCl_3$, was used to block the ion influx through the toxin pores. Lanthanides and other trivalent metal ions have been used before to block LLO-induced Ca^{2+} flow through plasma membranes (TranVan Nhieu *et al.*, 2004; Bittenbring, 2005; Butler, 2004; Repp *et al.*, 2002; Dramsi and Cossart, 2003) and La^{3+} was found to have the lowest $IC_{(50)}$ value (Bittenbring, 2005). Previous studies employing electrophysiological methods proposed pores consisting of as little as three toxin molecules when using low LLO concentration (Repp *et al.*, 2002; Butler, 2004). These pores would have a much smaller diameter than the ones consisting of up to 50 monomers described with electron microscopy. This might explain the pores' relative specificity for Ca^{2+} and how lanthanum ions are able to block them.

When cells were preincubated with 10 mM $LaCl_3$, no reaction to the addition of LLO was observed. Even very high concentrations (250 ng/ml) of DTT-activated LLO could not trigger changes in $[Ca^{2+}]_i$ or the cell surface area (Figure 3.1.4). When $LaCl_3$ was given one minute after the toxin, the increase in $[Ca^{2+}]_i$ stopped immediately and remained steady somewhat above the baseline. Also, no cell shrinking could be observed in this experiment. LLO alone at the same concentration (20 ng/ml) caused an approximately two times higher increase in $[Ca^{2+}]_i$ and a drop in the cell surface area. Finally, Thapsigargin was administered to see if the intracellular Ca^{2+}-stores were still intact. Thapsigargin inhibits the SERCA, which leads to a release of ER-stored Ca^{2+} that can be detected in the cytoplasm as a slow increase in $[Ca^{2+}]_i$ that forms a very broad peak (Thastrup *et al.*, 1990). In related experiments

with PLY the addition of Thapsigargin induced no further increase in $[Ca^{2+}]_i$ (see appendix section 8.2). This might be because the amount of Ca^{2+} released from the ER was not large enough and was covered by the massive influx through the pores in the plasma membrane. Alternatively, the ER might have been damaged by the toxin incubation in some way and subsequently was emptied of Ca^{2+}. As both LLO and PLY form Ca^{2+}-permeable pores, the results from one toxin probably resemble the ones of similarly-conducted experiments with the other. Therefore, it was presumed that administration of Thapsigargin after LLO incubation would also show no further increase in $[Ca^{2+}]_i$. When $LaCl_3$ was added before or shortly after LLO, the subsequent treatment with Thapsigargin triggered a slow increase in $[Ca^{2+}]_i$, indicating that the intracellular Ca^{2+}-stores were not affected. This indicates that blocking LLO pores protects intracellular Ca^{2+}-stores from direct or indirect effects the toxin might have on them. The release of ER-stored Ca^{2+} by Thapsigargin had no effect on the cell surface area. These findings indicate a direct link between the influx of extracellular Ca^{2+} and the shrinking of epithelial cells. The reason for the volume loss might be due to an osmotic reaction to the intracellular ion balance. When an imbalance was prevented by blocking the toxin pores the cells did not react with a reduction of their volume.

4.1.4 Lanthanum reduces *L. monocytogenes* invasiveness in epithelial monolayers and has bactericidal effects at millimolar concentrations

A reduction of the cell volume and ensuing strains or eventual breaks in intestinal epithelial monolayers might be helpful for *L. monocytogenes* in entering the host. The breaking of TJs and AJs would provide the bacteria access to ECad, the ligand for InlA, the virulence factor that triggers the bacterial uptake into epithelial cells (Figure 4.1.1). Therefore, it was tested if the action of LLO on epithelial monolayers *in vitro* would increase the amount of bacteria inside the cells. Again, $LaCl_3$ was used to block the shrinking of cells due to the toxin's action when incubated with bacteria. This group was compared to mock-treated cells that were also infected with the same MOI of *L. monocytogenes*.

To be sure that $LaCl_3$ had no deleterious effects on the pathogen the supernatants were also checked for bacterial numbers. The results showed that increasing concentrations of $LaCl_3$ could significantly reduce the number of bacteria inside cells and significantly increase their number in the supernatant in a dose-dependent

manner (Figure 3.1.5). This is in accordance to the observations of Dramsi and Cossart (Dramsi and Cossart, 2003). They also used $LaCl_3$ to reduce the internalisation of *L. monocytogenes* but did not dwell on the link between Ca^{2+}-influx and cell shrinking.

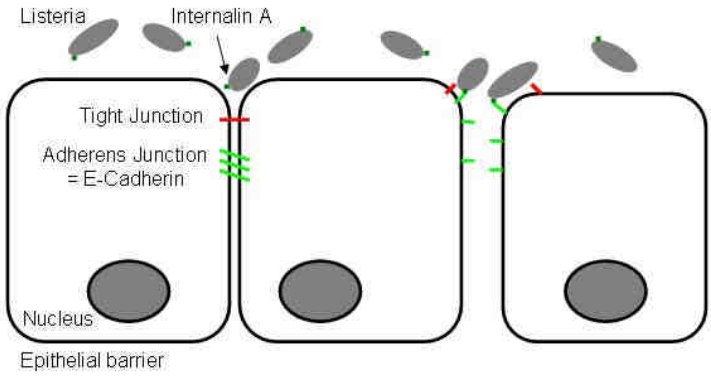

Fig. 4.1.1 Model for invasion of epithelial cells by *L. monocytogenes*. ECad is inaccessible to bacteria in functional epithelial barriers. Volume loss triggered by LLO would cause TJ breakdown, making ECad available.

Another interesting finding was that high amounts of $LaCl_3$ seemed to be toxic for the pathogen. At concentrations of 1 mM $LaCl_3$ and above, the bacterial numbers were strongly reduced inside as well as outside the cells. At concentrations of 5 mM and 10 mM, it was not possible to detect any CFUs on the agar plates when the cell lysates and supernatants were plated out undiluted.

To ensure that the observed reduction in bacterial numbers was indeed an effect of $LaCl_3$ the following experiment was conducted. The same amount of bacteria was incubated in exactly the same medium and $LaCl_3$ concentrations as in the previous experiment, but without the epithelial cells. Interestingly, the results were not the same as before. The bacteria did not only tolerate the presence of $LaCl_3$ better, but at a concentration of 1 mM they did actually grow to significantly higher numbers than the control group (Figure 3.1.6). This was surprising, taking into account the sparse composition of the medium used. HEPES medium basically is just an isotonic and buffered solution containing no growth essentials like amino acids or trace metals besides Ca^{2+} and glucose. In the presence of 2.5 mM $LaCl_3$; the bacterial count was unchanged in comparison to the control. At higher concentrations the numbers of live bacteria was reduced significantly. The CFUs went down by three log steps when incubated with 5 mM $LaCl_3$ and by six log steps with 10 mM, but there were still colonies found to be counted. The difference in bacterial resistance to $LaCl_3$ in the

presence or absence of cells could be caused by the active bacterial defence that is known from epithelial cells. This includes the production and release of antimicrobial peptides and reactive oxygen species. When the bacteria are subject to negative influences from both the cells and $LaCl_3$, it is to be expected that their survival suffers under double pressure.

The influence of $LaCl_3$ on bacterial growth and survival was tested in more detail by establishing growth curves of *L. monocytogenes* in different media and increasing concentrations of $LaCl_3$ (Figure 3.1.7). In HEPES medium, the untreated bacteria showed only a minimal increase in OD over the measurement period of ten hours. All groups grown together with $LaCl_3$, with the exception of the two highest concentrations, were able to reach OD levels twice as high as the control. When 5 and 10 mM $LaCl_3$ were added to the microplate wells used in this assay a cloudy, white precipitate formed that made it impossible to detect the minuscule changes in OD values in HEPES medium. Even the background correction with the same $LaCl_3$ concentrations measured without bacteria could not counter this effect. The other two media used were MM, a minimal growth medium for bacteria and BHI, a rich and complex medium to achieve fast proliferation and dense cultures. The outcome in MM was similar to HEPES. The bacteria achieved higher OD values when growing in media containing $LaCl_3$, except for the highest concentration. In 10 mM $LaCl_3$, the bacteria grew distinctly worse but were still able to increase the optical density of the culture. It appeared that the gain in growth compared to the control in all other groups was lower than in the previous experiment. Also, the problem with precipitations of high $LaCl_3$ concentrations was less pronounced so that all groups could be evaluated. When the bacteria were cultured in BHI, the presence of $LaCl_3$ had completely different effects on the growth curves. Here, lower concentrations of up to 0.5 mM $LaCl_3$ had no influence on the multiplication speed or maximum OD values when compared to the untreated control. The groups treated with higher amounts clearly showed a dose-dependent growth inhibition. At concentrations of 1 mM $LaCl_3$, the growth curve was identical to lower concentrations for up to five hours, after that it showed a weaker increase and levelled off shortly below the maximum OD of the control. Similar results were obtained in the 2.5 mM group that reached a plateau phase at a somewhat lower density. In the 5 mM group, the ascending slope of the growth curve was less steep and achieved a density that was about one third smaller than the control. High concentrations of $LaCl_3$ (10 mM) seemed to have almost

bacteriostatic properties in BHI, as bacterial proliferation was strongly inhibited and the maximum density was about 75% below control values. From these multifaceted results one might conclude that there is a link between the availability of growth factors in the environment and the tolerability and even use of $LaCl_3$ by the bacteria. There are reports that La^{3+} can increase the function of enzymes needing metal ions as cofactors or even replace the cations for enzymatic functions (Pang *et al.*, 2002; Zhang *et al.*, 2003, 2006). The most important cofactor for bacterial growth is iron (Fe). It is vital for energy production, gene regulation and DNA biosynthesis and therefore an absolute requirement for replication (Andrews *et al.*, 2003) . The fact that enzymes like catalase and superoxide dismutase are more active in the presence of La^{3+} indicates that it is able to assume some functions of Fe-ions. As the medium becomes more complex and complete this could turn into a negative effect, where lanthanum ions at high concentrations compete with other metal ions of better functionality. This has been reported for some enzymes (Huber and Frieden, 1970; Marquis and Black, 1985) and could cause the observed reduction in replication efficiency. There is only little information in the literature about the toxicity of lanthanum towards bacteria. Early works dealing with the effects of lanthanides on bacteria are reviewed by Burkes and McCleskey (Burkes and McCleskey, 1947). The authors report that there were several studies between 1894 and 1941 that came to the same conclusions about the conflicting effects of low and high concentrations of $LaCl_3$ on bacterial growth. The latest publications found that low amounts of La^{3+} increase the cell permeability of E. coli in a way that allows the bacteria to access nutrients in the medium more easily. Higher concentrations, on the other hand, were toxic to the bacteria because they accumulated inside the cells and disturbed their growth (Peng *et al.*, 2004; Liu *et al.*, 2006).

To summarize this section, it can be stated that $LaCl_3$ has differential effects on *L. monocytogenes* that are highly dependent on the environmental conditions. In the invasion model low concentrations reduced the number of bacteria found inside cells while increasing bacterial numbers in the supernatant. This strengthens the hypothesis that LLO-induced cell shrinking facilitates invasion of closed epithelial monolayers for *L. monocytogenes* by disrupting intercellular junctions and thereby making ECad accessible. The same low concentrations were found to be harmless to the bacteria; they even allowed better bacterial growth in the minimal medium used for these experiments. The latter is also true for higher $LaCl_3$ concentrations (1 and

2.5 mM) that were found to be non-toxic for the bacteria when applied in the absence of cells. In contrast to that, these two concentrations significantly reduced bacterial numbers in the invasion model. It seems like the bacteria can tolerate and even make use of $LaCl_3$ when no other factors, like the active bacterial defence of epithelial cells, cause disadvantageous conditions. The mechanisms the bacteria use to cope with unfavourable environments, whatever they might be, most likely fail when facing both cellular defences and higher $LaCl_3$ concentrations.

4.1.5 The assessment of LLO mutants allows insights into its function

The mechanism of pore formation by CDCs as it is understood today has been described in chapter 1.2. There are still plenty of open questions concerning the exact process of intermolecular binding and oligomerization of single toxin molecules after binding to a membrane.

Towards this end, there have been no studies focusing on the role of single amino acid residues in domain 1 of LLO. The single amino acid mutations already studied in LLO were located either in the signal peptide on the N-terminal side of the protein or in the tryptophan-rich undecapeptide. These were aimed to understand and manipulate the secretion of LLO and its binding to cholesterol dependent membranes respectively (Schnupf *et al.*, 2006; Lety *et al.*, 2002; Glomski *et al.*, 2002; Michel *et al.*, 1990; P. Tang *et al.*, 1996).

To address the functional role of domain 1, mutants were created by collaborators (see section 2.10). These were tested for their haemolytic activity and the ability to induce an increase of $[Ca^{2+}]_i$ and a reduction in cell surface area. The results (Table 3.2.1) might give an idea about the functional importance of the altered residues.

To generate comparable results, the toxins were tested at the same concentration in the microscopic experiments. The relative activity was expressed in percent of maximum increase in $[Ca^{2+}]_i$ and the percentage of lost surface area. In the haemolytic assay, the amount of toxin necessary for 50% of total lysis was determined by dilution and expressed as percent of control values. All mutation sites are indicated in figure 4.1.2.

The LLO mutants could be separated into three groups. The first yielded a stronger reaction throughout all three tested parameters. This group consisted of:

- A40W, where alanine was exchanged with tryptophan to see if a sterical hindrance by the introduction of a very large residue at this position would

interfere with toxin activity. This was obviously not the case as this mutant was highly lytic and induced a very strong influx of Ca^{2+} and reduction in cell surface area.

- S44D, where serine was exchanged with aspartic acid. From the literature it is known that an amino acid swap at this site could interfere with a possible phosphorylation of the serine residue (Schnupf *et al.*, 2006), which resulted in increased cytotoxicity. This finding contradicts the increased activity of the S44D mutant, as this exchange was aimed to simulate a permanently phosphorylated site. As the group of Schnupf *et al.* used intracellular bacteria and their survival in macrophages as indicators it is questionable whether the results are comparable to the use of purified toxin alone.
- delta 51 was a mutant lacking the first 51 amino acids, including the signal peptide and the PEST sequence. As both are only necessary if LLO is to be produced and secreted by L. monocytogenes in infection situations it was not expected that this mutant would suffer a loss in activity. Lety et al. (Lety et al., 2001) also reported an increased haemolytic activity in LLO mutants lacking the PEST sequence, a finding that correlates with the results presented in this work.
- N230W, where asparagine was exchanged with tryptophan. This was the only mutation lying outside domain 1. It was introduced to determine the importance of a polar uncharged side chain at this site. The introduction of a large hydrophobic residue resulted in a somewhat reduced haemolytic activity. Nonetheless the influx of extracellular Ca^{2+} and the cell shrinking were stronger than in the wild type.

In the second group, one parameter was increased compared to the control, whereas lower values were observed in the other two tests. This group consisted of:

- S44E, where serine was changed to glutamic acid. This mutant was constructed with the same intention as S44D. The idea was to emulate a constantly phosphorylated residue. In this case, the haemolytic activity and the ability to induce an influx of extracellular Ca^{2+} were somewhat lower than in the wild type, while the loss in cell surface area was higher. The reason for the stronger cell volume reduction is not clear but might be due to differences in the status of cultured cells.

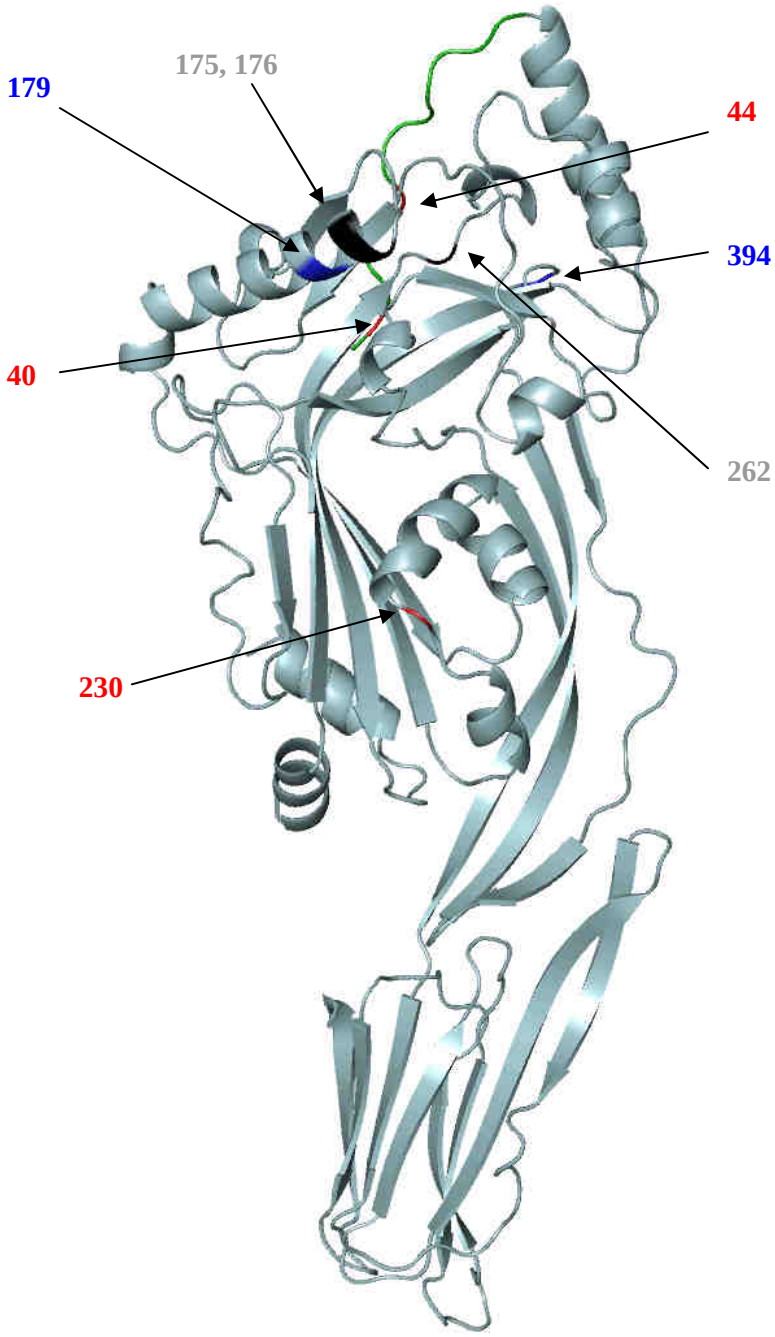

Fig. 4.1.2 A single LLO molecule including coloured mutation sites. The colour-coding is the same as in table 3.2.1. The green colour represents the first 51 amino acids at the N-terminus. Crystal structure of LLO as resolved by Köster (2010) used with permission from the authors.

- N179C, where asparagine was exchanged with cysteine. The idea was to enhance the oligomerization of LLO by introducing another possible site for disulfide bond formation. Indeed, this mutant was more haemolytic and triggered a stronger increase in $[Ca^{2+}]_i$, Only the loss of cell surface volume was not as pronounced as in the wild type.

- D394W, where aspartic acid was exchanged with tryptophan to reveal whether an acidic residue was necessary at this position. The introduction of a bulky side chain decreased the effects of the toxin on epithelial cells with slightly lower Ca^{2+} influx and less shrinking, but led to a better haemolytic activity.

It should be mentioned at this point that the previously described mutants yielded effects close to those of the wild type, regardless of minor deviations in the activities in the three test parameters. It was concluded that none of the substitutions mentioned above were actually inhibiting the functionality of LLO in a crucial fashion.

The third group of mutant toxins on the other hand displayed severe inabilities in lysing erythrocytes and triggering reactions in epithelial cells, hence it is concluded that they are crucial for LLO function. This group consisted of:

- K175E, where lysine was exchanged with glutamic acid. This mutant had no effects on epithelial cells and showed only very little haemolytic activity. The swap of a positively charged side chain with a negative one indicates that the correct charge at this position is vital for LLO's function.
- S176W, where a serine was exchanged for a tryptophan to evaluate the effects of a sterical hindrance at this position. The results were the same as for the previous mutant, indicating that this section of the molecule is important for toxin functionality.
- E262W, where glutamic acid was exchanged with tryptophan. The haemolytic activity of this mutant was reduced below 20% as compared to the wild type and epithelial cells did not react to this toxin. A negative charge at this site seems to plays an important role in toxin function.
- delta 51 + K175E, a combination that was only half as haemolytic as K175E alone. This mutant was produced to see if there was an interaction with the first 51 amino acids of neighbouring toxin molecules and the L175 site. This seemed to be the case as the double mutant performed much worse in lysing erythrocytes.
- delta 51 + S176W, a double mutant that had an activity that was reduced by a factor of 10^6. As in the previous mutant the idea was to check for interactions between the N-terminal region of the toxin and the α-helical region in which S176 is located. This mutant had the lowest activity of all

tested LLO variants, which points towards the importance of this site and its interactions with the N-terminal region of adjacent molecules.

- A40W + K175E, which was generated due to the same train of thought as the other two double mutants. Again, the question was if there were interactions between K175 and the N-terminal side of the bordering toxin molecules. The effect was a further reduction in haemolytic activity, similar to the delta 51 + K175E mutant. This indicated that single residues in the first 51 amino acids and their interactions with other side chains in domain 1 of the toxin are important for the functionality of LLO.

In conclusion, the results from the mutant toxins allowed an insight into the importance of single residues in domain 1 and the first 51 amino acids on the N-terminal side of LLO. The combination of changes in the α-helical region in which K175 and S176 are located and the deletion of the N-terminal region of the protein toxin produced mutants that were significantly less active than the single mutants. This led to the hypothesis that these two regions in domain 1 are important for the binding and oligomerization of LLO molecules to form a prepore complex. The mutations that did not yield a negative change in the toxins functionality were either not crucial for its activity or, like in the case of delta 51 or A40W, could be compensated for in some way. The exact mechanisms will have to be studied in more detail to increase the understanding of functional importance of residues in domain 1.

4.2 Effects of pneumolysin on epithelial monolayers

The most common cause for pneumonia are bacteria and especially *Streptococcus pneumoniae*, which is found in about half of all patient isolates (Sharma *et al.*, 2007; Anevlavis and Bouros, 2010; Frei *et al.*, 2011; Waterer *et al.*, 2011). The bacteria colonize the upper respiratory tract in a part of the healthy population and opportunistically establish infections in the very young, the elderly or immunocompromised individuals. In these risk groups, they may cause medical conditions like acute sinusitis, otitis media, meningitis, bacteraemia, sepsis, osteomyelitis, septic arthritis, endocarditis, peritonitis, pericarditis, cellulitis, and brain abscess (Siemieniuk *et al.*, 2011; Musher, 1992). *S. pneumoniae* carries an array of virulence factors (Mitchell and Mitchell, 2010). The most important ones are the polysaccharide capsule and PLY, the latter being found in all clinically relevant

isolates (Paton and Ferrante, 1983; Paton *et al.*, 1993). The bacterial capsule inhibits phagocytic clearance of the pathogen and hinders the recognition of bound complement and antibodies by the immune system (Jonsson *et al.*, 1985; Musher, 1992). Furthermore, it prevents the mechanical removal of the bacteria with mucus and reduces the exposure to antibiotics (van der Poll and Opal, 2009; Nelson *et al.*, 2007). PLY plays a crucial role in the pathogens ability to invade the host and cause detrimental invasive diseases like sepsis and meningitis (Kadioglu *et al.*, 2002; Orihuela *et al.*, 2004; Berry *et al.*, 1989). Unlike the other toxins in the group of CDCs, it is not actively secreted but stored in the cytoplasm of *S. pneumoniae* and is released upon lysis of the bacterial cells. This can be triggered by either the bacterial virulence factor autolysin, antimicrobial actions from the host immune system or antibiotics (Nau and Brück, 2002; Kalin *et al.*, 1987; Wheeler *et al.*, 1999; Howard and Gooder, 1974). Some PLY is also released during the growth of *S. pneumoniae* in an autolysin-independent manner (Balachandran *et al.*, 2001). The toxin has multiple effects on the host that prevent *S. pneumoniae* from being mechanically removed or killed (Rubins and Janoff, 1998). Moreover, it can promote the pathogen's invasiveness. This is due to the toxic effects of PLY on epithelial and endothelial cells (Rubins *et al.*, 1992, 1993; Steinfort *et al.*, 1989). There is also evidence from microscopic studies that the toxin disturbs the integrity of the epithelial barrier in primary tissue derived from the upper respiratory tract (Rayner *et al.*, 1995; Feldman *et al.*, 2002). Taking together the existing evidence, it can be assumed that PLY plays a critical role in the pathogens ability to cause pneumonia, cross the epithelial barrier in the lung and the blood-brain-barrier to induce meningitis.

The following experiments aimed to elucidate the role of the pore forming action of PLY and the subsequent influx of extracellular calcium in the disruption of pulmonary epithelial monolayers. The hypothesis was, much like as with LLO, that sublytic concentrations of the toxin can trigger cellular reactions that facilitate the entry of *S. pneumoniae* into the host. Most of the previous studies that were looking at the effects of PLY on the intracellular calcium homeostasis were done in neuronal or immune cells. These findings mainly focused on the induction of apoptosis (Stringaris *et al.*, 2002), the role of PLY in neuronal damage in general (Braun *et al.*, 2002) and the suppression of important defence mechanisms (Nandoskar *et al.*, 1986; Kadioglu *et al.*, 2000). In 2007, the group of Iliev *et al* (Iliev *et al.*, 2007) reported that PLY is able to induce changes in the actin cytoskeleton of human neuroblastoma cells. The

group further investigated the effects of PLY on other neuronal cell types and concluded that, although the toxin pores were necessary for the observed remodelling of the cytoskeleton, it was the influx of extracellular calcium ions through endogenous Ca^{2+}-channels that triggered the changes in cell morphology (Iliev *et al.*, 2009; Wippel *et al.*, 2011; Hupp *et al.*, 2012).

In order to investigate the ability of purified PLY to form Ca^{2+}-permeable pores at sublytic concentrations the same experimental approach was chosen as for LLO. The cell line used for all experiments with PLY is called H441 and consists of human lung adenocarcinoma epithelial cells. This cell line forms closed epithelial monolayers if grown to confluence and is widely used as a model for lung epithelium.

4.2.1 Purified pneumolysin forms Ca^{2+}-permeable pores in cultured epithelial cells

To verify the activity of purified PLY, the toxin was added to the cells at a concentration of 2000 ng/ml. The response to the presence of the toxin was an immediate increase in the 340/380 nm ratio, which indicated an influx of extracellular Ca^{2+} through the PLY-pores into the cytoplasm of H441 cells. This correlates with the previously described findings in other cell types that were incubated with PLY (Cockeran *et al.*, 2001; Braun *et al.*, 2002). Between single cells, the observed changes in $[Ca^{2+}]_i$ varied strongly (Figure 3.3.1A). The reason for this was most probably an uneven distribution of toxin molecules bound to the plasma membrane among the monitored cells. Similar effects occurred with LLO in this work and were also described by others working with the two toxins and looking at the calcium homeostasis of single cells (Braun *et al.*, 2002; Repp *et al.*, 2002).

Preincubation with the reducing agent DTT also increased the activity of PLY. This is consistent with one of the early discovered properties of CDCs. PLY under reducing conditions could be used at about 20 times lower concentrations than the untreated toxin to yield the same amount of Ca^{2+} influx into cells (Figure 3.3.1B) This is a considerably weaker activation than observed for LLO (see 4.1.2). The reason for this discrepancy in the reaction of the two toxins to reducing conditions is not clear; so far there is no information about this or other comparisons of CDCs in the literature. There was also a difference in the dynamics of the $[Ca^{2+}]_i$ increase between PLY and LLO. Cells treated with PLY showed a slow increase that reached a peak two to three minutes after the toxin was added and a steady decline of Ca^{2+}-levels from there until

the end of the experiment. In contrast to that, LLO triggered a sharp peak shortly after addition that declined to somewhat lower Ca^{2+}-levels which then remained constant for the rest of the experiment. The diverging reactions to PLY and LLO were not necessarily due to differences between the toxins but might have simply been caused by the use of two different cell lines.

Using PLY+DTT that was heat-inactivated at 65℃ for five minutes did not yield a response from the cells, indicating that the toxin was the only active substance used in the experiment.

4.2.2 Pneumolysin reduces the overall surface area of epithelial monolayers by toxin-induced influx of calcium ions into the cytoplasm

The evaluation of the single photographs taken by the video microscopy system revealed that almost confluent cells treated with sublytic concentrations of PLY (100 ng/ml) lost contact to one another and started to shrink (Figure 3.3.2A). This started approximately five minutes after the toxin was added and was represented by a loss of junctions between cells and a subsequent opening of intercellular space. Over time these openings increased in size as the single cells lost more and more of their original circumference. At the end of the experiment, large gaps had formed in a formerly closed epithelial layer. As with LLO-treated cells it was possible to quantify the loss of cell surface area. Figure 3.3.2B shows the decline of the total area covered by cells on the same experiment from which the single frames in 3.3.2A were taken. The sudden decline at around 360s was caused by the death of a single cell that is marked with a red arrowhead in part A of the Figure. Dead cells completely lose the fluorescent dye and therefore have a large impact on the whole surface area measurement. To avoid an interference of the data by dead or dying cells only experiments without any such occurrences were evaluated. The frequency of dead cells during all of the experiments was extremely low, indicating that the used PLY concentrations were not lethal to the great majority of cells for the chosen experimental times.

As a consequence of the observations made in the video microscopy footage the status of intercellular junctions in cells treated with PLY was assessed. Closed monolayers of H441 cells were incubated with 100 ng/ml PLY for six hours, fixed and stained with a fluorescence-labelled anti-ECad antibody. ECad is the building block of AJs, which lend physical strength and strain resistance to the epithelial barrier. If

PLY was able to damage the integrity of pulmonary epithelium, it should have a strong influence on AJs. The results obtained by confocal microscopy confirmed this hypothesis and were similar to the ones from the previous experiment (Figure 3.3.3). The control group showed a closed monolayer with strong ECad signals along the intercellular borders. Cells treated with PLY had a much weaker ECad signal and large gaps were found between them (white arrows). Taken together, the results of these last two experiments indicate that PLY has detrimental effects on the integrity of pulmonary epithelial barriers by weakening intercellular junctions and inducing volume loss in cells.

Next, it was examined whether the increase in $[Ca^{2+}]_i$ triggered by the influx of extracellular Ca^{2+} through toxin pores caused the destabilisation of epithelial integrity. Like in the experiments with LLO, the unspecific calcium channel inhibitor $LaCl_3$ was used to block any ion flux through the PLY pores. $LaCl_3$ was found to block Ca^{2+}-influx through PLY pores in patch-clamp experiments (Schramm, 2004). The same study claims the formation of PLY pores consisting of very few molecules when the toxin is used at nanomolar concentrations. In analogy to LLO (Repp *et al.*, 2002), it is likely that PLY also forms small pores at sublytic levels. Indeed, the diameter of PLY pores consisting of 38 subunits was described to be 40 nm in electron microscopy studies using lytic (micromolar) amounts of toxin (Tilley et al., 2005). Sublytic toxin concentrations, as used in here, probably allow only for smaller oligomers to form, as the amount of molecules per cell is limited. This would explain the relative selectivity of the pores for divalent cations (Schramm, 2004) and the blocking capability of the larger lanthanum ions.

When the cells were preincubated with $LaCl_3$, the administration of toxin (100 ng/ml) had no measurable effect on the calcium homeostasis or the cell surface area (Figure 3.3.4). When the inhibitor was given shortly after PLY, the influx of extracellular Ca^{2+} was stopped immediately and the $[Ca^{2+}]_i$ quickly returned to its basal level. There was no change in the cell surface area in this group. PLY alone triggered a strong and fast increase in $[Ca^{2+}]_i$ with peak levels about two fold higher than in cells at rest. This group was the only one to show a decrease in the total surface area covered by cells, which started shortly after the toxin was added and continued until the end of the experiment. In the groups employing $LaCl_3$, it was also checked whether the toxin was able to empty intracellular calcium stores. The SERCA-blocker Thapsigargin was added at the end of the experiments to examine whether the $[Ca^{2+}]_i$ would change

due to the release of calcium ions from the ER. Indeed, the cells in both groups reacted to the presence of Thapsigargin by a slow increase in intracellular calcium levels. This indicated that the incubation with PLY in combination with $LaCl_3$ did not damage the intracellular calcium stores. When the cells were treated with PLY alone, Thapsigargin was not administered because of the relatively small amount of Ca^{2+} stored inside the organelles. The peak caused by the small amount of ER-stored Ca^{2+} would probably not have been detectable due to the massive ion influx from the extracellular space through the toxin pores (see results from a similar experiment in appendix section 8.2).

4.2.3 Pneumolysin depletes intracellular calcium stores independent of endogenous ion channels.

The influence of PLY on intracellular calcium stores was examined in more detail to follow up on the existing evidence in the literature. In 2007, the group of Gekara *et al.* (Gekara *et al.*, 2007) described that LLO-producing *L. monocytogenes* and the purified toxin by itself were able to injure the ER of exposed cells. This group also observed an increase in $[Ca^{2+}]_i$ connected to the damaged organelles and concluded that LLO might directly trigger the release of ER-stored Ca^{2+}. The results in this study were not conclusive about the exact mechanisms behind this. The increase in $[Ca^{2+}]_i$ could be partially inhibited by blocking endogenous ER-calcium channels, hinting the involvement of cellular signalling events.

The following experiments were performed to test whether toxins from the group of CDCs are able to directly release Ca^{2+} from intracellular stores or if they hijack cellular signalling events to do so. By completely removing all extracellular Ca^{2+} before the administration of the toxin, it was possible to visualize the emptying of storage organelles into the cytoplasm. To achieve a completely Ca^{2+}-free extracellular environment, the cells were measured in medium that was prepared without $CaCl_2$. Additionally, the membrane-impermeable metal-ion chelator EGTA was added to remove all traces of Ca^{2+} from the medium before the start of the experiment. When cells were treated with PLY under these conditions, they reacted differently than in medium containing extracellular Ca^{2+} (Figure 3.3.5). The increase in $[Ca^{2+}]_i$ started with a few seconds delay and was represented by an almost symmetrical peak that quickly returned to basal levels. This progression might be interpreted as the release of Ca^{2+} from the stores in the ER until they were

completely depleted. As the internal Ca^{2+} stores were obviously not able to hold their cargo, the cells probably tried to remove excess Ca^{2+} from their cytoplasm to the extracellular space, where the ions would be chelated immediately by the dissolved EGTA. This gradient was probably responsible for the rapid return to initial calcium levels. To prove that the ER was the source of the Ca^{2+} entering the cytoplasm, Thapsigargin was added some time after the toxin. The SERCA-inhibitor did not trigger any further changes in the $[Ca^{2+}]_i$, indicating that the ER was completely depleted of Ca^{2+}. As a proof of concept, cells were treated with Thapsigargin first to empty the ER Ca^{2+}-stores. This treatment resulted in an immediate increase in $[Ca^{2+}]_i$. The reaction to Thapsigargin was stronger than to PLY, arguably because the diffusion through the membrane of the ER was slower than the release caused by PLY, as can be seen in figure 3.3.5. Therefore the $[Ca^{2+}]_i$ could reach higher levels before triggering the cells to remove the surplus ions from the cytoplasm. When PLY was added after Thapsigargin, $[Ca^{2+}]_i$ showed only a minuscule and short-lived fluctuation. The conclusion drawn from this behaviour is that PLY, while still able to perforate the plasma membrane of the cells, could not interfere with the calcium homeostasis because the internal stores were already depleted. These two experimental setups give strong evidence that PLY is indeed able to release ER-stored Ca^{2+} into the cytoplasm. The next question to answer was whether this effect was dependent on endogenous ER calcium-release channels. The two types of channels responsible for the controlled release of Ca^{2+} into the cytoplasm are ryanodine receptors (RyR), which are activated by elevated Ca^{2+}-levels in the cytoplasm, and inositol trisphosphate (IP_3) receptors (IP_3R), which are activated by the second messenger IP_3. To investigate an involvement of these two endogenous channels in the PLY-triggered ER-store depletion, they were pharmacologically deactivated with specific inhibitors. RyR were blocked by Ryanodine (Rya) and IP_3R were inhibited with Xestospongin C (XeC). Cells pretreated with a cocktail of both Rya and XeC showed a very similar reaction to PLY as did untreated cells. The maximum $[Ca^{2+}]_i$ reached was a little lower, but the kinetic of the reaction was basically identical. Thapsigargin was added again at the end of the experiment to verify the Ca^{2+}-depletion of the ER. The SERCA-inhibitor had no further effect, indicating that PLY released the stored Ca^{2+} independent from endogenous ER calcium-release channels. In connection to this, Stavru *et al.* (Stavru *et al.*, 2011) recently reported that LLO is able to interfere with mitochondrial dynamics and

energy production when applied extracellularly. This could also hint to a change in the mitochondrial Ca^{2+}-concentration due to the toxin, a possibility that was not addressed experimentally by the authors. Therefore, this is the first finding of a CDC directly depleting intracellular Ca^{2+}-stores without relying on host signalling pathways.

4.2.4 The effects of pneumolysin on epithelial cells mimic those of hyperosmotic conditions.

The reactions of cells to LLO and PLY, as described in sections 4.1.3 and 4.2.2, respectively, were reminiscent of those to hyperosmotic conditions found in the literature. Cells under hyperosmotic stress are known to show a number of changes in response to the non-physiological conditions (Burg *et al.*, 2007). These include, among others, a rapid loss in cell volume (Hazama and Okada, 1988), a transient increase in $[Ca^{2+}]_i$ (Dascalu *et al.*, 1995; Homsher *et al.*, 1974), the activation of MAP kinase p38 (Han *et al.*, 1994) and the subsequent translocation of the transcription factor NFAT5 from the cytoplasm to the nucleus (López-Rodríguez *et al.*, 2001). The incubation with PLY had triggered a loss in cell surface area that was dependent on the influx of extracellular Ca^{2+} in the previously discussed experiments (see section 4.2.2). Therefore, the toxin's effects were compared to those caused by hyperosmotic stress in the same cell type.

Sorbitol was used as a membrane impermeable solute to increase the osmolarity of the medium from 300 mOsm/kg to 500 mOsm/kg while the cells were monitored for their $[Ca^{2+}]_i$ and their total surface area. Upon addition of 200 mOsm Sorbitol, the $[Ca^{2+}]_i$ increased slightly and returned to basal levels within about four minutes (Figure 3.3.6). Thapsigargin had no effect when given after Sorbitol, suggesting that the ER stores were depleted of Ca^{2+} by the induction of hyperosmotic stress. When the Ca^{2+}-ionophore Iono was administered at the end of the experiment there was a fast and strong peak in $[Ca^{2+}]_i$ that showed an intact ion gradient between the intra- and extracellular space. These findings are consistent with the existing results from other groups (Homsher *et al.*, 1974; Hazama and Okada, 1988). To assess the influence of extracellular Ca^{2+}, a second group of cells was preincubated with $LaCl_3$ to block the ion flux through eventually opened endogenous membrane channels upon induction of hyperosmotic stress. The pretreated cells reacted differently to the hyperosmotic stimulus, their initial increase in $[Ca^{2+}]_i$ was slower but had an almost doubled magnitude compared to the non-pretreated cells. Over the next minutes the

calcium levels dropped only slightly and did not respond to the addition of Thapsigargin. The explanation for this diverging behaviour could be the same as in the case of Thapsigargin causing a stronger signal in Ca^{2+}-free medium than PLY (see section 4.2.2). The slower rise was possibly due to the unspecific calcium channel blocker $LaCl_3$ inhibiting migration of extracellular ions through membrane channels into the cytoplasm. In this scenario, all of the Ca^{2+} released would have originated from the ER, which fittingly did not react to incubation with Thapsigargin. Additionally, the presence of $LaCl_3$ was probably responsible for the permanently elevated Ca^{2+} levels as it prevented the active removal of the excess ions from the cytoplasm.

There were also changes in the second parameter measured. As soon as Sorbitol had been added, the cells in both groups immediately lost about 2% of their original surface area. The reaction was exactly the same in both setups independent of the preincubation with $LaCl_3$.This indicated that the inflow of Ca^{2+} into the cytoplasm from intracellular stores and not the extracellular medium was directly linked to the loss of cell surface area. The striking difference in the reaction of cells to hyperosmotic stress was the quick adaption to the changed environmental conditions. The loss in surface area was sudden but stopped again immediately, leaving the cells with a reduced but stable volume. Cells treated with PLY lost more and more surface area over time, the perforation of their membranes left them without a way to stabilize their volume again (see section 4.2.2).

The translocation of cytoplasmic NFAT5 into the nucleus is an important step in the adaptation of cells suffering from hyperosmotic stress. The transcription factor has been studied in detail in the last few years and was found to induce genes that have anti-apoptotic activities, activate the accumulation of organic osmolytes in the cytoplasm and facilitate the uptake of water into the cell (Woo *et al.*, 2002; Hasler *et al.*, 2005; Burg *et al.*, 2007; Ferraris and Burg, 2004).

Cells that were kept in regular medium (300 mOsm/kg) showed an almost even distribution of NFAT5 staining throughout the whole cell with a somewhat reduced signal in the nucleus (Figure 3.3.7). This is consistent with the literature, where it is described that NFAT5 is present in both nucleus and cytoplasm. The ratio of the transcription factor found in- and outside the nucleus at isotonic conditions is dependent on the cell type but is always directly responding to the osmotic conditions surrounding the cell (Dahl *et al.*, 2001; Lopez-Rodríguez *et al.*, 1999). Cells treated

with sublytic amounts of PLY (100 ng/ml) or kept in medium with an increased osmolarity (500 mOsm/kg) both featured a visible increase in NFAT5 signal colocalizing with the DAPI-stained nucleus. Translocation of NFAT5 to the nucleus under hyperosmotic stress is caused by a combination of increased intracellular ionic strength that is due to cell shrinking and the phosphorylation of the transcription factor by p38 and other kinases (Irarrazabal *et al.*, 2004, 2008; Dahl *et al.*, 2001; Ferraris *et al.*, 2002; Ko *et al.*, 2002). The fact that PLY is able to induce volume loss and thereby an increase in intracellular ionic strength together with the other finding that p38 is activated in epithelial cells in response to the presence of the toxin sufficiently explain why it also triggers the shift of NFAT5 into the nucleus. This is a previously undescribed effect of PLY or other members of the CDCs that allows further insights into the toxin's mode of action on host cells.

4.2.5 Blocking conventional PKC-activity and MLC-phosphorylation inhibits the pneumolysin-triggered loss of cell surface area

In the previous section it was established that cells react to the presence of sublytic concentrations of PLY in a way that is similar to hyperosmotic conditions. While volume loss due to an osmotic imbalance is easily explained, the question remained how the toxin could trigger the same effect. It had to be excluded that pore formation at the used concentration by itself was sufficient to cause the observed volume loss, *e.g.* by simply allowing the cellular content to exit through the pores. If this was the case, then interventions with the cells machinery should have no impact on the shrinking caused by the toxin. Promising targets to look at in this context were the cPKC. This subgroup of the PKC family is dependent on elevated Ca^{2+}-levels to be active, a prerequisite that is given in cells treated with PLY. The cPKC were found to be involved in the disassembly of TJs and there is evidence that their activation negatively affects the integrity of epithelial monolayers (Tai *et al.*, 1996; Chou *et al.*, 1998; Tepperman *et al.*, 2005). In most studies investigating this train of thought, inhibitors that act specifically on the different subsets of the PKC family were used to determine which isoforms were responsible for the loss of epithelial integrity. It was reported that inhibitors with selectivity towards cPKC and especially the isoform PKC-α prevented the detrimental effects of a general PKC activation. Furthermore PKC-α is involved in the regulation of the actin cytoskeleton (Larsson, 2006). It has functions in regulating the transport and distribution of integrins (Ng *et al.*, 1999), the

prevention of F-actin bundling (Anilkumar *et al.*, 2003) and the formation of stress fibres (Holinstat *et al.*, 2003).

Therefore, the effect of the PKC-α specific inhibitor Gö6976 (Martiny-Baron *et al.*, 1993) was tested on PLY-treated cells (Figure 3.3.8). The increase in $[Ca^{2+}]_i$ upon PLY administration showed an initial difference between cells pretreated with Gö6976 and those that were not pretreated. The Ca^{2+}-levels in the untreated group featured a characteristic peak right after the toxin was given and later dropped somewhat but stayed elevated the whole time. The initial peak in the inhibitor-pretreated group was visibly lower; however, this difference in peak height was not statistically significant. Approximately ten minutes after PLY was added, both curves met and had a similar progression until the end of the experiment. When Iono was given, both groups showed a strong peak, indicating that the $[Ca^{2+}]_i$ was not saturated. While the toxin-induced inflow of extracellular Ca^{2+} was not really disturbed by Gö6976, the loss in surface area covered by cells was clearly alleviated by preincubation with the inhibitor. Cells treated with PLY alone had lost almost 20% of their surface area at the end of the experiment. In contrast to that, the cells in the Gö6976-pretreated group did not shrink in the presence of the toxin. This group only suffered a loss in cell surface area upon the addition of Iono, indicating that it was still sensitive to the massive perforation and subsequent ion influx caused by the ionophore. This result indicates that the decrease in cellular volume was not due to the leaking of intracellular material through toxin pores but a cellular mechanism that is PKC-α – dependent.

Cells exposed to hypoosmotic medium are known to respond by the so called regulatory volume decrease (RVD), a cellular reaction to counteract excessive cell swelling and eventual membrane burst. To antagonise the increase of their volume, the cells follow a dual strategy. The first step is the release of intracellular osmolytes like taurine into the extracellular space in an attempt to equilibrate the osmotic pressure (Shennan *et al.*, 1993). The second step is a reorganisation of the actin cytoskeleton that actively stabilizes the cell size and initiates shrinking to return to the physiological volume (Schmidt-Nielsen, 1975). The trigger starting this process is an increase in $[Ca^{2+}]_i$ (Grinstein *et al.*, 1982) followed by the activation of PKC-α (Liu *et al.*, 2003). This in turn causes the phosphorylation of a part of the actin cytoskeleton, myosin light chain (MLC) (Marshall *et al.*, 2005). Phosphorylated MLC induces a contraction of the actin cytoskeleton that has been shown to reduce epi -and

endothelial monolayer integrity and cause the formation of intercellular gaps (Turner *et al.*, 1997; Kawkitinarong *et al.*, 2004; Wu *et al.*, 2010; Garcia *et al.*, 1995; Verin *et al.*, 1995). With the previous results of this work in mind, it was hypothesized that PLY at sublytic concentrations could simulate hypoosmotic conditions, thereby triggering a RVD-response in affected cells. This cellular reaction could explain the continuous loss in cell surface area, as it would go on as long as there is an elevated level of Ca^{2+} in the cytoplasm. It would also fit with the finding that the area loss is stopped immediately by $LaCl_3$ through the blocking of Ca^{2+}-permeable pores and prohibited by Gö6976 by inhibiting PKC-α activity. The formation of intercellular gaps in long-term PLY exposed cells (Figure 3.3.7) also points towards this explanation.

To check the hypothesis that PLY induces counteractions to simulated hypoosmotic conditions rather than mimicking hyperosmotic ones, it was tried to interfere with the last step in the cellular RVD-reaction, the phosphorylation of MLC. To do so, cells were preincubated with a peptide called TIP. This is a circular 17 amino acid peptide that mimics the lectin-like (TIP) domain of tumor necrosis factor (TNF) (Lucas *et al.*, 1994). The TIP peptide was described to restore the fluid balance and reduce the vascular permeability in an acute lung injury model (Elia *et al.*, 2003; Vadász *et al.*, 2008; Hamacher *et al.*, 2010; Bloc *et al.*, 2002) and to ameliorate LLO-induced hyperpermeability in endothelial cells by inhibiting MLC phosphorylation (Xiong *et al.*, 2010; Lucas *et al.*, 2009; Yang *et al.*, 2010).

Cells preincubated with the TIP peptide were compared to a control group that was left untreated and a group of cells that was pretreated with a peptide containing the same amino acids as TIP but arranged in a random order, called scrambled TIP (sTIP). These three groups were treated with PLY like in the previous experiment and monitored for changes in $[Ca^{2+}]_i$ and the surface area covered by cells (Figure 3.3.9). Control cells and those preincubated with the non-functional sTIP featured changes in $[Ca^{2+}]_i$ that were characteristic for PLY-treated cells. The TIP-preincubated cells produced an initial peak that was a little smaller than in the other two groups. Interestingly the Ca^{2+} levels dropped below the baseline after a few minutes and stayed low until the end of the experiment in this group. These differences were not statistically significant, which might be due to the low number of replicates and the high deviations between them. It is not clear how the functional peptide affected the cells' Ca^{2+}-homeostasis, as it does not bind PLY or directly inhibits the inflow of extracellular ions (Xiong *et al.*, 2010). A possible explanation for the continuously

reduced but still fluctuating Ca^{2+} levels could be that the peptide stimulates export mechanisms to reduce the cytoplasmic Ca^{2+} concentration, thereby effectively working against the PLY induced ion influx. Due to PLY, the sTIP-pretreated and control group both suffered a major decrease in the surface area covered by cells. Although the cells preincubated with the non-functional peptide were somewhat more affected, there was no significant difference to cells in the control group. Pretreatment with TIP had an effect similar to that observed by the use of the PKC-inhibitor in the previous experiment. Cells that were preincubated with the functional peptide before PLY was added showed only a minor decrease in cell surface area upon treatment with the toxin. The difference between this group and the control was found to be significant for the second half of the experiment. These results point towards the induction of a certain subset of cellular machinery by PLY via the simulation of hypoosmotic conditions, caused by continuously elevated $[Ca^{2+}]_i$ due to toxin pores in the plasma membrane.

4.3 Summary

The motivation for working with sub-lytic concentrations of two long-known and generally well-characterized toxins like LLO and PLY was that there are still open questions about their role in pathogenicity. The findings described in this work are summarized in figure 4.3.1.

An important finding not mentioned before was the similarity of the cellular reactions to the toxins. Both LLO and PLY triggered a fast and permanent increase in $[Ca^{2+}]_i$ at sublytic concentrations. They were also causing a loss of cell surface area that was causally linked to an influx of extracellular Ca^{2+}. Seeing the similarities of the toxins' effects, it is assumed that any effect observed with one toxin might be also found with others sharing the same mode of action. As an example, the ability of PLY to empty the ER stores of Ca^{2+} is probably shared by LLO and other members of the CDC family. Also the inhibitory effect of Gö6976 and TIP on the loss of cell surface area is assumed to be similar in LLO-treated cells, although any of these hypotheses have to be tested experimentally.

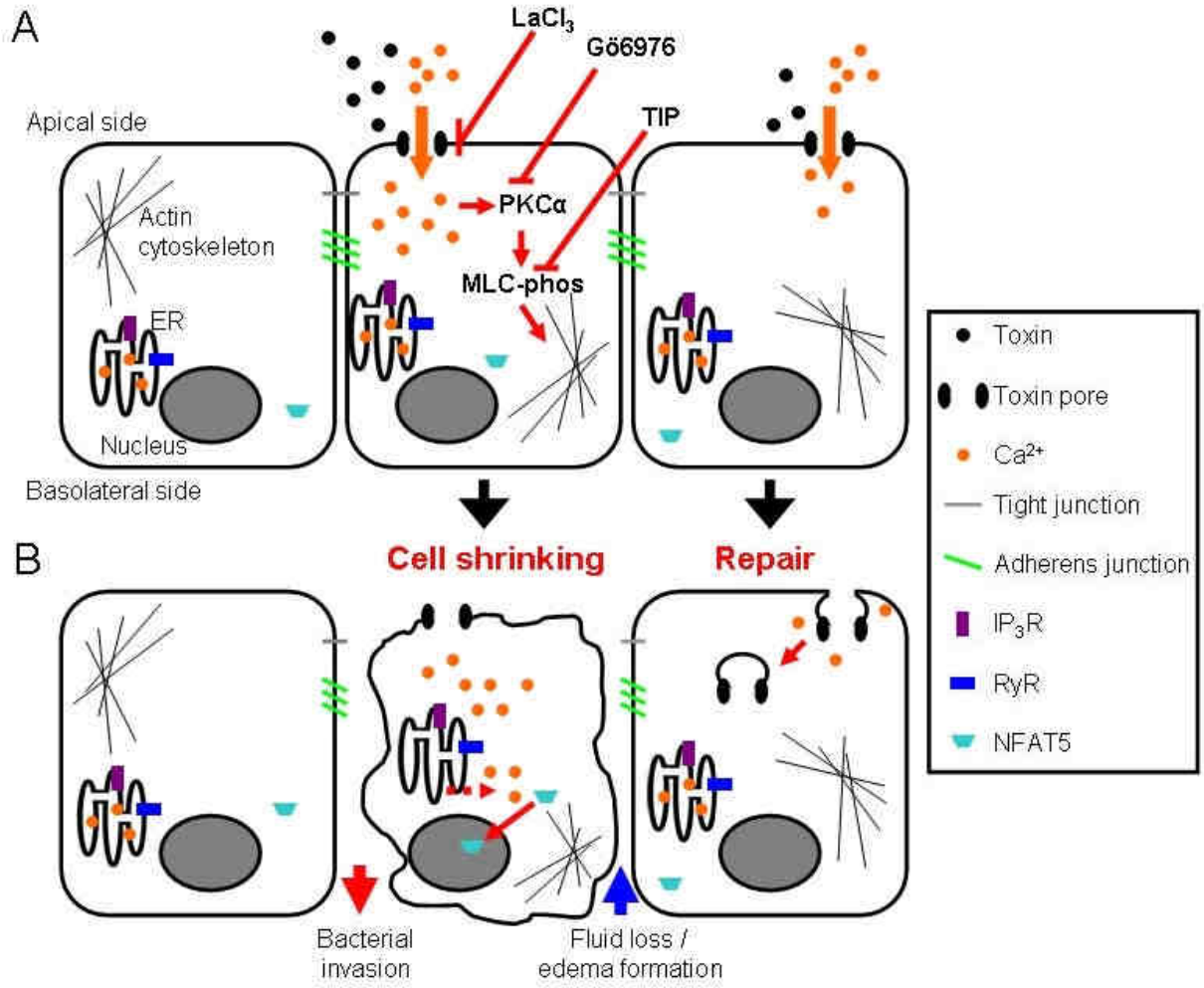

Fig 4.3.1 Model of toxin effects on epithelial cells as described in this work.
A) depicts epithelial cells confronted with a toxin like LLO or PLY.
Middle cell: toxin pores allow influx of extracellular Ca^{2+}, leading to the activation of PKC-α. Activated PKC-α in turn mediates the phosphorylation of MLC, which leads to a contraction of the actin cytoskeleton. $LaCl_3$ stops the Ca^{2+} influx and thereby inhibits all sequential effects of the toxins. Cell shrinking is also significantly reduced when PKC- α or MLC phosphorylation are inhibited (by Gö6976 or the TIP-peptide, respectively).
Right cell: if the number of toxin pores is small enough, a Ca^{2+}-dependent membrane repair mechanism is induced (see Corrotte *et al.*, 2012)
B) shows the effects of toxins on epithelial monolayers.
Middle cell: in Ca^{2+}-free medium it was found that toxin incubation rapidly empties the ER-Ca^{2+}-stores into the cytoplasm. This reaction is independent from endogenous ER Ca^{2+}-channels like IP_3 receptors (IP_3R) and ryanodine receptors (RyR). The shrinking of cells disrupts intercellular junctions, leading to a loss of tight junction integrity. When the epithelial barrier becomes leaky it cannot fulfil its function to hinder pathogens from entering and fluid loss into the lumen of the lung or intestines. After a few hours of incubation with PLY the translocation of NFAT5 from the cytoplasm into the nucleus was observed, probably due to the increasing intracellular ionic strength in shrinking cells.
Right cell: successful repair by endocytosis of toxin pores and subsequent resealing of the membrane.

It was also observed that the cells incubated with toxins had, depending on the concentrations used, a certain capability to counteract the Ca^{2+} influx caused by LLO or PLY. It was found that the $[Ca^{2+}]_i$ started to oscillate after the addition of toxin and that cells exposed to low concentrations could stabilize their Ca^{2+} homeostasis back

to basal levels after a few minutes (Figure 3.1.1 and 3.3.1). The cellular reaction obviously included the removal of excess Ca^{2+} from the cytoplasm, *e.g.* by the plasma membrane Ca^{2+} ATPase, but must have also had a kind of repair mechanism to remove or seal perforated areas of the plasma membrane. This is deduced by the wavelike changes in $[Ca^{2+}]_i$ that indicate the continuous opening and closing of Ca^{2+} channels.

A mechanism that re-establishes the cellular homeostasis has been described for SLO by Corrotte *et al.* (Corrotte *et al.*, 2012). This group found that cells are able to reseal their membranes by forming endocytic vesicles of the perforate membrane areas in a Ca^{2+} dependent manner. Comparable results have been produced with perforin, an effector secreted by cytotoxic T lymphocytes that shares several structural and functional features of CDCs (Praper *et al.*, 2011). It was published that perforin triggers invaginations and formation of internal vesicles much like the ones described with SLO.

In conclusion, it can be stated that the role of LLO and PLY in host-pathogen interactions is multifaceted and complex. Further research is necessary to unravel all the distinct functions of the toxins in bacterial pathogenicity

4.4 Outlook

In this work it was possible to clarify several functional aspects of the two bacterial protein toxins LLO and PLY. It could be shown that sublytic concentrations of LLO induce a reduction of the overall surface area of closed epithelial monolayers that is dependent on the influx of extracellular Ca^{2+} through toxin pores into the cytoplasm of affected cells. The ability of LLO to disturb the integrity of epithelial monolayers with this mechanism was found to benefit the invasiveness of *L. monocytogenes*, as the blocking of the toxin pores reduced the number of bacteria found intracellularly and increased the amount of bacteria in the extracellular space. Therefore, the hypothesis was established that the toxin is increasing the availability of the cellular receptor ECad, which is needed by the bacteria to invade host cells. This needs further investigation, for example by using bacterial strains in infection experiments that express toxin mutants. By using a completely non-functional mutant or one that can bind the plasma membrane of cells but is unable to form ion-permeable pores, it could be excluded that the effects seen are due to a cellular response. This could be either a receptor recognizing the toxin molecule or some mechanism triggered by

LLO binding to the membrane, which could both lead to the opening of endogenous Ca^{2+} channels that could be responsible for the increase in $[Ca^{2+}]_i$. The used channel blocker ($LaCl_3$) is too unspecific to exclude this possibility, as it acts on all channels allowing a Ca^{2+} flux (Lansman, 1990; Hagiwara and Takahashi, 1967). It was also seen that $LaCl_3$ had a diverging effect on the growth capability of *L. monocytogenes* that depended not only on the concentration of the chemical but also on the composition of the medium used to grow the bacteria. The few publications dealing with the effects of lanthanides on the growth of bacteria do not reveal the mechanisms behind the inhibition or stimulation of bacterial growth. Therefore, it would be very interesting to test the bacteriostatic and bactericidal capacity of $LaCl_3$ on other bacteria to check if it is limited to the one strain used in this work or active on bacteria in general. The therapeutic potential of $LaCl_3$ in infectious diseases is presumably very limited, as it acts on the ion homeostasis via multiple targets in a number of human tissues (Weiss, 1974; Huettner *et al.*, 1998; Wengler *et al.*, 2007; Herscher and Rega, 1997). Understanding of the mode of action of $LaCl_3$ on bacterial growth and survival is still desirable, as it could help to develop new antibacterial treatments.

The LLO mutants tested in this study revealed an important role of single amino acids for the function of the toxin in the so far neglected domain 1. It was found that some mutations were without a measurable effect on the activity of LLO, while others were either increasing the cellular reaction to the toxin or were corrupting it. The logical continuation would be to test the less active mutants for their ability to bind cholesterol-containing membranes, multimerise on them and form prepore complexes. This could be done using electron microscopy and artificial membranes. The knowledge gained from these experiments would be the role of each single mutated amino acid, and domain 1 as a whole, in the process of pore formation of a typical CDC. Non-functional toxin mutants could also be used to test whether pore formation and concomitant influx of Ca^{2+} are necessary to trigger cellular reactions or if toxin binding to the membrane is sufficient. The pores of CDCs (up to 45 nm diameter) are large enough for large molecules to passage directly into the cytoplasm. Mutants could be developed to form pores of a distinct size or selectivity as system for intracellular delivery. If the conformational changes in the process of pore formation were elucidated it might even be possible to generate toxin mutants that can be opened or closed at will via a switch-like mechanism.

The experiments with PLY on respiratory epithelial cells revealed that the potential to increase the $[Ca^{2+}]_i$ and to damage the monolayer integrity is the same for both toxins used in this study. It was also shown that long-term incubation with sublytic concentrations of PLY caused a reduction in the amount of ECad present at intercellular junctions and the formation of large gaps in previously closed monolayers. When taken together, these results led to the hypothesis that all members of the CDC are able to injure epithelial barriers in the human host with the same mechanism, as all of them are able to form pores in the plasma membrane. This should be investigated further by testing other members of this group for their ability to disturb the Ca^{2+} homeostasis of host cells and their effect on epithelial monolayer integrity.

The cellular reactions to sublytic PLY concentrations were studied in more detail. It was found that the toxin is able to trigger an increase in $[Ca^{2+}]_i$ even when the affected cells were kept in Ca^{2+}-free medium. A further investigation showed that the intracellular stores were emptied independently of endogenous channels in the presence of PLY. It was not clear how the release of Ca^{2+} from the intracellular stores was mediated. However, there is a publication that found related results in cells treated with LLO (Gekara *et al.*, 2007). The authors observed an increase in the permeability of the ER membrane and a concomitant release of stored Ca^{2+} into the cytoplasm, concluding that the toxin was in some way directly damaging the organelle. Furthermore, Stavru *et al.* (Stavru *et al.*, 2011) reported that LLO is able to interfere with mitochondrial morphology and energy production in a manner that is dependent on the influx of extracellular Ca^{2+}. While this publication supports the hypothesis that CDCs can influence organelles when applied extracellularly, it strictly links the mitochondrial damage to an influx of extracellular Ca^{2+}. The idea of LLO and PLY being able to directly affect the organelles of a cell is intriguing and should be followed in further studies. It should be considered that toxin binding to the plasma membranes by itself might trigger an unknown signalling pathway that causes the depletion of cellular Ca^{2+} stores and changes in organelle morphology. The possibility that toxins can enter cells through their own pores and perforate internal membranes should also be explored. Here, electron microscopy in combination with toxin specific gold-labelled antibodies can be used. Another way to detect interactions with organelles would be to separate them from the other cell components by ultracentrifugation and subsequent detection of the toxins using SDS-PAGE and

western blot. When looking at intracellular toxin actions, LLO has to be considered separately from all other CDCs. Due to its unique PEST-like sequence, LLO was described to be ubiquitinated and degraded quickly in the cytoplasm of eukaryotic cells (Decatur and Portnoy, 2000; Lety *et al.*, 2001). Nevertheless, other publications (Quinn *et al.*, 1993; Viala *et al.*, 2008) showed an intracellular accumulation of the toxin after infection with L. monocytogenes, restoring the possibility of LLO having direct intracellular effects.

Incubation with PLY for several hours induced the translocation of the transcription factor NFAT5 from the cytoplasm into the nucleus, an event that has been described to occur as a response to hyperosmotic stress. NFAT5 mobilisation is triggered by phosphorylation through activated p38 and increasing ionic strength in the cytoplasm, both occurring due to hyperosmotic conditions and toxin incubation. The question arising here was whether the active transcription factor could counteract the toxin's impact on the cell physiology. To answer this it would be necessary to block NFAT5 either by siRNA or by inhibitors in long term experiments to see if the cells would fare better or worse without it.

In the last part of this work it was demonstrated that the volume loss of epithelial cells triggered by PLY can be inhibited by blocking PKC-α and the phosphorylation of MLC. The hypothesis derived was that the toxin-induced inflow of extracellular Ca^{2+} is responsible for the RVD activation. To substantiate this it could be tested if cells still shrink without Ca^{2+} being present in the medium. Additionally, one could remove all intracellular Ca^{2+} by using cell permeable chelators like BAPTA-AM and depleting intracellular Ca^{2+} stores with Thapsigargin. This way it would be possible to differentiate whether inflow of extracellular Ca^{2+} alone is sufficient to activate PKC-α and MLC phosphorylation or if an increase in $[Ca^{2+}]_i$ mediated by the opening of intracellular stores triggers the same reaction.

5 Summary

Listeriolysin O (LLO) and pneumolysin (PLY) are two bacterial protein toxins from the family of cholesterol dependent cytolysins (CDC) that are produced by *Listeria monocytogenes* and *Streptococcus pneumoniae*, respectively. The toxins are found in all clinically relevant bacterial isolates, highlighting their importance for the virulence of these bacterial pathogens. Both LLO and PLY generate pores in the plasma membrane of host cells. High toxin concentrations directly lyse affected cells, while lower (sublytic) concentrations trigger an influx of extracellular calcium ions (Ca^{2+}) into the cytoplasm. Ca^{2+} is an important intracellular second messenger. An increase in its cytoplasmic concentration ($[Ca^{2+}]_i$) results in the activation of signalling pathways.

Both toxins were tested for their ability to create an imbalance in the Ca^{2+}-homeostasis of epithelial cells at sublytic concentrations. It was shown that the toxins triggered a concentration-dependent increase in $[Ca^{2+}]_i$ and caused the cells to shrink. This loss in cell surface area was dependent on the influx of extracellular Ca^{2+}, as it could be inhibited with $LaCl_3$, an unspecific ion channel blocker. LLO variants harbouring single amino acid exchanges were compared to wild-type toxin to asses their functionality and gain further insights in the mechanism of pore formation.

In infection experiments, it was determined that *L. monocytogenes'* ability to invade closed epithelial monolayers was reduced by $LaCl_3$ in a concentration-dependent manner. This implies that the LLO-induced increase in $[Ca^{2+}]_i$ and the accompanying loss of intercellular connections are important for the bacteria to overcome epithelial barriers.

Using PLY-treated epithelial cells, it was demonstrated that the toxin is able to empty intracellular Ca^{2+} stores independently of endogenous channels. No influx of extracellular Ca^{2+} was involved in this reaction, as these experiments were performed in Ca^{2+}-free medium. Finally, the effects of PLY were compared to those of hyperosmotic conditions. It was shown that increased osmolarity and toxin administration had similar effects on the calcium homeostasis, intracellular Ca^{2+} stores and cell volume, which were accompanied by the translocation of the cell volume transcriptional regulator NFAT5. PLY-induced cell shrinking did not occur when PKC-α and MLC-phosphorylation were blocked. These inhibitors did not prevent the influx of extracellular Ca^{2+}, suggesting that cellular signalling events are responsible for the loss in cell surface volume upon toxin treatment.

6 Zusammenfassung

Listeriolysin O (LLO) und Pneumolysin (PLY) sind bakterielle Toxine, welche der Familie der Cholesterin-abhängigen Cytolysine (cholesterol dependent cytolysins, CDC) angehören und von *Listeria monocytogenes* bzw. *Streptococcus pneumoniae* produziert werden. Die Toxine werden von allen klinisch relevanten Stämmen dieser beiden Krankheitserreger gebildet, was ihre Bedeutung als Virulenzfaktoren aufzeigt. LLO und PLY entfalten ihre Wirkung durch die Bildung von Poren in der Zellmembran von Wirtszellen. Hohe Konzentrationen bewirken die sofortige Lyse der betroffenen Zellen, während geringere (nicht-lytische) Mengen den Einstrom von extrazellulären Calcium-Ionen (Ca^{2+}) in das Zytoplasma ermöglichen. Unkontrollierte Veränderungen der intrazellulären Ca^{2+}-Konzentrationen ($[Ca^{2+}]_i$) können verschiedenste Signalkaskaden aktivieren, da Ca^{2+} ein wichtiger intrazellulärer sekundärer Botenstoff ist.

Es wurde untersucht ob nicht-lytische Mengen der beiden Toxine in der Lage sind, die Ca^{2+}-Homöostase von Epithelzellen zu stören. Beide Toxine lösten einen konzentrationsabhängigen Anstieg der $[Ca^{2+}]_i$ und eine Verminderung der Zelloberfläche aus. Beides konnte durch den Einsatz von $LaCl_3$, einem unspezifischen Ionenkanalblocker, gestoppt werden. Dies zeigt, dass die Verminderung der Zelloberfläche durch den Einstrom extrazellulären Ca^{2+} ausgelöst wird. Um den Mechanismus der Porenbildung besser zu verstehen wurden LLO-Mutanten, bei denen einzelne Aminosäuren ausgetauscht waren, auf ihre Aktivität getestet und mit dem Wildtyp verglichen. Des Weiteren wurde durch Infektionsversuche gezeigt, dass *L. monocytogenes* durch $LaCl_3$ an einer effektiven Invasion von geschlossenen Epithelzellrasen gehindert wurde. Dies spricht dafür, dass der von LLO ausgelöste Anstieg der $[Ca^{2+}]_i$ und das damit verbundene Schrumpfen der Zellen den Bakterien hilft, die epitheliale Barriere zu überwinden.

In Zellen die mit PLY behandelt wurden konnte gezeigt werden, dass das Toxin die Entleerung der intrazellulären Ca^{2+}-Speicher unabhängig von endogenen Kanälen auslösen kann. Da die Versuche in Ca^{2+}-freiem Medium durchgeführt wurden, basierte dieser Effekt nicht auf einem Einstrom von extrazellulärem Ca^{2+}. Zuletzt wurde untersucht, ob sich die zellulären Reaktionen auf PLY und hyperosmolare Bedingungen unterscheiden. Die Behandlung mit Toxin und eine erhöhte Osmolarität hatten ähnliche Auswirkungen auf die Ca^{2+}-Homöostase, die intrazellulären Ca^{2+}-Speicher und das Zellvolumen, welche von der Translokation des Volumen-

regulierenden Transkriptionsfaktors NFAT5 begleitet wurden. Durch die Inhibition von PKC-α und der Phosphorylierung von MLC konnte der von PLY ausgelöste Volumenverlust gestoppt werden. Dies verhinderte jedoch nicht den Einstrom von extrazellulärem Ca^{2+}, was darauf hindeutet, dass das Schrumpfen der Zellen durch endogene Signalwege ausgelöst wird.

7 References

Alexander, J. E., Berry, A. M., Paton, J C, Rubins, J B, Andrew, P W, and Mitchell, T J (1998). Amino acid changes affecting the activity of pneumolysin alter the behaviour of pneumococci in pneumonia. *Microbial pathogenesis*, **24**, 167–74.

Allen, I. V. (1965). The effect of bacterial pyrogen on the blood-brain barrier for trypan blue. *The Journal of Pathology and Bacteriology*, **89**, 481–494.

Alouf, J. and Popoff, M. (2005). The comprehensive sourcebook of bacterial protein toxins Third Edit. Alouf, J. and Popoff, M. (eds) Academic Press.

Alouf, Joseph E. and Müller-Alouf, H. (2003). Staphylococcal and streptococcal superantigens: molecular, biological and clinical aspects. *International Journal of Medical Microbiology*, **292**, 429–440.

Anderson, R., Steel, H. C., Cockeran, R., von Gottberg, A., de Gouveia, L., Klugman, K. P., Mitchell, T J, and Feldman, C. (2007). Comparison of the effects of macrolides, amoxicillin, ceftriaxone, doxycycline, tobramycin and fluoroquinolones, on the production of pneumolysin by Streptococcus pneumoniae in vitro. *The Journal of antimicrobial chemotherapy*, **60**, 1155–8.

Andrews, S. C., Robinson, A. K., and Rodríguez-Quiñones, F. (2003). Bacterial iron homeostasis. *FEMS microbiology reviews*, **27**, 215–37.

Anevlavis, S. and Bouros, D. (2010). Community acquired bacterial pneumonia. *Expert opinion on pharmacotherapy*, **11**, 361–74.

Anilkumar, N., Parsons, M., Monk, R., Ng, Tony, and Adams, J. C. (2003). Interaction of fascin and protein kinase Calpha: a novel intersection in cell adhesion and motility. *The EMBO journal*, **22**, 5390–402.

Avery, O. T. and Neill, J. M. (1924). Studies on Oxidation and Reduction by Pneumococcus: IV. Oxidation of Hemotoxin in Sterile Extracts of Pneumococcus. *The Journal of experimental medicine*, **39**, 745–55.

Balachandran, P., Hollingshead, S. K., Paton, J C, and Briles, D. E. (2001). The autolytic enzyme LytA of Streptococcus pneumoniae is not responsible for releasing pneumolysin. *Journal of bacteriology*, **183**, 3108–16.

Bavdek, A., Kostanjšek, R., Antonini, V., Lakey, J. H., Dalla Serra, M., Gilbert, R. J. C., and Anderluh, G. (2012). pH dependence of listeriolysin O aggregation and pore-forming ability. *The FEBS journal*, **279**, 126–41.

Bernheimer, a W. and Avigad, L. S. (1970). Streptolysin o: activation by thiols. *Infection and immunity*, **1**, 509–10.

Bernheimer, Alan W and Rudy, B. (1986). Interactions between membranes and cytolytic peptides. *Biochimica et biophysica acta*, **864**, 123–41.

Berridge, M. J., Lipp, P., and Bootman, M. D. (2000). The versatility and universality of calcium signalling. *Nature Reviews Molecular Cell Biology*, **1**, 11–21.

Berry, A. M., Lock, R. A., Hansman, D., and Paton, J C (1989). Contribution of autolysin to virulence of Streptococcus pneumoniae. *Infection and immunity*, **57**, 2324–30.

Berry, A. M., Paton, J C, and Hansman, D. (1992). Effect of insertional inactivation of the genes encoding pneumolysin and autolysin on the virulence of Streptococcus pneumoniae type 3. *Microbial pathogenesis*, **12**, 87–93.

Berry, A. M., Yother, J., Briles, D. E., Hansman, D., and Paton, J C (1989). Reduced virulence of a defined pneumolysin-negative mutant of Streptococcus pneumoniae. *Infection and immunity*, **57**, 2037–42.

Bhakdi, S. and Tranum-Jensen, J. (1988). Damage to cell membranes by pore-forming bacterial cytolysins. *Progress in allergy*, **40**, 1–43.

Billington, S J, Jost, B H, Cuevas, W. A., Bright, K. R., and Songer, J G (1997). The Arcanobacterium (Actinomyces) pyogenes hemolysin, pyolysin, is a novel member of the thiol-activated cytolysin family. *Journal of bacteriology*, **179**, 6100–6.

Billington, Stephen J, Jost, B Helen, and Songer, J Glenn (2000). Thiol-activated cytolysins: structure, function and role in pathogenesis. *FEMS microbiology letters*, **182**, 197–205.

Billington, Stephen J, Songer, J Glenn, and Jost, B Helen (2002). The variant undecapeptide sequence of the Arcanobacterium pyogenes haemolysin, pyolysin, is required for full cytolytic activity. *Microbiology (Reading, England)*, **148**, 3947–54.

Binz, T., Blasi, J., Yamasaki, S., Baumeister, A., Link, E., Südhof, T. C., Jahn, R., and Niemann, H. (1994). Proteolysis of SNAP-25 by types E and A botulinal neurotoxins. *The Journal of biological chemistry*, **269**, 1617–20.

Bittenbring, J. T. (2005). Elektrophysiologische Charakterisierung und pharmakologische Blockade von Listeriolysin O-induzierten Membranporen.

Blencowe, H., Lawn, J., Vandelaer, J., Roper, M., and Cousens, S. (2010). Tetanus toxoid immunization to reduce mortality from neonatal tetanus. *International journal of epidemiology*, **39 Suppl 1**, i102–9.

Bloc, A., Lucas, R., Van Dijck, E., Bilej, M., Dunant, Y., De Baetselier, Patrick, and Beschin, A. (2002). An invertebrate defense molecule activates membrane conductance in mammalian cells by means of its lectin-like domain. *Developmental and comparative immunology*, **26**, 35–43.

Bolton, B. M. and Fish, C. (1902). An estimate of the amount of toxin in the blood of horses infected with tetanus. *Transactions of the Association of American Physicians*, **14**, 462–467.

Boyle-Vavra, S. and Daum, R. S. (2007). Community-acquired methicillin-resistant Staphylococcus aureus: the role of Panton-Valentine leukocidin. *Laboratory investigation; a journal of technical methods and pathology*, **87**, 3–9.

Braun, J. S., Sublett, J. E., Freyer, D., Mitchell, Tim J, Cleveland, J. L., Tuomanen, Elaine I, and Weber, J. R. (2002). Pneumococcal pneumolysin and H(2)O(2) mediate brain cell apoptosis during meningitis. *The Journal of clinical investigation*, **109**, 19–27.

Braun, V., Neuss, B., Ruan, Y., Schiebel, E., Schöffler, H., and Jander, G. (1987). Identification of the Serratia marcescens hemolysin determinant by cloning into Escherichia coli. *Journal of bacteriology*, **169**, 2113–20.

Brillard, J., Duchaud, E., Boemare, N., Kunst, F., and Givaudan, A. (2002). The PhlA hemolysin from the entomopathogenic bacterium Photorhabdus luminescens belongs to the two-partner secretion family of hemolysins. *Journal of bacteriology*, **184**, 3871–8.

Brown, M. L., O'Hara, F. P., Close, N. M., Mera, R. M., Miller, L. A., Suaya, J. A., and Amrine-Madsen, H. (2011). Prevalence and Sequence Variation of Panton-Valentine Leukocidin in the

United States among Methicillin-Resistant and Methicillin-Susceptible Staphylococcus aureus. *Journal of clinical microbiology*.

Bryan-Lluka, L. J. and Bönisch, H. (1997). Lanthanides inhibit the human noradrenaline, 5-hydroxytryptamine and dopamine transporters. *Naunyn-Schmiedeberg's archives of pharmacology*, **355**, 699–706.

Bryant, A. E., Bayer, C. R., Hayes-Schroer, S. M., and Stevens, Dennis L (2003). Activation of platelet gpIIbIIIa by phospholipase C from Clostridium perfringens involves store-operated calcium entry. *The Journal of infectious diseases*, **187**, 408–17.

Burg, M. B., Ferraris, J. D., and Dmitrieva, N. I. (2007). Cellular response to hyperosmotic stresses. *Physiological reviews*, **87**, 1441–74.

Burkes, S. and McCleskey, C. S. (1947). The Bacteriostatic Activity of Cerium, Lanthanum, and Thallium. *Journal of bacteriology*, **54**, 417–24.

Butler, R. S. (2004). Elektrophysiologische Charakterisierung der durch Listeriolysin O von Listeria monocytogenes und chromosomaler Punktmutanten induzierten Membranporen in humanen embryonalen Nierenzellen.

Carrero, J. a, Calderon, B., and Unanue, E. R. (2004). Listeriolysin O from Listeria monocytogenes is a lymphocyte apoptogenic molecule. *Journal of immunology (Baltimore, Md.□: 1950)*, **172**, 4866–74.

Charpentier, E., Novak, R., and Tuomanen, E. (2000). Regulation of growth inhibition at high temperature, autolysis, transformation and adherence in Streptococcus pneumoniae by clpC. *Molecular microbiology*, **37**, 717–26.

Chou, C. Y., Shen, M. R., Hsu, K. S., Huang, H. Y., and Lin, H. C. (1998). Involvement of PKC-alpha in regulatory volume decrease responses and activation of volume-sensitive chloride channels in human cervical cancer HT-3 cells. *The Journal of physiology*, **512 (Pt 2**, 435–48.

Cockeran, R., Theron, a J., Steel, H. C., Matlola, N. M., Mitchell, T J, Feldman, C., and Anderson, R. (2001). Proinflammatory interactions of pneumolysin with human neutrophils. *The Journal of infectious diseases*, **183**, 604–11.

Cohen, B., Halbert, S. P., and Perkins, M. E. (1942). Pneumococcal Hemolysin: The Preparation of Concentrates, and Their Action on Red Cells. *Journal of bacteriology*, **43**, 607–27.

Cohen, B., Shwachman, H., and Perkins, M. E. (1937). Inactivation of Pneumococcal Hemolysin by Certain Sterols. *Proc Soc Exp Biol Med*, **35**, 586–591.

Cole, R. (1914). PNEUMOCOCCUS HEMOTOXIN. *The Journal of experimental medicine*, **20**, 346–62.

Corrotte, M., Fernandes, M. C., Tam, C., and Andrews, N. W. (2012). Toxin Pores Endocytosed During Plasma Membrane Repair Traffic into the Lumen of MVBs for Degradation. *Traffic (Copenhagen, Denmark)*, **13**, 483–94.

Curtis, D. R., Game, C. J., Lodge, D., and McCulloch, R. M. (1976). A pharmacological study of Renshaw cell inhibition. *The Journal of physiology*, **258**, 227–42.

Czajkowsky, D. M., Hotze, Eileen M, Shao, Z., and Tweten, R. K. (2004). Vertical collapse of a cytolysin prepore moves its transmembrane beta-hairpins to the membrane. *The EMBO journal*, **23**, 3206–15.

Dahl, S. C., Handler, J. S., and Kwon, H M (2001). Hypertonicity-induced phosphorylation and nuclear localization of the transcription factor TonEBP. *American journal of physiology. Cell physiology*, **280**, C248–53.

Darji, a, Niebuhr, K, Hense, M., Wehland, J, Chakraborty, T, and Weiss, S (1996). Neutralizing monoclonal antibodies against listeriolysin: mapping of epitopes involved in pore formation. *Infection and immunity*, **64**, 2356–8.

Darji, A., Chakraborty, Trinad, Niebuhr, Kirsten, Tsonis, N., Wehland, Jiirgen, and Weiss, Siegfried (1995). Hyperexpression of listeriolysin in the nonpathogenic species Listeria innocua and high yield purification. *Journal of biotechnology*, **43**, 205–212.

Dascalu, a, Oron, Y., Nevo, Z., and Korenstein, R. (1995). Hyperosmotic modulation of the cytosolic calcium concentration in a rat osteoblast-like cell line. *The Journal of physiology*, **486 (Pt 1**, 97–104.

Decatur, A L and Portnoy, D A (2000). A PEST-like sequence in listeriolysin O essential for Listeria monocytogenes pathogenicity. *Science (New York, N.Y.)*, **290**, 992–5.

Dramsi, S. and Cossart, Pascale (2003). Listeriolysin O-mediated calcium influx potentiates entry of Listeria monocytogenes into the human Hep-2 epithelial cell line. *Infection and immunity*, **71**, 3614–8.

Ehrlich, P. (1898). Diskussionsbemerkung: Crotin und Tetanolysin. *Berliner Klinische Wochenschrift*, **12**, 273–274.

Elia, N., Tapponnier, M., Matthay, M. a, Hamacher, Jurg, Pache, J.-C., Brundler, M.-A., Totsch, M., De Baetselier, Patrick, Fransen, L., Fukuda, N., et al. (2003). Functional identification of the alveolar edema reabsorption activity of murine tumor necrosis factor-alpha. *American journal of respiratory and critical care medicine*, **168**, 1043–50.

Endo, Y., Tsurugi, K., Yutsudo, T., Takeda, Y., Ogasawara, T., and Igarashi, K. (1988). Site of action of a Vero toxin (VT2) from Escherichia coli O157:H7 and of Shiga toxin on eukaryotic ribosomes. RNA N-glycosidase activity of the toxins. *European journal of biochemistry / FEBS*, **171**, 45–50.

FDA (2009). U.S. Food and Drug Administration on Bacterial Endotoxins/Pyrogens.

Feldman, C., Anderson, R., Cockeran, R., Mitchell, T J, Cole, P., and Wilson, R. (2002). The effects of pneumolysin and hydrogen peroxide, alone and in combination, on human ciliated epithelium in vitro. *Respiratory Medicine*, **96**, 580–585.

Feldman, C., Munro, N. C., Jeffery, P. K., Mitchell, T J, Andrew, P W, Boulnois, G J, Guerreiro, D., Rohde, J. A., Todd, H. C., and Cole, P. J. (1991). Pneumolysin induces the salient histologic features of pneumococcal infection in the rat lung in vivo. *American journal of respiratory cell and molecular biology*, **5**, 416–23.

Felmlee, T., Pellett, S., and Welch, R. A. (1985). Nucleotide sequence of an Escherichia coli chromosomal hemolysin. *Journal of bacteriology*, **163**, 94–105.

Ferrante, A., Rowan-Kelly, B., and Paton, James C (1984). Inhibition of in vitro human lymphocyte response by the pneumococcal toxin pneumolysin. *Infection and immunity*, **46**, 585–9.

Ferraris, J. D. and Burg, M. B. (2004). Drying and salting send different messages. *The Journal of physiology*, **558**, 3.

Ferraris, J. D., Persaud, P., Williams, C. K., Chen, Y., and Burg, M. B. (2002). cAMP-independent role of PKA in tonicity-induced transactivation of tonicity-responsive enhancer/ osmotic response

element-binding protein. *Proceedings of the National Academy of Sciences of the United States of America*, **99**, 16800–5.

Fickl, H., Cockeran, R., Steel, H. C., Feldman, C., Cowan, G., Mitchell, T J, and Anderson, R. (2005). Pneumolysin-mediated activation of NFkappaB in human neutrophils is antagonized by docosahexaenoic acid. *Clinical and experimental immunology*, **140**, 274–81.

Field, M., Fromm, D., al-Awqati, Q., and Greenough, W. B. (1972). Effect of cholera enterotoxin on ion transport across isolated ileal mucosa. *The Journal of clinical investigation*, **51**, 796–804.

Field, M., Rao, M. C., and Chang, E. B. (1989). Intestinal electrolyte transport and diarrheal disease (1). *The New England journal of medicine*, **321**, 800–6.

Foran, P., Lawrence, G. W., Shone, C. C., Foster, K. A., and Dolly, J. O. (1996). Botulinum neurotoxin C1 cleaves both syntaxin and SNAP-25 in intact and permeabilized chromaffin cells: correlation with its blockade of catecholamine release. *Biochemistry*, **35**, 2630–6.

Freer, J. H. and Arbuthnott, J. P. (1982). Toxins of Staphylococcus aureus. *Pharmacology & therapeutics*, **19**, 55–106.

Freer, J. H., Arbuthnott, J. P., and Bernheimer, A W (1968). Interaction of staphylococcal alpha-toxin with artificial and natural membranes. *Journal of bacteriology*, **95**, 1153–68.

Frei, C. R., Bell, A. M., Traugott, K. a, Jaso, T. C., Daniels, K. R., Mortensen, E. M., Restrepo, M. I., Oramasionwu, C. U., Ruiz, A. D., Mylchreest, W. R., et al. (2011). A Clinical Pathway for Community-Acquired Pneumonia: An Observational Cohort Study. *BMC infectious diseases*, **11**, 188.

Garcia, J. G., Davis, H. W., and Patterson, C. E. (1995). Regulation of endothelial cell gap formation and barrier dysfunction: role of myosin light chain phosphorylation. *Journal of cellular physiology*, **163**, 510–22.

Garred, O., van Deurs, B., and Sandvig, K (1995). Furin-induced cleavage and activation of Shiga toxin. *The Journal of biological chemistry*, **270**, 10817–21.

Gedde, M M, Higgins, D E, Tilney, L. G., and Portnoy, D a (2000). Role of listeriolysin O in cell-to-cell spread of Listeria monocytogenes. *Infection and immunity*, **68**, 999–1003.

Gekara, N. O., Groebe, L., Viegas, N., and Weiss, Siegfried (2008). Listeria monocytogenes desensitizes immune cells to subsequent Ca2+ signaling via listeriolysin O-induced depletion of intracellular Ca2+ stores. *Infection and immunity*, **76**, 857–62.

Gekara, N. O., Westphal, K., Ma, B., Rohde, M., Groebe, L., and Weiss, Siegfried (2007). The multiple mechanisms of Ca2+ signalling by listeriolysin O, the cholesterol-dependent cytolysin of Listeria monocytogenes. *Cellular microbiology*, **9**, 2008–21.

Genestier, A.-L., Michallet, M.-C., Prévost, G., Bellot, G., Chalabreysse, L., Peyrol, S., Thivolet, F., Etienne, J., Lina, G., Vallette, F. M., et al. (2005). Staphylococcus aureus Panton-Valentine leukocidin directly targets mitochondria and induces Bax-independent apoptosis of human neutrophils. *The Journal of clinical investigation*, **115**, 3117–27.

Geoffroy, C., Gaillard, J. L., Alouf, J E, and Berche, P (1989). Production of thiol-dependent haemolysins by Listeria monocytogenes and related species. *Journal of general microbiology*, **135**, 481–7.

Geoffroy, C., Gaillard, J. L., Alouf, J E, and Berche, P (1987). Purification, characterization, and toxicity of the sulfhydryl-activated hemolysin listeriolysin O from Listeria monocytogenes. *Infection and immunity*, **55**, 1641–6.

Gill, D. M. (1982). Bacterial toxins: a table of lethal amounts. *Microbiological reviews*, **46**, 86–94.

Glaser, P., Frangeul, L., Buchrieser, C., Rusniok, C., Amend, A., Baquero, F., Berche, P, Bloecker, H., Brandt, P., Chakraborty, T, et al. (2001). Comparative genomics of Listeria species. *Science (New York, N.Y.)*, **294**, 849–52.

Glomski, I. J., Gedde, Margaret M, Tsang, A. W., Swanson, J. a, and Portnoy, Daniel a (2002). The Listeria monocytogenes hemolysin has an acidic pH optimum to compartmentalize activity and prevent damage to infected host cells. *The Journal of cell biology*, **156**, 1029–38.

Goebel, W., Chakraborty, T, and Kreft, J. (1988). Bacterial hemolysins as virulence factors. *Antonie van Leeuwenhoek*, **54**, 453–63.

Goldfine, H. and Wadsworth, S. J. (2002). Macrophage intracellular signaling induced by Listeria monocytogenes. *Microbes and infection / Institut Pasteur*, **4**, 1335–43.

Grinstein, S, Dupre, A., and Rothstein, A. (1982). Volume regulation by human lymphocytes. Role of calcium. *The Journal of general physiology*, **79**, 849–68.

Guzmán, C. a., Domann, E., Ronde, M., Bruder, D., Darji, A., Weiss, Siegfried, Wehland, Jürgen, Chakraborty, Trinad, and Timmis, K. N. (1996). Apoptosis of mouse dendritic cells is triggered by listeriolysin, the major virulence determinant of Listeria monocytogenes. *Molecular Microbiology*, **20**, 119–126.

Hagiwara, S. and Takahashi, K. (1967). Surface density of calcium ions and calcium spikes in the barnacle muscle fiber membrane. *The Journal of general physiology*, **50**, 583–601.

Hamacher, Jürg, Stammberger, U., Roux, J., Kumar, S., Yang, G., Xiong, C., Schmid, R. a, Fakin, R. M., Chakraborty, Trinad, Hossain, H. M. D., et al. (2010). The lectin-like domain of tumor necrosis factor improves lung function after rat lung transplantation--potential role for a reduction in reactive oxygen species generation. *Critical care medicine*, **38**, 871–8.

Hamon, M. A., Batsché, E., Régnault, B., Tham, T. N., Seveau, Stéphanie, Muchardt, C., and Cossart, Pascale (2007). Histone modifications induced by a family of bacterial toxins. *Proceedings of the National Academy of Sciences of the United States of America*, **104**, 13467–72.

Hamon, M., Bierne, H., and Cossart, Pascale (2006). Listeria monocytogenes: a multifaceted model. *Nature reviews. Microbiology*, **4**, 423–34.

Han, J., Lee, J. D., Bibbs, L., and Ulevitch, R. J. (1994). A MAP kinase targeted by endotoxin and hyperosmolarity in mammalian cells. *Science (New York, N.Y.)*, **265**, 808–11.

Harvey, P. C. and Faber, J. E. (1941). Studies on the Listerella Group: I. Biochemical and Hemolytic Reactions. *Journal of bacteriology*, **42**, 677–87.

Hasler, U., Vinciguerra, M., Vandewalle, A., Martin, P.-Y., and Féraille, E. (2005). Dual effects of hypertonicity on aquaporin-2 expression in cultured renal collecting duct principal cells. *Journal of the American Society of Nephrology□: JASN*, **16**, 1571–82.

Hazama, A. and Okada, Y. (1988). Ca2+ sensitivity of volume-regulatory K+ and Cl- channels in cultured human epithelial cells. *The Journal of physiology*, **402**, 687–702.

Hepler, J. R. and Gilman, A. G. (1992). G proteins. *Trends in biochemical sciences*, **17**, 383–7.

Herscher, C. J. and Rega, A. F. (1997). On the mechanism of inhibition of the PMCa(2+)-ATPase by lanthanum. *Annals of the New York Academy of Sciences*, **834**, 407–9.

Hertle, R., Hilger, M., Weingardt-Kocher, S., and Walev, I. (1999). Cytotoxic action of Serratia marcescens hemolysin on human epithelial cells. *Infection and immunity*, **67**, 817–25.

Heuck, A. P., Moe, P. C., and Johnson, B. B. (2010). The cholesterol-dependent cytolysin family of gram-positive bacterial toxins. *Sub-cellular biochemistry*, **51**, 551–77.

Heuck, A. P., Tweten, R. K., and Johnson, A. E. (2003). Assembly and topography of the prepore complex in cholesterol-dependent cytolysins. *The Journal of biological chemistry*, **278**, 31218–25.

Hidalgo, I. J., Raub, T. J., and Borchardt, R. T. (1989). Characterization of the human colon carcinoma cell line (Caco-2) as a model system for intestinal epithelial permeability. *Gastroenterology*, **96**, 736–49.

Hippenstiel, S. and Suttorp, N. (2003). Interaction of pathogens with the endothelium. *Thrombosis and haemostasis*, **89**, 18–24.

Hirst, R. A., Kadioglu, A, O'callaghan, C., and Andrew, P W (2004). The role of pneumolysin in pneumococcal pneumonia and meningitis. *Clinical and experimental immunology*, **138**, 195–201.

Hoheisel, P. and Hoheisel, E. (1968). [On the average tetanus immunization rate]. *Das Deutsche Gesundheitswesen*, **23**, 360–5.

Holinstat, M., Mehta, D., Kozasa, T., Minshall, R. D., and Malik, A. B. (2003). Protein kinase Calpha-induced p115RhoGEF phosphorylation signals endothelial cytoskeletal rearrangement. *The Journal of biological chemistry*, **278**, 28793–8.

Homsher, E., Briggs, F. N., and Wise, R. M. (1974). Effects of hypertonicity on resting and contracting frog skeletal muscles. *The American journal of physiology*, **226**, 855–63.

Hotze, E M, Wilson-Kubalek, E M, Rossjohn, J., Parker, M. W., Johnson, a E., and Tweten, R. K. (2001). Arresting pore formation of a cholesterol-dependent cytolysin by disulfide trapping synchronizes the insertion of the transmembrane beta-sheet from a prepore intermediate. *The Journal of biological chemistry*, **276**, 8261–8.

Howard, L. V. and Gooder, H. (1974). Specificity of the autolysin of Streptococcus (Diplococcus) pneumoniae. *Journal of bacteriology*, **117**, 796–804.

Howard, P. and Riley, H. D. (1965). Tetanus: epidemiologic and clinical aspects of 72 cases. *The Journal-lancet*, **85**, 472–7.

Huber, C. T. and Frieden, E. (1970). The inhibition of ferroxidase by trivalent and other metal ions. *The Journal of biological chemistry*, **245**, 3979–84.

Huettner, J. E., Stack, E., and Wilding, T. J. (1998). Antagonism of neuronal kainate receptors by lanthanum and gadolinium. *Neuropharmacology*, **37**, 1239–47.

Hupp, S., Heimeroth, V., Wippel, C., Förtsch, C., Ma, J., Mitchell, Timothy J, and Iliev, Asparouh I (2012). Astrocytic tissue remodeling by the meningitis neurotoxin pneumolysin facilitates pathogen tissue penetration and produces interstitial brain edema. *Glia*, **60**, 137–46.

Iliev, A.I., Djannatian, J.R., Nau, R., Mitchell, T J, and Wouters, F.S. (2007). Cholesterol-dependent actin remodeling via RhoA and Rac1 activation by the Streptococcus pneumoniae toxin pneumolysin. *Proceedings of the National Academy of Sciences*, **104**, 2897.

Iliev, Asparouh I, Djannatian, Jasmin Roya, Opazo, F., Gerber, J., Nau, R., Mitchell, Timothy J, and Wouters, Fred S (2009). Rapid microtubule bundling and stabilization by the Streptococcus

pneumoniae neurotoxin pneumolysin in a cholesterol-dependent, non-lytic and Src-kinase dependent manner inhibits intracellular trafficking. *Molecular microbiology*, **71**, 461–77.

Irarrazabal, C. E., Liu, J. C., Burg, M. B., and Ferraris, J. D. (2004). ATM, a DNA damage-inducible kinase, contributes to activation by high NaCl of the transcription factor TonEBP/OREBP. *Proceedings of the National Academy of Sciences of the United States of America*, **101**, 8809–14.

Irarrazabal, C. E., Williams, C. K., Ely, M. A., Birrer, M. J., Garcia-Perez, A., Burg, M. B., and Ferraris, J. D. (2008). Activator protein-1 contributes to high NaCl-induced increase in tonicity-responsive enhancer/osmotic response element-binding protein transactivating activity. *The Journal of biological chemistry*, **283**, 2554–63.

Janeway, C. A., Travers, P., Walport, M., and Shlomchik, M. J. (2001). Immunobiology 5th ed. Garland Science, New York.

Jedrzejas, M. J. (2001). Pneumococcal virulence factors: structure and function. *Microbiology and molecular biology reviews□: MMBR*, **65**, 187–207□; first page, table of contents.

Jefferies, J., Nieminen, L., Kirkham, L.-A., Johnston, C., Smith, A., and Mitchell, Tim J (2007). Identification of a secreted cholesterol-dependent cytolysin (mitilysin) from Streptococcus mitis. *Journal of bacteriology*, **189**, 627–32.

Johnson, M. K. and Aultman, K. S. (1977). Studies on the mechanism of action of oxygen-labile haemolysins. *Journal of general microbiology*, **101**, 237–41.

Jonsson, S., Musher, D. M., Chapman, A., Goree, A., and Lawrence, E. C. (1985). Phagocytosis and killing of common bacterial pathogens of the lung by human alveolar macrophages. *The Journal of infectious diseases*, **152**, 4–13.

Jounblat, R., Kadioglu, Aras, Mitchell, Tim J, and Andrew, Peter W (2003). Pneumococcal behavior and host responses during bronchopneumonia are affected differently by the cytolytic and complement-activating activities of pneumolysin. *Infection and immunity*, **71**, 1813–9.

Kadioglu, A, Gingles, N. A., Grattan, K., Kerr, A., Mitchell, T J, and Andrew, P W (2000). Host cellular immune response to pneumococcal lung infection in mice. *Infection and immunity*, **68**, 492–501.

Kadioglu, Aras, Taylor, S., Iannelli, F., Pozzi, G., Mitchell, Tim J, and Andrew, Peter W (2002). Upper and lower respiratory tract infection by Streptococcus pneumoniae is affected by pneumolysin deficiency and differences in capsule type. *Infection and immunity*, **70**, 2886–90.

Kalin, M., Kanclerski, K., Granström, M., and Möllby, R. (1987). Diagnosis of pneumococcal pneumonia by enzyme-linked immunosorbent assay of antibodies to pneumococcal hemolysin (pneumolysin). *Journal of clinical microbiology*, **25**, 226–9.

Kanclerski, K. and Möllby, R. (1987). Production and purification of Streptococcus pneumoniae hemolysin (pneumolysin). *Journal of clinical microbiology*, **25**, 222–5.

Kawkitinarong, K., Linz-McGillem, L., Birukov, K. G., and Garcia, J. G. N. (2004). Differential regulation of human lung epithelial and endothelial barrier function by thrombin. *American journal of respiratory cell and molecular biology*, **31**, 517–27.

Kayal, S., Lilienbaum, A., Poyart, C., Memet, S., Israel, A., and Berche, Patrick (1999). Listeriolysin O-dependent activation of endothelial cells during infection with Listeria monocytogenes: activation of NF-kappa B and upregulation of adhesion molecules and chemokines. *Molecular microbiology*, **31**, 1709–22.

Kingdon, G. C. and Sword, C. P. (1970). Effects of Listeria monocytogenes Hemolysin on Phagocytic Cells and Lysosomes. *Infection and immunity*, **1**, 356–62.

Ko, B. C. B., Lam, A. K. M., Kapus, A., Fan, L., Chung, S. K., and Chung, S. S. M. (2002). Fyn and p38 signaling are both required for maximal hypertonic activation of the osmotic response element-binding protein/tonicity-responsive enhancer-binding protein (OREBP/TonEBP). *The Journal of biological chemistry*, **277**, 46085–92.

Köster, S. (2010). Strukturelle und funktionelle Charakterisierung ausgewählter Membranproteine. **2010**.

Lam, G. Y., Fattouh, R., Muise, A. M., Grinstein, Sergio, Higgins, Darren E., and Brumell, J. H. (2011). Listeriolysin O Suppresses Phospholipase C-Mediated Activation of the Microbicidal NADPH Oxidase to Promote Listeria monocytogenes Infection. *Cell Host & Microbe*, **10**, 627–634.

Lansman, J. B. (1990). Blockade of current through single calcium channels by trivalent lanthanide cations. Effect of ionic radius on the rates of ion entry and exit. *The Journal of general physiology*, **95**, 679–96.

Larsson, C. (2006). Protein kinase C and the regulation of the actin cytoskeleton. *Cellular signalling*, **18**, 276–84.

Leimeister-Wächter, M. and Chakraborty, T (1989). Detection of listeriolysin, the thiol-dependent hemolysin in Listeria monocytogenes, Listeria ivanovii, and Listeria seeligeri. *Infection and immunity*, **57**, 2350–7.

Lety, M A, Frehel, C., Dubail, I., Beretti, J. L., Kayal, S., Berche, Patrick, and Charbit, Alain (2001). Identification of a PEST-like motif in listeriolysin O required for phagosomal escape and for virulence in Listeria monocytogenes. *Molecular microbiology*, **39**, 1124–39.

Lety, Marie Annick, Frehel, C., Berche, Patrick, and Charbit, Alain (2002). Critical role of the N-terminal residues of listeriolysin O in phagosomal escape and virulence of Listeria monocytogenes. *Molecular microbiology*, **46**, 367–79.

Libman, E. (1905). A pneumococcus producing a peculiar form of hemolysis. *Proc. N.Y. Pathol. Soc.*, **5**, 168.

Liu, P., Xiao, H., Li, X., Zhang, C., and Liu, Yi (2006). Study on the toxic mechanism of La3+ to Escherichia coli. *Biological trace element research*, **114**, 293–9.

Liu, X., Zhang, M. I. N., Peterson, L. B., and O'Neil, R. G. (2003). Osmomechanical stress selectively regulates translocation of protein kinase C isoforms. *FEBS Letters*, **538**, 101–106.

Lo, R. Y., Strathdee, C. A., and Shewen, P. E. (1987). Nucleotide sequence of the leukotoxin genes of Pasteurella haemolytica A1. *Infection and immunity*, **55**, 1987–96.

Lopez-Rodríguez, C., Aramburu, J., Rakeman, a S., and Rao, a (1999). NFAT5, a constitutively nuclear NFAT protein that does not cooperate with Fos and Jun. *Proceedings of the National Academy of Sciences of the United States of America*, **96**, 7214–9.

Lucas, R., Magez, S., De Leys, R., Fransen, L., Scheerlinck, J. P., Rampelberg, M., Sablon, E., and De Baetselier, P (1994). Mapping the lectin-like activity of tumor necrosis factor. *Science (New York, N.Y.)*, **263**, 814–7.

Lucas, R., Sridhar, S., Rick, F. G., Gorshkov, B., Umapathy, N. S., Yang, G., Oseghale, A., Verin, Alexander D, Chakraborty, Trinad, Matthay, M. a, et al. (2012). Agonist of growth hormone-

releasing hormone reduces pneumolysin-induced pulmonary permeability edema. *Proceedings of the National Academy of Sciences of the United States of America*, **109**, 2084–9.

Lucas, R., Verin, Alexander D, Black, S. M., and Catravas, J. D. (2009). Regulators of endothelial and epithelial barrier integrity and function in acute lung injury. *Biochemical pharmacology*, **77**, 1763–72.

Lyerly, D. M. and Kreger, A. S. (1983). Importance of serratia protease in the pathogenesis of experimental Serratia marcescens pneumonia. *Infection and immunity*, **40**, 113–9.

López-Rodríguez, C., Aramburu, J., Jin, L., Rakeman, a S., Michino, M., and Rao, a (2001). Bridging the NFAT and NF-kappaB families: NFAT5 dimerization regulates cytokine gene transcription in response to osmotic stress. *Immunity*, **15**, 47–58.

Macfarlane, M. G. and Knight, B. C. (1941). The biochemistry of bacterial toxins: The lecithinase activity of Cl. welchii toxins. *The Biochemical journal*, **35**, 884–902.

Maki, D. G., Hennekens, C. G., Phillips, C. W., Shaw, W. V., and Bennett, J. V. (1973). Nosocomial urinary tract infection with Serratia marcescens: an epidemiologic study. *The Journal of infectious diseases*, **128**, 579–87.

Marquis, J. K. and Black, E. E. (1985). Activation and inactivation of bovine caudate acetylcholinesterase by trivalent cations. *Biochemical pharmacology*, **34**, 533–8.

Marshall, W. S., Ossum, C. G., and Hoffmann, E. K. (2005). Hypotonic shock mediation by p38 MAPK, JNK, PKC, FAK, OSR1 and SPAK in osmosensing chloride secreting cells of killifish opercular epithelium. *The Journal of experimental biology*, **208**, 1063–77.

Martiny-Baron, G., Kazanietz, M. G., Mischak, H., Blumberg, P. M., Kochs, G., Hug, H., Marmé, D., and Schächtele, C. (1993). Selective inhibition of protein kinase C isozymes by the indolocarbazole Gö 6976. *The Journal of biological chemistry*, **268**, 9194–7.

Maus, U. A., Backi, M., Winter, C., Srivastava, M., Schwarz, M. K., Rückle, T., Paton, James C, Briles, D., Mack, M., Welte, T., et al. (2007). Importance of phosphoinositide 3-kinase gamma in the host defense against pneumococcal infection. *American journal of respiratory and critical care medicine*, **175**, 958–66.

Maus, U. a, Srivastava, M., Paton, James C, Mack, M., Everhart, M. B., Blackwell, T. S., Christman, J. W., Schlöndorff, D., Seeger, W., and Lohmeyer, J. (2004). Pneumolysin-induced lung injury is independent of leukocyte trafficking into the alveolar space. *Journal of immunology (Baltimore, Md.□: 1950)*, **173**, 1307–12.

Mayer, M. M. (1972). Mechanism of cytolysis by complement. *Proceedings of the National Academy of Sciences of the United States of America*, **69**, 2954–8.

McCormick, J. K., Yarwood, J. M., and Schlievert, P. M. (2001). Toxic shock syndrome and bacterial superantigens: an update. *Annual review of microbiology*, **55**, 77–104.

McRoberts, J. A., Beuerlein, G., and Dharmsathaphorn, K. (1985). Cyclic AMP and Ca2+-activated K+ transport in a human colonic epithelial cell line. *The Journal of biological chemistry*, **260**, 14163–72.

Mengaud, J., Ohayon, H., Gounon, P., Mege R-M, and Cossart, P (1996). E-cadherin is the receptor for internalin, a surface protein required for entry of L. monocytogenes into epithelial cells. *Cell*, **84**, 923–32.

Meyer, K. F. and Eddie, B. (1951). Perspectives concerning botulism. *Zeitschrift für Hygiene und Infektionskrankheiten; medizinische Mikrobiologie, Immunologie und Virologie*, **133**, 255–63.

Michel, E., Reich, K. A., Favier, R., Berche, P, and Cossart, P (1990). Attenuated mutants of the intracellular bacterium Listeria monocytogenes obtained by single amino acid substitutions in listeriolysin O. *Molecular microbiology*, **4**, 2167–78.

Mitchell, A. M. and Mitchell, T J (2010). Streptococcus pneumoniae: virulence factors and variation. *Clinical microbiology and infection□: the official publication of the European Society of Clinical Microbiology and Infectious Diseases*, **16**, 411–8.

Mitchell, T J, Walker, J. A., Saunders, F. K., Andrew, P W, and Boulnois, G J (1989). Expression of the pneumolysin gene in Escherichia coli: rapid purification and biological properties. *Biochimica et biophysica acta*, **1007**, 67–72.

Mlinar, B. and Enyeart, J. J. (1993). Block of current through T-type calcium channels by trivalent metal cations and nickel in neural rat and human cells. *The Journal of physiology*, **469**, 639–52.

Morgan, P. J., Andrew, P. w, and Mitchell, T J (1996). Thiol-activated cytolysins.pdf. *Reviews in Medical Microbiology*, **7**, 221–229.

Musher, D. M. (1992). Infections caused by Streptococcus pneumoniae: clinical spectrum, pathogenesis, immunity, and treatment. *Clinical infectious diseases□: an official publication of the Infectious Diseases Society of America*, **14**, 801–7.

Nandoskar, M., Ferrante, a, Bates, E. J., Hurst, N., and Paton, J C (1986). Inhibition of human monocyte respiratory burst, degranulation, phospholipid methylation and bactericidal activity by pneumolysin. *Immunology*, **59**, 515–20.

Nassif, X., Bourdoulous, S., Eugène, E., and Couraud, P.-O. (2002). How do extracellular pathogens cross the blood-brain barrier? *Trends in microbiology*, **10**, 227–32.

Nato, F., Reich, K., Lhopital, S., Rouyre, S., Geoffroy, C., Mazie, J. C., and Cossart, P (1991). Production and characterization of neutralizing and nonneutralizing monoclonal antibodies against listeriolysin O. *Infection and immunity*, **59**, 4641–6.

Nau, R. and Brück, W. (2002). Neuronal injury in bacterial meningitis: mechanisms and implications for therapy. *Trends in neurosciences*, **25**, 38–45.

Nelson, A. L., Roche, A. M., Gould, J. M., Chim, K., Ratner, A. J., and Weiser, Jeffrey N (2007). Capsule enhances pneumococcal colonization by limiting mucus-mediated clearance. *Infection and immunity*, **75**, 83–90.

Ng, T, Shima, D., Squire, A., Bastiaens, P. I., Gschmeissner, S., Humphries, M. J., and Parker, P. J. (1999). PKCalpha regulates beta1 integrin-dependent cell motility through association and control of integrin traffic. *The EMBO journal*, **18**, 3909–23.

Nikitas, G., Deschamps, C., Disson, O., Niault, T., Cossart, Pascale, and Lecuit, M. (2011). Transcytosis of Listeria monocytogenes across the intestinal barrier upon specific targeting of goblet cell accessible E-cadherin. *The Journal of experimental medicine*, **208**, 2263–2277.

Nishibori, T., Xiong, H., Kawamura, I., Arakawa, M., and Mitsuyama, M. (1996). Induction of cytokine gene expression by listeriolysin O and roles of macrophages and NK cells. *Infection and immunity*, **64**, 3188–95.

Nishiwaki, H., Nakashima, K., Ishida, C., Kawamura, T., and Matsuda, K. (2007). Cloning, functional characterization, and mode of action of a novel insecticidal pore-forming toxin, sphaericolysin, produced by Bacillus sphaericus. *Applied and environmental microbiology*, **73**, 3404–11.

Orihuela, C. J., Gao, G., Francis, K. P., Yu, J., and Tuomanen, Elaine I (2004). Tissue-specific contributions of pneumococcal virulence factors to pathogenesis. *The Journal of infectious diseases*, **190**, 1661–9.

Pang, X., Wang, D. H., Xing, X. Y., Peng, A., Zhang, F. S., and Li, C. J. (2002). Effect of La3+ on the activities of antioxidant enzymes in wheat seedlings under lead stress in solution culture. *Chemosphere*, **47**, 1033–9.

Pany, S. and Krishnasastry, M V (2007). Aromatic residues of Caveolin-1 binding motif of alpha-hemolysin are essential for membrane penetration. *Biochemical and biophysical research communications*, **363**, 197–202.

Paton, J C, Berry, A. M., Lock, R. A., Hansman, D., and Manning, P. A. (1986). Cloning and expression in Escherichia coli of the Streptococcus pneumoniae gene encoding pneumolysin. *Infection and immunity*, **54**, 50–5.

Paton, J C and Ferrante, a (1983). Inhibition of human polymorphonuclear leukocyte respiratory burst, bactericidal activity, and migration by pneumolysin. *Infection and immunity*, **41**, 1212–6.

Paton, J C, Lock, R. a, and Hansman, D. J. (1983). Effect of immunization with pneumolysin on survival time of mice challenged with Streptococcus pneumoniae. *Infection and immunity*, **40**, 548–52.

Paton, James C, Andrew, Peter W, Boulnois, Graham J, and Mitchell, Timothy J (1993). Molecular analysis of the pathogenicity of Streptococcus pneumoniae: the role of pneumococcal proteins. *Annual review of microbiology*, **47**, 89–115.

Peng, L., Yi, L., Zhexue, L., Juncheng, Z., Jiaxin, D., Daiwen, P., Ping, S., and Songsheng, Q. (2004). Study on biological effect of La3+ on Escherichia coli by atomic force microscopy. *Journal of Inorganic Biochemistry*, **98**, 68–72.

Pentecost, M., Otto, G., Theriot, J. A., and Amieva, M. R. (2006). Listeria monocytogenes invades the epithelial junctions at sites of cell extrusion. *PLoS pathogens*, **2**, e3.

Pillich, H., Loose, M., Zimmer, K.-P., and Chakraborty, Trinad (2012). Activation of the unfolded protein response by Listeria monocytogenes. *Cellular microbiology*.

Podack, E. R. and Konigsberg, P. J. (1984). Cytolytic T cell granules. Isolation, structural, biochemical, and functional characterization. *The Journal of experimental medicine*, **160**, 695–710.

van der Poll, T. and Opal, S. M. (2009). Pathogenesis, treatment, and prevention of pneumococcal pneumonia. *Lancet*, **374**, 1543–56.

Poltorak, a. (1998). Defective LPS Signaling in C3H/HeJ and C57BL/10ScCr Mice: Mutations in Tlr4 Gene. *Science*, **282**, 2085–2088.

Poole, K., Schiebel, E., and Braun, V. (1988). Molecular characterization of the hemolysin determinant of Serratia marcescens. *Journal of bacteriology*, **170**, 3177–88.

Praper, T., Sonnen, A. F.-P., Kladnik, A., Andrighetti, A. O., Viero, G., Morris, K. J., Volpi, E., Lunelli, L., Dalla Serra, M., Froelich, C. J., et al. (2011). Perforin activity at membranes leads to invaginations and vesicle formation. *Proceedings of the National Academy of Sciences of the United States of America*, **108**, 21016–21.

Prevost, G., Bouakham, T., Piemont, Y., and Monteil, H. (1995). Characterisation of a synergohymenotropic toxin produced by Staphylococcus intermedius. *FEBS letters*, **376**, 135–40.

Quinn, F., Pine, L., White, E., George, V., Gutekunst, K., and Swaminathan, B. (1993). Immunogold labelling of Listeria monocytogenes virulence-related factors within Caco-2 cells. *Research in microbiology*, **144**, 597–608.

Raichvarg, D., Siou, G., Dubreuil, A., Bonnaire, Y., Brossard, C., and Boudène, C. (1982). In vivo and in vitro effect of the Haemophilus influenzae lipopolysaccharide on ciliated respiratory epithelium. *Journal of hygiene, epidemiology, microbiology, and immunology*, **26**, 112–6.

Ramachandran, R., Heuck, A. P., Tweten, R. K., and Johnson, A. E. (2002). Structural insights into the membrane-anchoring mechanism of a cholesterol-dependent cytolysin. *Nature structural biology*, **9**, 823–7.

Rangel-González, F. J., García-Colunga, J., and Miledi, R. (2002). Inhibition of neuronal nicotinic acetylcholine receptors by La(3+). *European journal of pharmacology*, **441**, 15–21.

Ratner, A. J., Hippe, K. R., Aguilar, J. L., Bender, M. H., Nelson, A. L., and Weiser, Jeffrey N (2006). Epithelial cells are sensitive detectors of bacterial pore-forming toxins. *The Journal of biological chemistry*, **281**, 12994–8.

Rayner, C. F., Jackson, A. D., Rutman, A., Dewar, A., Mitchell, T J, Andrew, P W, Cole, P. J., and Wilson, R. (1995). Interaction of pneumolysin-sufficient and -deficient isogenic variants of Streptococcus pneumoniae with human respiratory mucosa. *Infection and immunity*, **63**, 442–7.

Repp, H., Pamukçi, Z., Koschinski, A., Domann, E., Darji, A., Birringer, J., Brockmeier, D., Chakraborty, Trinad, and Dreyer, F. (2002). Listeriolysin of Listeria monocytogenes forms Ca2+-permeable pores leading to intracellular Ca2+ oscillations. *Cellular microbiology*, **4**, 483–91.

Ribet, D., Hamon, M., Gouin, E., Nahori, M.-A., Impens, F., Neyret-Kahn, H., Gevaert, K., Vandekerckhove, J., Dejean, A., and Cossart, Pascale (2010). Listeria monocytogenes impairs SUMOylation for efficient infection. *Nature*, **464**, 1192–5.

Richter, J. F., Gitter, A. H., Günzel, D., Weiss, Siegfried, Mohamed, W., Chakraborty, Trinad, Fromm, M., and Schulzke, J. D. (2009). Listeriolysin O affects barrier function and induces chloride secretion in HT-29/B6 colon epithelial cells. *American journal of physiology. Gastrointestinal and liver physiology*, **296**, G1350–9.

Ring, a, Weiser, J N, and Tuomanen, E I (1998). Pneumococcal trafficking across the blood-brain barrier. Molecular analysis of a novel bidirectional pathway. *The Journal of clinical investigation*, **102**, 347–60.

Rogers, P. D., Thornton, J., Barker, K. S., McDaniel, D. O., Sacks, G. S., Swiatlo, E., and McDaniel, L. S. (2003). Pneumolysin-dependent and -independent gene expression identified by cDNA microarray analysis of THP-1 human mononuclear cells stimulated by Streptococcus pneumoniae. *Infection and immunity*, **71**, 2087–94.

Rossjohn, J., Feil, S. C., McKinstry, W. J., Tweten, R. K., and Parker, M. W. (1997). Structure of a cholesterol-binding, thiol-activated cytolysin and a model of its membrane form. *Cell*, **89**, 685–92.

Rottini, G., Dobrina, a, Forgiarini, O., Nardon, E., Amirante, G. a, and Patriarca, P. (1990). Identification and partial characterization of a cytolytic toxin produced by Gardnerella vaginalis. *Infection and immunity*, **58**, 3751–8.

Rowe, G. E. and Welch, R. A. (1994). Assays of hemolytic toxins. *Methods in enzymology*, **235**, 657–67.

Rubins, J B, Charboneau, D, Fasching, C., Berry, A. M., Paton, J C, Alexander, J. E., Andrew, P W, Mitchell, T J, and Janoff, E N (1996). Distinct roles for pneumolysin's cytotoxic and

complement activities in the pathogenesis of pneumococcal pneumonia. *American journal of respiratory and critical care medicine*, **153**, 1339–46.

Rubins, J B and Janoff, E N (1998). Pneumolysin: a multifunctional pneumococcal virulence factor. *The Journal of laboratory and clinical medicine*, **131**, 21–7.

Rubins, Jeffrey B, Duane, P. G., Charboneau, Darlene, and Janoff, Edward N (1992). Toxicity of pneumolysin to pulmonary endothelial cells in vitro. *Infection and immunity*, **60**, 1740–6.

Rubins, Jeffrey B, Duane, P. G., Clawson, D., Charboneau, Darlene, Young, J., and Niewoehner, D. E. (1993). Toxicity of pneumolysin to pulmonary alveolar epithelial cells. *Infection and immunity*, **61**, 1352–8.

Russell, R. J., Wilkinson, P. C., McInroy, R. J., McKay, S., McCartney, A. C., and Arbuthnott, J. P. (1976). Effects of staphylococcal products on locomotion and chemotaxis of human blood neutrophils and monocytes. *Journal of medical microbiology*, **9**, 433–9.

Sanchez-Puelles, J. M., Ronda, C., Garcia, J. L., Garcia, P., Lopez, R., and Garcia, E. (1986). Searching for autolysin functions. Characterization of a pneumococcal mutant deleted in the lytA gene. *European journal of biochemistry / FEBS*, **158**, 289–93.

Sandvig, K, Garred, O., Prydz, K., Kozlov, J. V., Hansen, S. H., and van Deurs, B. (1992). Retrograde transport of endocytosed Shiga toxin to the endoplasmic reticulum. *Nature*, **358**, 510–2.

Sandvig, Kirsten, Torgersen, M. L., Engedal, N., Skotland, T., and Iversen, T.-G. (2010). Protein toxins from plants and bacteria: probes for intracellular transport and tools in medicine. *FEBS letters*, **584**, 2626–34.

Saunders, F. K., Mitchell, T J, Walker, J. a, Andrew, P W, and Boulnois, G J (1989). Pneumolysin, the thiol-activated toxin of Streptococcus pneumoniae, does not require a thiol group for in vitro activity. *Infection and immunity*, **57**, 2547–52.

Schiavo, G., Rossetto, O., Catsicas, S., Polverino de Laureto, P., DasGupta, B. R., Benfenati, F., and Montecucco, C. (1993). Identification of the nerve terminal targets of botulinum neurotoxin serotypes A, D, and E. *The Journal of biological chemistry*, **268**, 23784–7.

Schiavo, G., Shone, C. C., Rossetto, O., Alexander, F. C., and Montecucco, C. (1993). Botulinum neurotoxin serotype F is a zinc endopeptidase specific for VAMP/synaptobrevin. *The Journal of biological chemistry*, **268**, 11516–9.

Schmidt-Nielsen, B. (1975). Comparative physiology of cellular ion and volume regulation. *The Journal of experimental zoology*, **194**, 207–19.

Schnupf, P., Portnoy, Daniel a, and Decatur, Amy L (2006). Phosphorylation, ubiquitination and degradation of listeriolysin O in mammalian cells: role of the PEST-like sequence. *Cellular microbiology*, **8**, 353–64.

Schramm, P. (2004). Elektrophysiologische Charakterisierung und pharmakologische Beeinflussung von durch Pneumolysin aus Streptococcus pneumoniae gebildeten Poren.

Sekino-Suzuki, N., Nakamura, M., Mitsui, K. I., and Ohno-Iwashita, Y. (1996). Contribution of individual tryptophan residues to the structure and activity of theta-toxin (perfringolysin O), a cholesterol-binding cytolysin. *European journal of biochemistry / FEBS*, **241**, 941–7.

Sharma, S., Maycher, B., and Eschun, G. (2007). Radiological imaging in pneumonia: recent innovations. *Current opinion in pulmonary medicine*, **13**, 159–69.

Shatursky, O., Heuck, a P., Shepard, L. a, Rossjohn, J., Parker, M. W., Johnson, a E., and Tweten, R. K. (1999). The mechanism of membrane insertion for a cholesterol-dependent cytolysin: a novel paradigm for pore-forming toxins. *Cell*, **99**, 293–9.

Shaughnessy, L. M., Lipp, P., Lee, K.-D., and Swanson, J. A. (2007). Localization of protein kinase C epsilon to macrophage vacuoles perforated by Listeria monocytogenes cytolysin. *Cellular microbiology*, **9**, 1695–704.

Shen, X. Y., Hamilton, T. a, and DiCorleto, P. E. (1989). Lipopolysaccharide-induced expression of the competence gene KC in vascular endothelial cells is mediated through protein kinase C. *Journal of cellular physiology*, **140**, 44–51.

Shennan, D. B., McNeillie, S. a, and Curran, D. E. (1993). Stimulation of taurine efflux from human placental tissue by a hypoosmotic challenge. *Experimental physiology*, **78**, 843–6.

Shepard, L. a, Heuck, a P., Hamman, B. D., Rossjohn, J., Parker, M. W., Ryan, K. R., Johnson, a E., and Tweten, R. K. (1998). Identification of a membrane-spanning domain of the thiol-activated pore-forming toxin Clostridium perfringens perfringolysin O: an alpha-helical to beta-sheet transition identified by fluorescence spectroscopy. *Biochemistry*, **37**, 14563–74.

Sheppard, J. D., Jumarie, C., Cooper, D. G., and Laprade, R. (1991). Ionic channels induced by surfactin in planar lipid bilayer membranes. *Biochimica et biophysica acta*, **1064**, 13–23.

Siemieniuk, R. A., Gregson, D. B., and Gill, M. J. (2011). The persisting burden of invasive pneumococcal disease in HIV patients: an observational cohort study. *BMC infectious diseases*, **11**, 314.

Singh, R., Jamieson, A., and Cresswell, P. (2008). GILT is a critical host factor for Listeria monocytogenes infection. *Nature*, **455**, 1244–7.

Smyth, C. J. and Duncan, J. L. (1978). Thiol-activated (oxygen labile) cytolysins. In, Jeljaszewicz, J. and Wadstrbm, T. (eds), *Bacterial Toxins and Cell Membranes*. Academic Press, New York, pp. 129–183.

Soltani, C. E., Hotze, Eileen M, Johnson, A. E., and Tweten, R. K. (2007). Structural elements of the cholesterol-dependent cytolysins that are responsible for their cholesterol-sensitive membrane interactions. *Proceedings of the National Academy of Sciences of the United States of America*, **104**, 20226–31.

Song, L., Hobaugh, M. R., Shustak, C., Cheley, S., Bayley, H., and Gouaux, J. E. (1996). Structure of staphylococcal alpha-hemolysin, a heptameric transmembrane pore. *Science (New York, N.Y.)*, **274**, 1859–66.

Stavru, F., Bouillaud, F., Sartori, A., Ricquier, D., and Cossart, Pascale (2011). Listeria monocytogenes transiently alters mitochondrial dynamics during infection. *Proceedings of the National Academy of Sciences of the United States of America*, **108**, 3612–7.

Stavru, F. and Cossart, Pascale (2011). Listeria infection modulates mitochondrial dynamics. *Communicative & integrative biology*, **4**, 364–6.

Steinfort, C., Wilson, R., Mitchell, T J, Feldman, C., Rutman, A., Todd, H., Sykes, D., Walker, J., Saunders, K., and Andrew, P W (1989). Effect of Streptococcus pneumoniae on human respiratory epithelium in vitro. *Infection and immunity*, **57**, 2006–13.

Stevens, D L, Tanner, M. H., Winship, J., Swarts, R., Ries, K. M., Schlievert, P. M., and Kaplan, E. (1989). Severe group A streptococcal infections associated with a toxic shock-like syndrome and scarlet fever toxin A. *The New England journal of medicine*, **321**, 1–7.

Stringaris, A. K., Geisenhainer, J., Bergmann, F., Balshüsemann, C., Lee, U., Zysk, G., Mitchell, Timothy J, Keller, B. U., Kuhnt, U., Gerber, J., et al. (2002). Neurotoxicity of Pneumolysin, a Major Pneumococcal Virulence Factor, Involves Calcium Influx and Depends on Activation of p38 Mitogen-Activated Protein Kinase. *Neurobiology of Disease*, **11**, 355–368.

Stuart, R. O. and Nigam, Sanjay K (1995). Regulated assembly of tight junctions by protein kinase C. *Proceedings of the National Academy of Sciences of the United States of America*, **92**, 6072–6.

Tai, Y. H., Flick, J., Levine, S. A., Madara, J. L., Sharp, G. W., and Donowitz, M. (1996). Regulation of tight junction resistance in T84 monolayers by elevation in intracellular Ca2+: a protein kinase C effect. *The Journal of membrane biology*, **149**, 71–9.

Takano, K. (1985). Neurophysiological aspects of tetanus toxin effects on the motor system. *European journal of epidemiology*, **1**, 193–201.

Tang, C. T., Nguyen, D. T., Ngo, T. H., Nguyen, T. M. P., Le, V. T., To, S. D., Lindsay, J., Nguyen, T. D., Bach, V. C., Le, Q. T., et al. (2007). An outbreak of severe infections with community-acquired MRSA carrying the Panton-Valentine leukocidin following vaccination. *PloS one*, **2**, e822.

Tang, P., Rosenshine, I., Cossart, Pascale, and Finlay, B. B. (1996). Listeriolysin O activates mitogen-activated protein kinase in eucaryotic cells. *Infection and immunity*, **64**, 2359–61.

Tappin, M. J., Pastore, A., Norton, R. S., Freer, J. H., and Campbell, I. D. (1988). High-resolution 1H NMR study of the solution structure of delta-hemolysin. *Biochemistry*, **27**, 1643–7.

Tepperman, B. L., Soper, B. D., and Chang, Q. (2005). Effect of protein kinase C activation on intracellular Ca2+ signaling and integrity of intestinal epithelial cells. *European journal of pharmacology*, **518**, 1–9.

Thastrup, O., Cullen, P. J., Drøbak, B. K., Hanley, M. R., and Dawson, a P. (1990). Thapsigargin, a tumor promoter, discharges intracellular Ca2+ stores by specific inhibition of the endoplasmic reticulum Ca2(+)-ATPase. *Proceedings of the National Academy of Sciences of the United States of America*, **87**, 2466–70.

Thornton, J. and McDaniel, L. S. (2005). THP-1 monocytes up-regulate intercellular adhesion molecule 1 in response to pneumolysin from Streptococcus pneumoniae. *Infection and immunity*, **73**, 6493–8.

Tilley, S. J., Orlova, E. V., Gilbert, R. J. C., Andrew, Peter W, and Saibil, H. R. (2005). Structural basis of pore formation by the bacterial toxin pneumolysin. *Cell*, **121**, 247–56.

Tilney, L. G. and Portnoy, D a (1989). Actin filaments and the growth, movement, and spread of the intracellular bacterial parasite, Listeria monocytogenes. *The Journal of cell biology*, **109**, 1597–608.

Todd, J., Fishaut, M., Kapral, F., and Welch, T. (1978). Toxic-shock syndrome associated with phage-group-I Staphylococci. *Lancet*, **2**, 1116–8.

TranVan Nhieu, G., Clair, C., Grompone, G., and Sansonetti, P. (2004). Calcium signalling during cell interactions with bacterial pathogens. *Biology of the cell / under the auspices of the European Cell Biology Organization*, **96**, 93–101.

Tsukamoto, T. and Nigam, S.K. (1999). Role of tyrosine phosphorylation in the reassembly of occludin and other tight junction proteins. *American Journal of Physiology-Renal Physiology*, **276**, F737.

Turner, J. R., Rill, B. K., Carlson, S. L., Carnes, D., Kerner, R., Mrsny, R. J., and Madara, J. L. (1997). Physiological regulation of epithelial tight junctions is associated with myosin light-chain phosphorylation. *The American journal of physiology*, **273**, C1378–85.

Vadia, S., Arnett, E., Haghighat, A.-C., Wilson-Kubalek, Elisabeth M., Tweten, R. K., and Seveau, Stephanie (2011). The Pore-Forming Toxin Listeriolysin O Mediates a Novel Entry Pathway of L. monocytogenes into Human Hepatocytes. *PLoS Pathogens*, **7**, e1002356.

Vadász, I., Schermuly, R. T., Ghofrani, H. A., Rummel, S., Wehner, S., Mühldorfer, I., Schäfer, K. P., Seeger, W., Morty, R. E., Grimminger, F., et al. (2008). The lectin-like domain of tumor necrosis factor-alpha improves alveolar fluid balance in injured isolated rabbit lungs. *Critical care medicine*, **36**, 1543–50.

Verin, A D, Patterson, C. E., Day, M. A., and Garcia, J. G. (1995). Regulation of endothelial cell gap formation and barrier function by myosin-associated phosphatase activities. *The American journal of physiology*, **269**, L99–108.

Viala, J. P. M., Mochegova, S. N., Meyer-Morse, N., and Portnoy, Daniel A (2008). A bacterial pore-forming toxin forms aggregates in cells that resemble those associated with neurodegenerative diseases. *Cellular microbiology*, **10**, 985–93.

Vijayvargia, R., Suresh, C. G., and Krishnasastry, Musti V (2004). Functional form of Caveolin-1 is necessary for the assembly of alpha-hemolysin. *Biochemical and biophysical research communications*, **324**, 1130–6.

Vázquez-Boland, J. A., Kuhn, M., Berche, P, Chakraborty, T, Domínguez-Bernal, G., Goebel, W., González-Zorn, B., Wehland, J, and Kreft, J. (2001). Listeria pathogenesis and molecular virulence determinants. *Clinical microbiology reviews*, **14**, 584–640.

Wadsworth, S. J. and Goldfine, H. (2002). Mobilization of protein kinase C in macrophages induced by Listeria monocytogenes affects its internalization and escape from the phagosome. *Infection and immunity*, **70**, 4650–60.

Walker, J. A., Allen, R. L., Falmagne, P., Johnson, M. K., and Boulnois, G J (1987). Molecular cloning, characterization, and complete nucleotide sequence of the gene for pneumolysin, the sulfhydryl-activated toxin of Streptococcus pneumoniae. *Infection and immunity*, **55**, 1184–9.

Waterer, G. W., Rello, J., and Wunderink, R. G. (2011). Management of community-acquired pneumonia in adults. *American journal of respiratory and critical care medicine*, **183**, 157–64.

Weiss, G. B. (1974). Cellular Pharmacology of Lanthanum. *Annual Review of Pharmacology*, **14**, 343–354.

Welch, R. A. (1987). Identification of two different hemolysin determinants in uropathogenic Proteus isolates. *Infection and immunity*, **55**, 2183–90.

Welch, R. A. (2001). RTX toxin structure and function: a story of numerous anomalies and few analogies in toxin biology. *Current topics in microbiology and immunology*, **257**, 85–111.

Wengler, Gerd, Wengler, Gisela, and Koschinski, A. (2007). A short treatment of cells with the lanthanide ions La3+, Ce3+, Pr3+ or Nd3+ changes the cellular chemistry into a state in which RNA replication of flaviviruses is specifically blocked without interference with host-cell multiplication. *The Journal of general virology*, **88**, 3018–26.

Westbrook, D. G. and Bhunia, A. K. (2000). Dithiothreitol enhances Listeria monocytogenes mediated cell cytotoxicity. *Microbiology and immunology*, **44**, 431–8.

Wheeler, J., Freeman, R., Steward, M., Henderson, K., Lee, M. J., Piggott, N. H., Eltringham, G. J., and Galloway, A. (1999). Detection of pneumolysin in sputum. *Journal of medical microbiology*, **48**, 863–6.

Wippel, C., Förtsch, C., Hupp, S., Maier, E., Benz, R., Ma, J., Mitchell, Timothy J, and Iliev, Asparouh I (2011). Extracellular calcium reduction strongly increases the lytic capacity of pneumolysin from streptococcus pneumoniae in brain tissue. *The Journal of infectious diseases*, **204**, 930–6.

Woo, S. K., Lee, S. D., Na, K. Y., Park, W. K., and Kwon, H Moo (2002). TonEBP/NFAT5 stimulates transcription of HSP70 in response to hypertonicity. *Molecular and cellular biology*, **22**, 5753–60.

Woodin, A. M. (1961). Assay of the two components of staphylococcal leucocidin and their antibodies. *The Journal of pathology and bacteriology*, **81**, 63–8.

Woodin, A. M. (1960). Purification of the two components of leucocidin from Staphylococcus aureus. *The Biochemical journal*, **75**, 158–65.

Wu, C.-C., Lu, Y.-Z., Wu, L.-L., and Yu, L. C. (2010). Role of myosin light chain kinase in intestinal epithelial barrier defects in a rat model of bowel obstruction. *BMC gastroenterology*, **10**, 39.

Xiong, C., Yang, G., Kumar, S., Aggarwal, S., Leustik, M., Snead, C., Hamacher, Juerg, Fischer, B., Umapathy, N. S., Hossain, H., et al. (2010). The lectin-like domain of TNF protects from listeriolysin-induced hyperpermeability in human pulmonary microvascular endothelial cells - a crucial role for protein kinase C-alpha inhibition. *Vascular pharmacology*, **52**, 207–13.

Yamada, O., Moldow, C. F., Sacks, T., Craddock, P. R., Boogaerts, M., and Jacob, H. S. (1981). Deleterious effects of endotoxin on cultured endothelial cells: an in vitro model of vascular injury. *Inflammation*, **5**, 115–126.

Yang, G., Hamacher, Jürg, Gorshkov, B., White, R., Sridhar, S., Verin, A., Chakraborty, Trinad, and Lucas, R. (2010). The dual role of TNF in pulmonary edema. *Journal of cardiovascular disease research*, **1**, 29.

Zhang, L., Yang, T., Gao, Y., Liu, Yubing, Zhang, T., Xu, S., Zeng, F., and An, L. (2006). Effect of lanthanum ions (La3+) on ferritin-regulated antioxidant process under PEG stress. *Biological trace element research*, **113**, 193–208.

Zhang, L., Zeng, F., and Xiao, R. (2003). Effect of lanthanum ions (La3+) on the reactive oxygen species scavenging enzymes in wheat leaves. *Biological trace element research*, **91**, 243–52.

8 Appendix

8.1 Graphs for ratiometric Ca^{2+} and total cell surface area measurements of single LLO mutants

A)

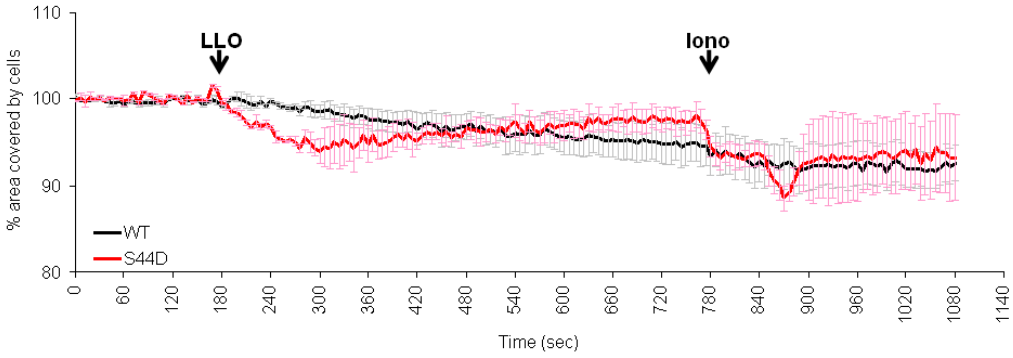

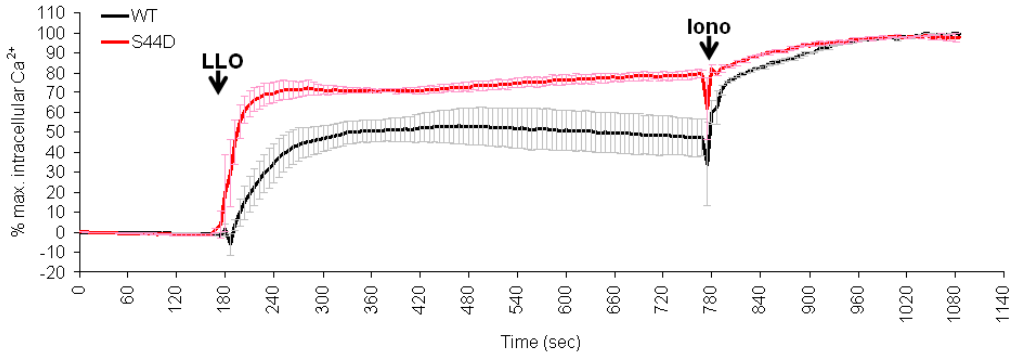

B)

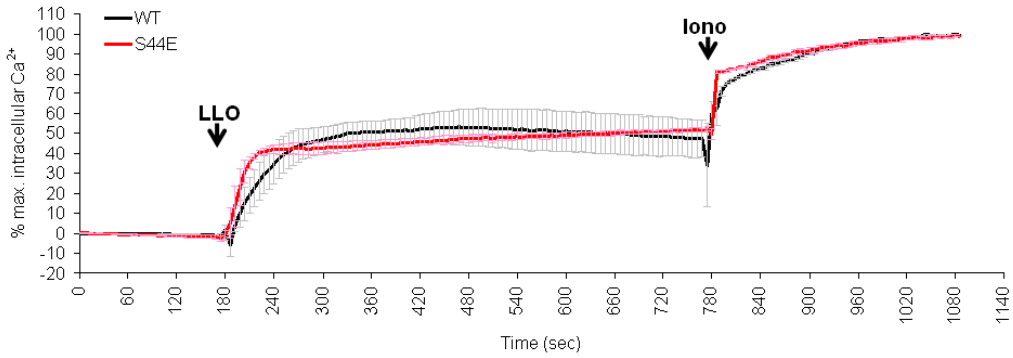

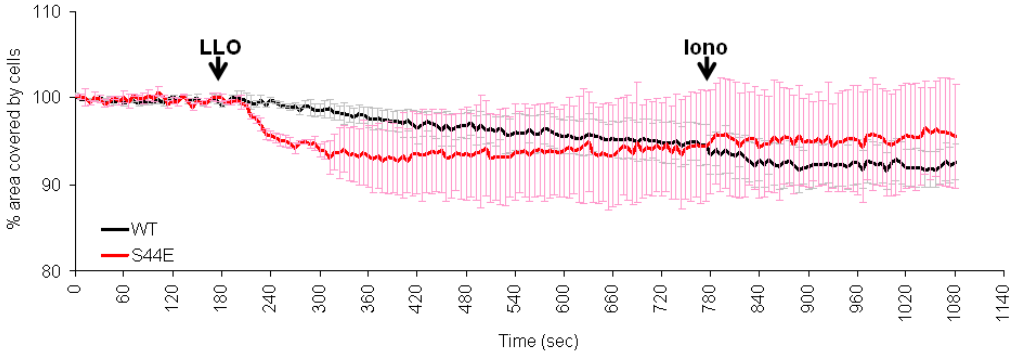

C)

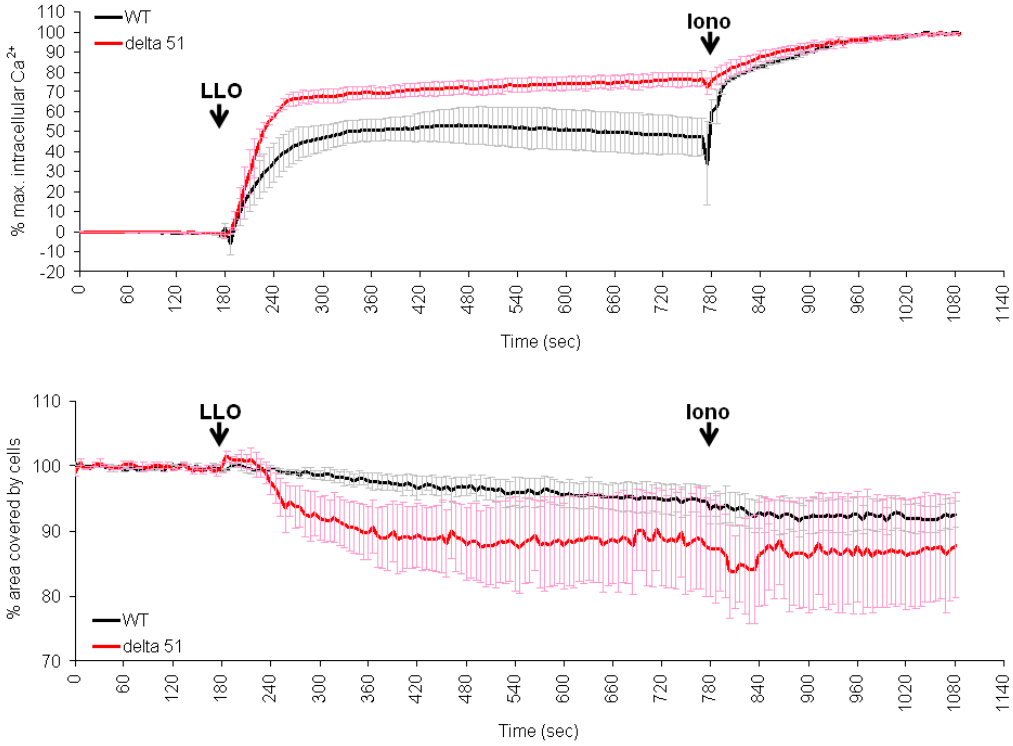
WT
delta 51
LLO
Iono
% max. intracellular Ca2+
Time (sec)
% area covered by cells
WT
delta 51
LLO
Iono
Time (sec)

D)

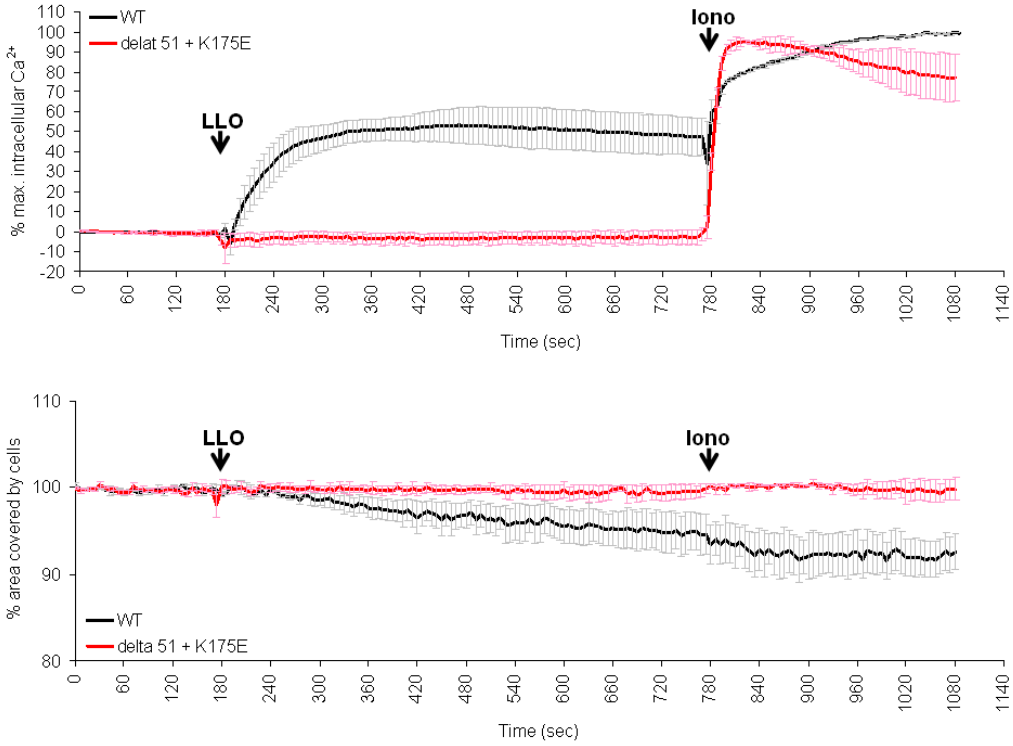
WT
delat 51 + K175E
LLO
Iono
% max. intracellular Ca2+
Time (sec)
% area covered by cells
WT
delta 51 + K175E
LLO
Iono
Time (sec)

E)

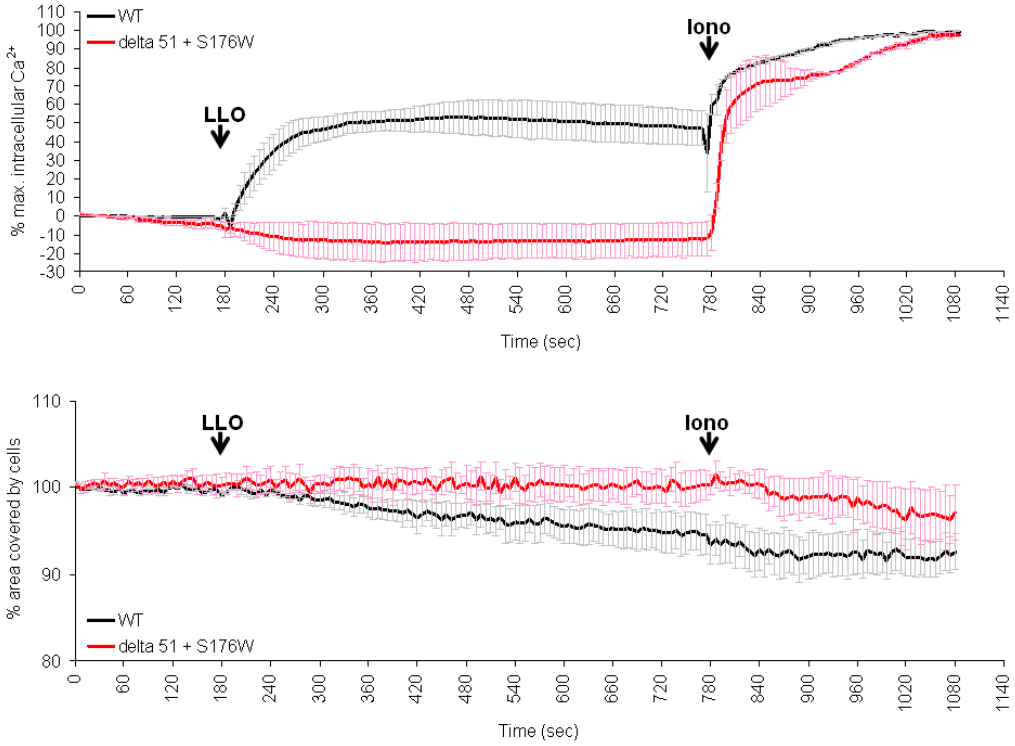
WT
delta 51 + S176W
LLO
Iono
% max. intracellular Ca2+
Time (sec)
% area covered by cells
Time (sec)

F)

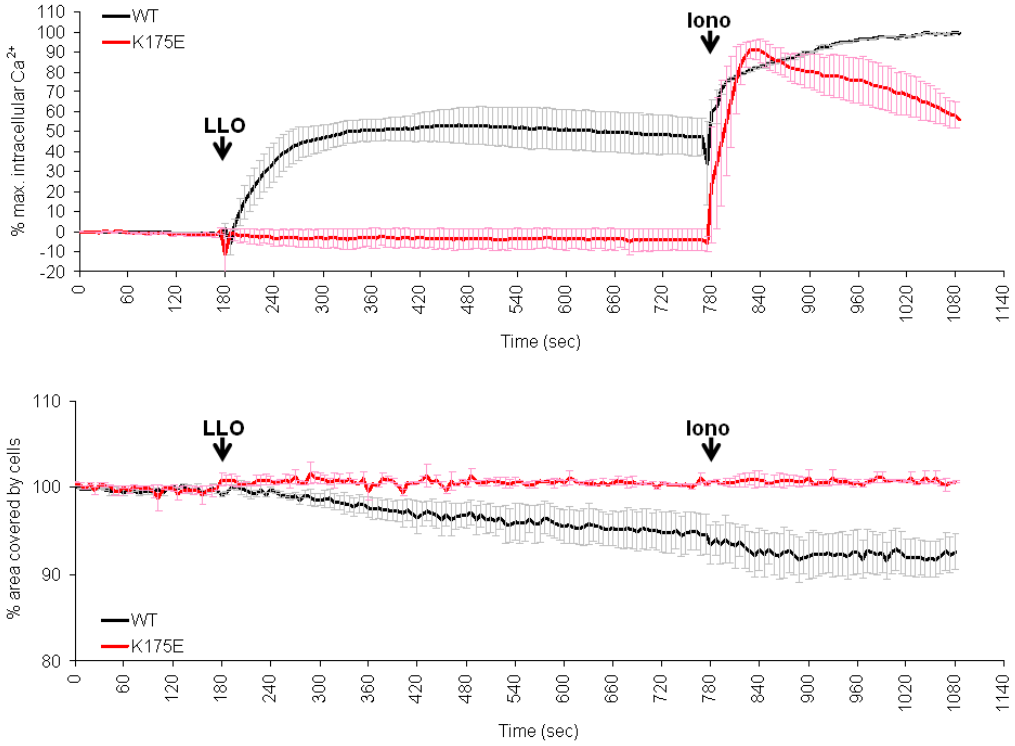
WT
K175E
LLO
Iono
% max. intracellular Ca2+
Time (sec)
% area covered by cells
Time (sec)

G)

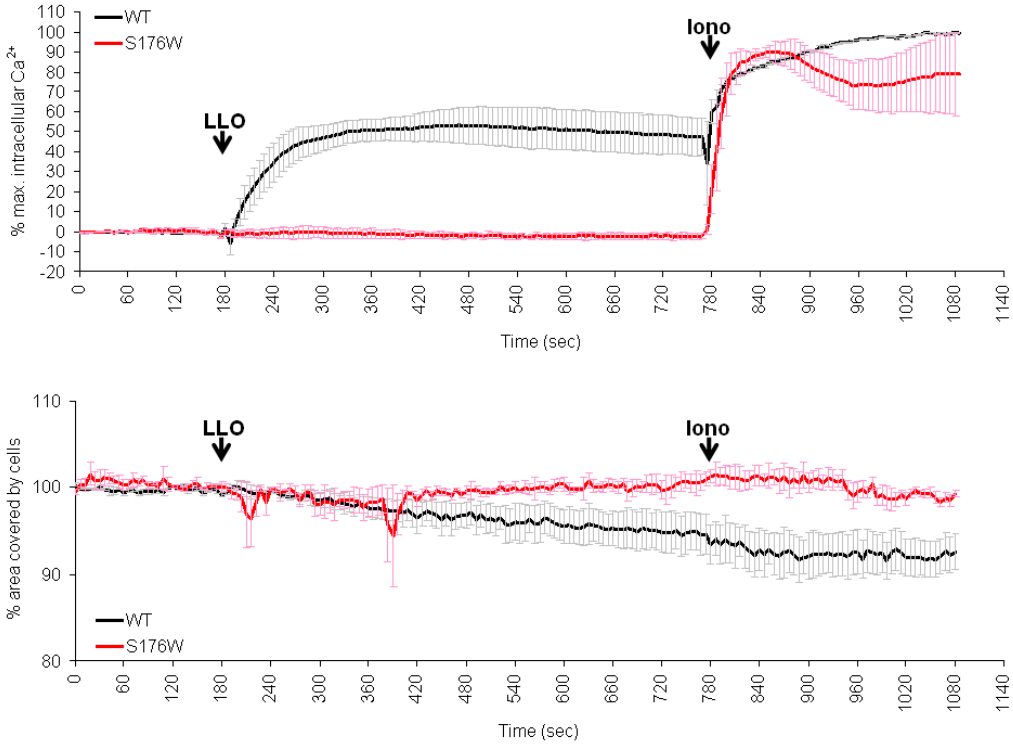
WT
S176W
LLO
Iono
% max. intracellular Ca2+
Time (sec)
% area covered by cells
WT
S176W
Time (sec)

H)

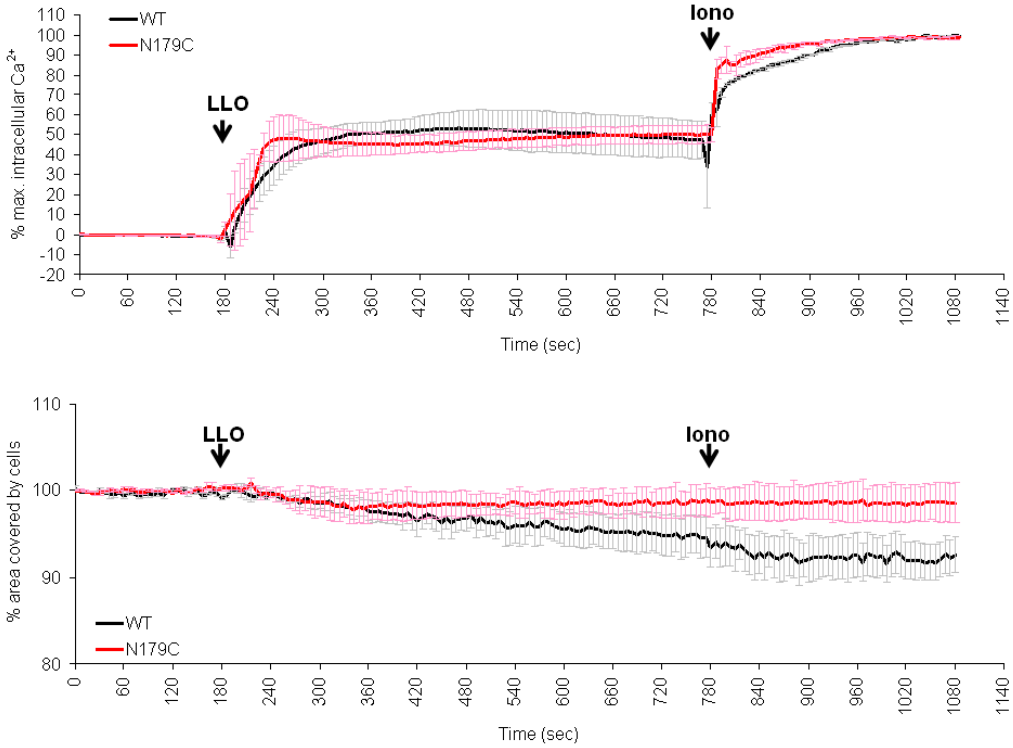
WT
N179C
LLO
Iono
% max. intracellular Ca2+
Time (sec)
% area covered by cells
WT
N179C
Time (sec)

I)

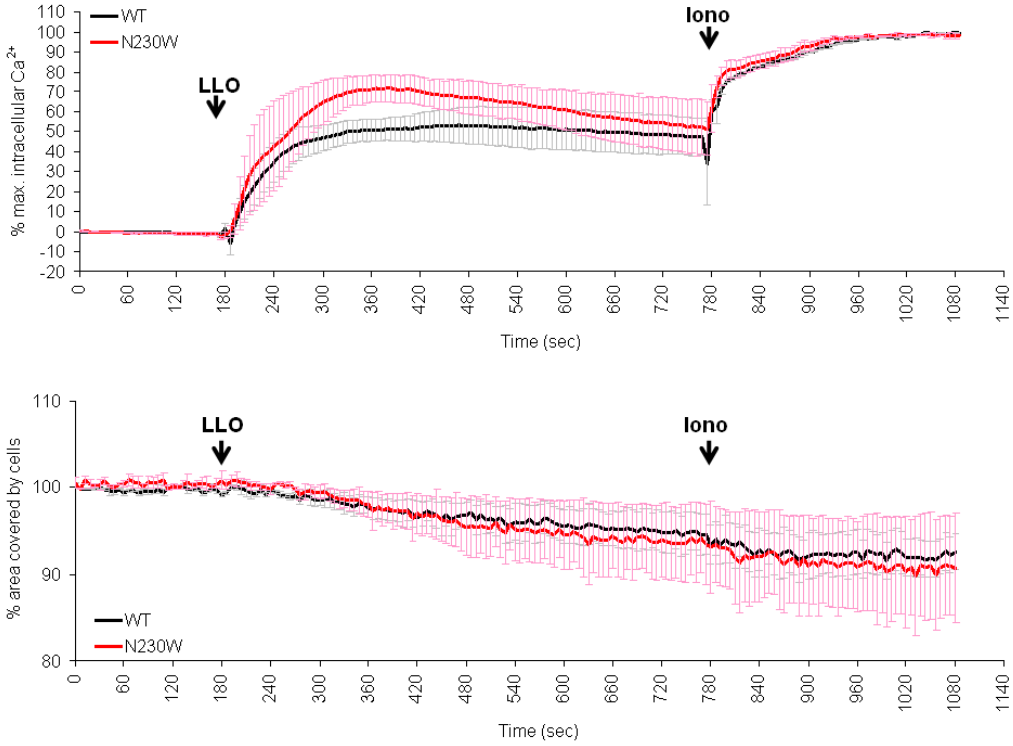
WT
N230W
LLO
Iono
% max. intracellular Ca2+
Time (sec)
% area covered by cells
WT
N230W
LLO
Iono
Time (sec)

J)

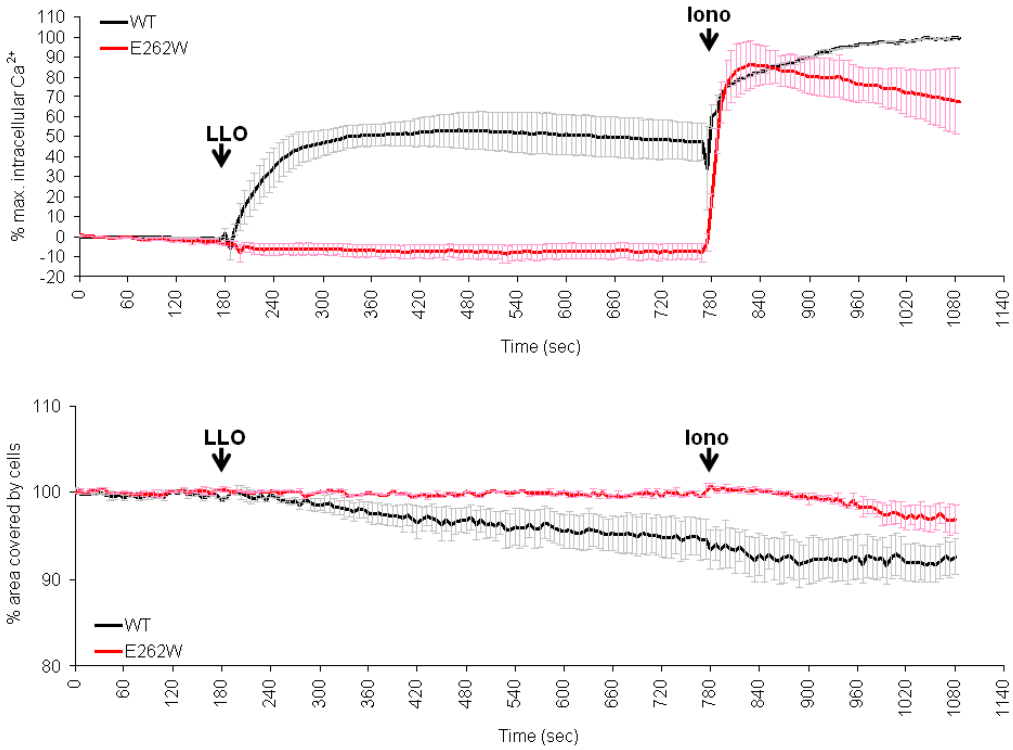
WT
E262W
LLO
Iono
% max. intracellular Ca2+
Time (sec)
% area covered by cells
WT
E262W
LLO
Iono
Time (sec)

K)

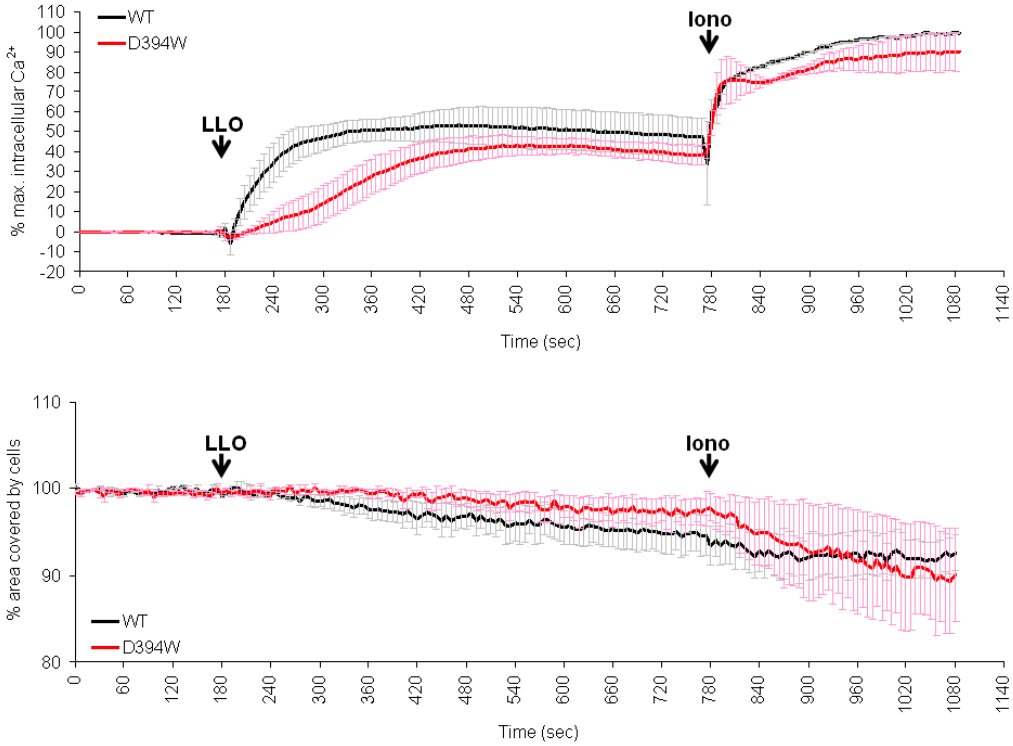

Fig 8.1.1 LLO mutants and their effect on the $[Ca^{2+}]_i$ and the cell surface area.
A)-K) Caco-2 cells were loaded with Fura-2 AM and monitored for changes in the emission at 340 and 380nm when excited at 510nm. From the emission readings the 340/380nm ratio was calculated. The maximum signal measured after adding Iono (5µM) at the end of the experiment was used to express the relative change in $[Ca^{2+}]_i$. LLO WT and mutants, all preincubated with DTT, were added at 50ng/ml and cells were measured for 10min before Iono was added. In the same experiments the cell surface area was determined by counting the pixels in the acquired images that had a signal above background levels. The pixel count in cells at rest was set to 100%.
The graph shows the mean values + SEM of three independent experiments for each group.

8.2 Thapsigargin is without effect on $[Ca^{2+}]_i$ when administered after PLY

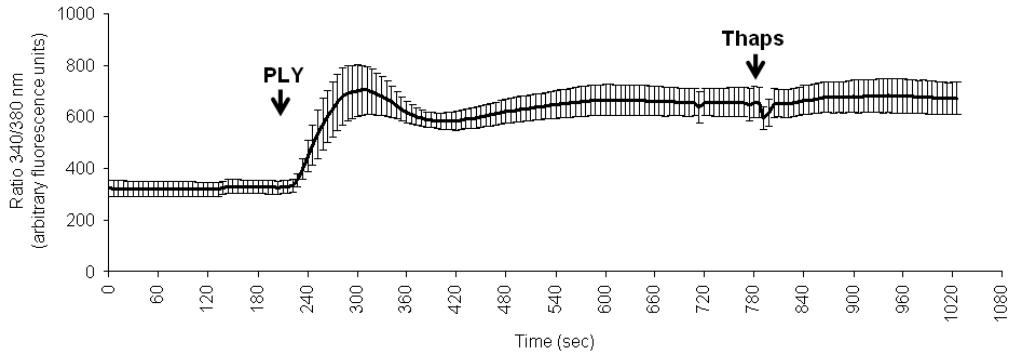

Fig 8.2.1 The addition of Thaps after PLY has no effect on the $[Ca^{2+}]_i$. H441 cells were loaded with Fura-2 AM and monitored for changes in the emission at 340 and 380nm when excited at 510nm. From the emission readings the 340/380nm ratio was calculated and used to express the relative change in $[Ca^{2+}]_i$ as arbitrary fluorescence units. 100ng/ml PLY+DTT and 100nM Thapsigargin (Thaps) were added at the indicated time points
Results are shown as mean values ± SEM of at least three independent experiments

.

Acknowledgements

I would never have been able to finish my dissertation without the guidance of my supervisor, help from co-workers and colleagues, and support from my family and friends.

I wish to express my deepest gratitude to my advisor, Prof. Dr. Trinad Chakraborty, for providing me with this project and his excellent guidance, caring, patience, and constant support.

Dr. Hamid Hossain has been a patient listener and has provided me with valuable advice and counsel. I am thankful for his supervision and expertise.

I am also thankful to Prof. Dr. Andreas Vilcinskas for accepting to co-supervise my dissertation.

Dr. Helena Pillich patiently thought me most of the basic techniques I used in my dissertation and how to design and interpret experiments correctly. She was always a great source for constructive criticism and advice, I am very grateful for all of her help and her proofreading of this work.

I would like to thank Dr. Svetlin Tchatalbachev for answering every possible question, be it technical or theoretical, and helping me in every other way imaginable.

The toxins produced by Martina Hudel have been a cornerstone of my dissertation; I could have not succeeded without her expertise in protein isolation and purification. I also want to thank her for general assistance in many technical aspects.

Large parts of my work were done in the Calcium Lab of the Institute of Physiology, JLU-Giessen. I would like to specially thank Dr. Yaser Abdallah, Dr. Sascha Kasseckert and Mustafa Micoogullari Gattuso for introducing me to the methods of calcium imaging, the possibility to use the equipment and always being there for questions and technical support.

I am very thankful to our partners at the Max Planck Institute of Biophysics for the productive cooperation. The work of Dr. Özkan Yildiz and Stefan Köster was indispensable for the crystallization of LLO and the generation of mutants.

I would like to thank my colleagues Maria Loose and Moritz Fritzenwanker for countless discussions about my data and, together with Madhu Singh, for proofreading this manuscript.

Dr. Rudolph Lucas was an inspiration long before I started to work on my dissertation. He was one of the most dedicated professors during my academic studies and since then had a very positive influence on my professional progress. I would like to thank him for his guidance and the supply of the TIP peptide.

Dr. Christiane Riedel always had constructive criticism and moral support for me; I am grateful for her patience and help with simplifying complex matters and proofreading my dissertation.

Most importantly, I could have not accomplished this without my family. Dieter, Erika, Simone and Philipp have been a constant source of loving concern, unconfined support, motivation and strength in all these years.

Curriculum Vitae

Der Lebenslauf wurde aus der elektronischen Version der Arbeit entfernt.
The CV was removed from the electronic version of this work.

édition scientifique
VVB LAUFERSWEILER VERLAG

VVB LAUFERSWEILER VERLAG
STAUFENBERGRING 15
D-35396 GIESSEN

Tel: 0641-5599888 Fax: -5599890
redaktion@doktorverlag.de
www.doktorverlag.de

ISBN: 978-3-8359-5996-5